‘Lipocalin 2, an essential multi-regulator of hepatic homeostasis during a Methionine & Choline deficient diet-induced Non-alcoholic steatohepatitis in mice’

Von der Fakultät für
Mathematik, Informatik und Naturwissenschaften der
RWTH Aachen University

zur Erlangung des akademischen Grades einer
Doktorin der Naturwissenschaften genehmigten Dissertation

vorgelegt von
M.Sc.-Biologin Anastasia Asimakopoulou
aus Sydney, Australien

Berichter: Univ.-Prof. Dr. rer. nat. R. Weiskirchen
Univ.- Prof. Dr. M. Spehr

Tag der mündlichen Prüfung: 29. Juni 2015

Diese Dissertation ist auf den Internetseiten der Universitätsbibliothek online verfügbar.

Die vorliegende Doktorarbeit wurde in der Zeit vom 1. Januar 2012 bis zum 31. Marz 2015 im Institut für Molekulare Pathobiochemie, Experimentelle Gentherapie und Klinische Chemie (IFMPEGKC) angefertigt und ist in englischer Sprache verfasst.

Doctoral Advisor and 1st Examiner:
Prof. Dr. rer. nat. R. Weiskirchen
Institute of Molecular Pathobiochemistry, Experimental Gene Therapy
and Clinical Chemistry,
University Hospital Aachen (Germany)

2nd Examiner:
Prof. Dr. rer. nat. M. Spehr
Department of Chemosensation,
RWTH University Aachen (Germany)

3rd Examiner:
Prof. Dr. rer. nat. J. Bernhagen
Department of Biochemistry and Molecular Cell Biology,
RWTH University Aachen (Germany)

Head of the Committee:
Prof. Dr. rer. nat. J. Bohrmann
Department of Zoology and Human Biology,
RWTH University Aachen (Germany)

Acknowledgements

I would like to express my graditude to the people that supported me during this work. First of all I want to thank Prof. Weiskirchen Ralf for giving me the opportunity to work with him on a very interesting project, for his advice and support through out the thesis and secondary for giving me the chance to get to know Germany. Moreover i have to thank Dr. Borkham-Kamphorst Erawan who made my introduction to the subject smoother, that she solved any experimental questions that arised and for her guidance throughout my thesis.

I would also like to thank the professionals that supported my thesis with the technical work and their advice and these are: Haas Ute, Van de Leur Eddy, Tag Carmen, Sauer-Lehnen Sibile, Weiskirchen Sabine and Uerlings Ricarda. Valuable also was the contribution of Dr. Yagmur Eray and Dr. Nikolaus Gassler. I need to express my appreciation to my other two examiners Prof. Spehr and Prof. Bernhagen for taking the time to evaluate my thesis. Pr. Bernhagen helped me as well with many things that could cause confusion. He always had the way/knowledge to solve it.

Furthermore at this laboratory I met people that without asking anything in return they helped me a lot in the work as much as in non-related to work needs. I enjoyed our discussions and their presence more than anything at this lab and these people are Dr. Meurer Steffen, Boaru Sorina and Kim Philipp.

A huge thanks goes to my parents for allowing me to folow my dream and study abroad and for supporting me all these years of studies. Studying in Germany gave me new friends like Zalake Deepak and Avoodapaian Padagaligam that together we went through many enjoyable experiences during these 3 years and i consider them as life-time friends, thank you for being by my side.

Last but not least I am grateful to Fernandez Andrea, the person that has been next to me the last years supporting me literally in every single thing. Thanks for your patience!

Table of Contents

Acknowledgements ... 3

Table of Contents ... 4

1 Summary ... 7

2 Highlights ... 9

3 Abbreviations ... 10

4 Introduction ... 13

4.1 Lipocalins ... 13

4.1.1 General structure and function of Lipocalins ... 13

4.1.2 Lipocalins in hepatic disease initiation and progression ... 15

4.2 Lipocalin 2 ... 16

4.2.1 Lipocalin 2 in fatty liver disease ... 23

4.2.2 Lipocalin 2 in the diagnosis of hepatic disease ... 24

4.3 The liver ... 25

4.3.1 Functions and anatomy of the liver ... 25

4.3.2 Hepatocytes in fatty liver disease ... 27

4.4 NAFLD-NASH ... 28

4.4.1 Diagnosis of NAFLD ... 28

4.4.2 NASH models and MCD diet ... 29

4.4.3 The mouse as experimental animal in NASH ... 29

4.4.4 Aim of the study ... 30

5 Experimental Methods ... 31

5.1 Animal model ... 31

5.2 High Fat Diet animal model ... 31

5.3 Blood sampling, serum analysis ... 31

5.4 Liver steatosis and inflammation scoring ... 32

5.5 Isolation of primary hepatocytes and cell culture ... 32

5.6 Stimulation with fatty acids or Rosiglitazone ... 33

5.7 Adenoviral vector preparation 33
5.8 Infection of primary hepatocytes 34
5.9 Plasmid DNA preparation (small prep) 34
5.10 Plasmid preparation (large prep) 35
5.11 Rubidium competent cells 36
5.12 Transformation of competent cells 37
5.13 Transfection of primary hepatocytes 37
5.14 RNA isolation of primary hepatocytes 37
5.15 RNA isolation from liver sections 38
5.16 Complementary DNA (cDNA) synthesis 39
5.17 PCR for cDNA synthesis check up 39
5.18 Quantitative real time PCR (qRT-PCR) 39
5.19 Protein extraction 40
5.20 Protein quantification (DC assay) 40
5.21 SDS-PAGE and Western blot analysis 40
5.22 Immunohistochemistry 41
5.23 Immunofluoresence-histochemistry 41
5.24 Immunofluorescence in primary hepatocytes 42
5.25 Cell quantification 42
5.26 Oil Red O staining of neutral lipids on liver sections 42
5.27 Oil Red O staining of neutral lipids on hepatocytes 43
5.28 Nile red staining on primary hepatocytes 43
5.29 Triglyceride assay 43
5.30 Free fatty acid assay 43
5.31 Myeloperoxidase (MPO) activity quantification assay 43
5.32 RNA and DNA quantification 44
5.33 Statistical analysis 44
6 Lipocalin 2 regulates PLIN5 expression and intracellular lipid formation in the liver .. 45

6.1 Introduction 45
6.2 Results 47
6.3 Discussion 64
7 Lipocalin-2 (NGAL/LCN2), a "HELP-ME" Signal in hepatic inflammation 69
7.1 Introduction 69
7.2 Results 70
7.3 Discussion 76
8 General conclusion and future aspects 79
9 References 80
10 Appendix 90
10.1 Supplementary tables 91
10.2 Solutions and buffers 103
10.3 Table of figures 108
10.4 Table of tables 109
10.5 Curriculum vitae 110

1 Summary

Lipocalin-2 (LCN2) is a 25-kDa secretory protein with great importance as a sensitive and specific screening and diagnostic biomarker for hepatic inflammation, acute hepatic injury, hepatic cancer, radiation-induced early phase hepatic damage and lipid abnormalities. However, little is known about LCN2's functions in the homeostasis and metabolism of hepatic lipids or in the development of steatosis as well as its actual role in the event of inflammation.

The aim of this study was to prospectively evaluate the LCN2 role in the 'two-hit' development of Non-alcoholic steatohepatitis (NASH) meaning the steatosis and the injury, observed by the appearance of inflammation. NASH is a condition where fatty liver is accompanied with inflammation. The objective of this study was to determine in wild type (WT) and *Lcn2*-deficient (*Lcn2*$^{-/-}$) mice the possible differences in their biological reactions after a Methionine and Choline deficient diet (MCD), a nutritional model used to induce the pathological condition of NASH.

The current study compares initially the intrahepatic lipid accumulation, lipid droplet formation, mitochondrial content, and expression of the Perilipin proteins known to regulate cellular lipid metabolism. *Lcn2*$^{-/-}$ mice fed with MCD diet accumulated more lipids in the liver than WT controls, and that the basal expression of the lipid droplet coat protein Perilipin 5 (PLIN5) was significantly reduced in these animals. Similarly, the overexpression of LCN2 and PLIN5 were also found in animals that were fed with a high fat diet. Furthermore, the loss of LCN2 and/or PLIN5 in hepatocytes prevented normal intracellular lipid droplet formation both *in vitro* and *in vivo*. In *in vitro* experimentation the restoration of LCN2 in *Lcn2*$^{-/-}$ primary hepatocytes by either transfection or adenoviral vector infection induced PLIN5 expression and restored proper lipid droplet formation.

The other section of this study targeted the role of LCN2 specifically in the inflammation process accompanying hepatic injury after administration of the MCD diet. Therefore, the hepatic LCN2 and inflammatory cytokines' interleukin- 6 and interleukin-1β (IL-6, IL-1β), tumor necrosis factor α (TNF-α), chemokine (C-C motif) ligand 2 (CCL2), and chemokine (C-C motif) receptor 2 (CCR2) expression was compared between the two genotypes. The expression of the activated forms of the Signal Transducers and Activators of Transcription (STAT1 and STAT3) were tested as well. Additionally, histology inflammation score and immunohistochemistry stainings with leukocytes and neutrophil granulocyte markers were performed. Both genotypes had inflammation sites as a result of the MCD diet, however the WT mice recruited more inflammatory cells than the *Lcn2*$^{-/-}$ accompanied with a strong upregulation of LCN2. Moreover, the WT mice fed with MCD diet, presented a remarkably stronger expression of phosphorylated forms of STAT1 and STAT3.

In conclusion this study shows that LCN2 is a protein of high significance with multiple functions in MCD-induced NASH in mice. The presented findings indicate that first of all, LCN2 is a key modulator of hepatic lipid homeostasis that controls the formation of intracellular lipid droplets by regulating PLIN5 expression while a second significant role in inflammation is that its upregulation serves as a 'HELP-ME' signal while inflammation appears. The upregulation of the LCN2-'HELP-ME'-factor, enhances the recruitment of neutrophil granulocytes and leukocytes towards resolution of the inflammation protecting the liver from progression to further hepatic damage agreeing to previous reports of LCN2's hepato-protective role in liver injury models. LCN2 may therefore represent a novel therapeutic drug target for the treatment of liver diseases associated with inflammation and elevated fat accumulation.

In the present dissertation the results that will be discussed have been published already in the following research papers:

- **Asimakopoulou** A, Borkham-Kamphorst E, Henning M, Yagmur E, Gassler N, Liedtke C, Berger T, Mak TW, Weiskirchen R. Lipocalin - 2 [LCN2] regulates PLIN5 expression and intracellular lipid droplet formation in the liver. Biochim. Biophys. Acta (2014), 1841:1513 - 1524.
- **Asimakopoulou** A, Borkham-Kamphorst E, Tacke F, Weiskirchen R. Lipocalin-2 (NGAL/LCN2), a "HELP-ME" signal in organ inflammation. Hepatology (2015), 62, in press.
- **Asimakopoulou** A, Weiskirchen R. Lipocalin 2 in the pathogenesis of fatty liver disease and nonalcoholic statohepatitis. Clin Lipidology (2015), 10:47-67.

2 Highlights

- A lack of LCN2 predisposes mice to develop hepatic steatosis.
- LCN2 is involved in intracellular lipid droplet formation.
- LCN2 regulates the expression of the lipid droplet coat protein PLIN5.
- Transient LCN2 expression can restore proper intracellular lipid droplet formation in *Lcn2*$^{-/-}$hepatocytes.
- LCN2 represents the 'HELP-ME' signal after inflammation develops.
- The LCN2-'HELP ME' signal contributes to the resolution of inflammation by recruiting leukocytes and mainly neutrophil granulocytes in the NASH mouse model.
- LCN2 is involved in the inflammation pathway mediated by STAT3 and STAT1.

3 Abbreviations

°C	degrees Celsius
µ	micro ($x10^{-6}$)
ADRP or PLIN2	adipocyte differentiation-related protein
AFLD	alcoholic fatty liver disease
AKI	acute kidney injury
ALT	alanine transaminase
ASH	alcoholic steatohepatitis
AST	aspartate transaminase
BSA	bovine serum albumin
CCL2	chemokine (C-C motif) ligand 2
CCl_4	carbon tetrachloride
CCR2	chemokine (C-C motif) receptor 2
CD45	cluster of differentiation 45
cDNA	complementary deoxyribonucleic acid
$CHCl_3$	chloroform
Conc.	concentration
Cont.	continue
Da	dalton
DAKO	3.3′-diaminobenzidine substrate
DAPI	4',6-diamidino-2-phenylindole
dH_2O	distilled water
DNA	deoxyribonucleic acid
DNAse	deoxyribonuclease
dNTP	nucleoside triphosphates containing deoxyribose
DTT	dithiothreitol
E.coli	Escherichia coli
et al.	et alii (and others)
EtOH	ethanol
FABP(s)-	fatty acid-binding proteins(s)-
FCS	fetal calf serum
FFA	free fatty acid
FLD	fatty liver disease
FLS	fatty liver Shionogi
g	gram
g	gravitational force
GAPDH	glyceraldehyde 3-phosphate dehydrogenase
H&E	haematoxylin and Eosin
HCC	hepatocellular carcinoma
HCl	hydrogen chloride
HCV	hepatitis C virus
HFD	high fat diet
HGNC	HUGO Gene Nomenclature Committee guidelines
hr(s)	hour(s)

IFN-γ	interferon gamma
IgG	immunoglobulin
IL-1β	interleukin 1β
IL-6	interleukin 6
in vitro	in artificial culture
in vivo	within the living
k	kilo
L	litre
LCN(s)-	lipocalin(s)-
***Lcn2*$^{-/-}$**	*Lcn2*-deficient
LDC	Lieber-DeCarli diet
LPS	lipopolysaccharide
LSDP5	lipid storage droplet protein 5
m	milli
M	mole per litre
MCD	Methionine and Choline deficient diet
MES	2-(N-morpholino)ethanesulfonic acid
MLDP	myocardial lipid droplet protein
mM	milli mole per litre
MOPS	morpholinopropanesulfonic acid
MPO	myeloid peroxidase
mRNA	messenger ribonucleic acid
n	number
n	nano (x10^{-9})
NAFLD	non-alcoholic fatty liver disease
NASH	non-alcoholic steatohepatitis
NGAL	neutrophil gelatinase associated lipocalin
NL or HNL	(Human) Neutrophil Lipocalin
NP-40	nonyl-phenoxypolyethoxylethanol
OD_{600}	optical density at 600 nm
OXPAT	oxidative tissue-enriched PAT
PAGE	polyacrilamide gel electrophoresis
PBS	phosphate-buffered saline
PBST	phosphate-buffered saline supplemented with Tween20
PCR	polymerase chain reaction
PEG	polyethylene Glycol
PFA	paraformaldehyde
PLIN-	perilipin-
PLIN4 or S3-12	perilipin4
PLIN5	perilipin 5
PPAR-γ	peroxisome proliferator-activated receptor γ,
qRT-PCR	quantitative real-time PCR
RBP(s)-	retinol-binding protein(s)-
RNA	ribonucleic acid
RNase	ribonuclease

rpm	round per minute
RT	room temperature
SD	standard deviation
SDS	sodium dodecyl sulfate
sec	second
Sip24	24 kDa super-inducible protein
STAT1	signal transducers and activators of transcription 1
STAT3	signal transducers and activators of transcription 3
TBST	tris-buffered saline supplemented with 1% Tween20
TE	tris and EDTA buffer
TIP47 or PLIN3	tail-interacting protein-47
TNF-α	tumor necrosis factor-α
v/v	volume /volume
VLDL	very low density lipoproteins
w/v	weight /volume
WT	wild type

4 Introduction

4.1 Lipocalins

The lipocalins form a family of proteins originally classified as a widespread group of transport proteins for small hydrophobic molecules. They share a limited homological sequence. However, they have a common three dimensional structure architecture. Their common structure is comprised of an eight stranded antiparallel β-barrel which encloses an internal hydrophobic binding domain. Research of the last decades, has instated the wide family of lipocalins in an extended spectrum of biological processes that most often become visible during disease formation. Important biological functions of the lipocalins include transport of iron, pheromone, retinoids, arachidonic acid, steroids, colouring pigments, histamine and lipids, control of cell regulation, and the enzymatic synthesis of prostaglandins [Flower et al., 1996; Cianci et al., 2002; Marchese et al., 1998; Beynon et al., 2003; Andersen et al., 1998].

4.1.1 General structure and function of Lipocalins

Members of the broad lipocalin protein family are found in several organisms including bacteria, plants, insects, and mammals such as human [Ganfornina et al., 2000]. In mid-80's Pervaiz and Brew categorised the first proteins of the lipocalin family [Pervaiz and Brew 1985]. They, as well gave the name ’lipo-calins’ to these proteins in order to describe their common ability to bind lipophilic molecules such as drugs and certain steroids in a way to protect them from degrading [Pervaiz and Brew 1985; Pervaiz et al., 1987]. The lipocalin family grew in members when methods such as informatics, sequence analysis, crystallography and nuclear magnetic resonance spectrometry were applied. Numerous extracellular and intracellular proteins with sequence homology, secondary structures and three-dimensional structure, similar to the first lipocalins, were identified and classified into the continuously extending Lipocalin superfamily [Pervaiz and Brew, 1985; Flower et al., 1991]. All the known members of the Lipocalin family in humans are depicted in Figure 4-i.

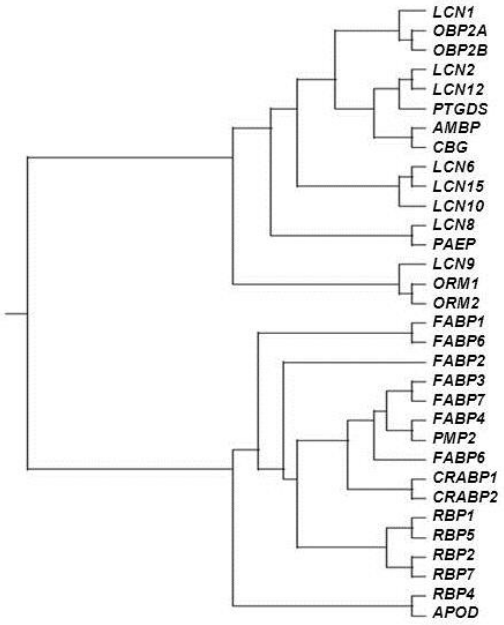


Figure 4-i: Phylogenetic tree for human Lipocalins. The tree includes human lipocalins that are deposited in GenBank database under accession numbers. CAI14045 (LCN1), CAG46889.(LCN2), NP_945184 (LCN6), NP_848564 (LCN8), NP_001001676 (LCN9), NP_001001712 (LCN10), NP_848631 (LCN12), NP_976222 (LCN15), CAG46887 (FABP1), AAH69617 (FABP2), CAG33148 (FABP3), CAG33184 (FABP4), NP_001435 (FABP5), AAB82751 (FABP6), CAG33338 (FABP7), CAG46802 (RBP1), AAH69513 (RBP2), CAH72328 (RBP4), NP_113679 (RBP5), CAI14685 (RBP7), N P_001624 (AMBP), CAG46572 (APOD), NP_000597 (C8G), CAG33298 (CRABP1), CAG29353 (CRABP2), CAI14043 (OBP2A), AAQ89340 (OBP2B), NP_000598 (ORM1), NP_000599 (ORM2), NP_002562 (PAEP), CAG46538 (PMP2) and NP_000945 (PTGDS), respectively. The sequence alignment and generation of phylogenetic tree was done at the GenomeNet Database Resource that is available at http://www.genome.jp/tools/clustalw. **(Source: Asimakopoulou and Weiskirchen 2015).**

Although some proteins of the lipocalin family share only an overall small sequence homology, all members of this protein family have a highly conserved structure with highly conserved folding segments, known as the lipocalin folds. This characteristic lipocalin fold is composed of a single eight-stranded continuously anti-parallel β-barrel that forms an integral hydrophobic pocket in which the different ligands are embedded. This ligand binding site is the special tool that the lipocalins use to function as transport proteins [Flower et al., 1996]. In Figure 4-ii the characteristic structure of the Lipocalin 2 is depicted.

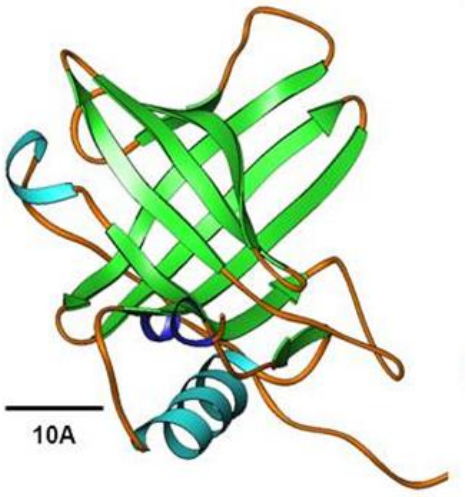


Figure 4-ii: Three dimensional structural architecture of Lipocalin 2. (A) In the monomeric structure of the human Gelatinase-associated Lipocalin (NGAL/LCN2) that was determined by Nuclear Magnetic Resonance (NMR) Spectroscopy the typical three dimensional lipocalin fold is recognizable. It consists of an eight-stranded antiparallel β-barrel. In the cavity of this barrel hydrophobic molecules can be incorporated. More details of the solution structure and dynamics of human LCN2 are given elsewhere [Coles et al., 1999]. The coordinates of the respective protein (1NGL, human NGAL) was taken from the RCSB Protein Data Bank repository that can be found at http://www.rcsb.org. The image was generated using the Ribbons XP software (Version 3.0) [Carson 1997**]. (Source: Asimakopoulou and Weiskirchen 2015).**

Additional advantageous characteristics of the lipocalins are their general small size, their ability to be secreted from various cells and that they contain ligand binding sites that target the multitude of specific substances with high specificity [Godovac-Zimmermann 1988]. These major features have involved the lipocalins in many biological processes. Bright examples of lipocalins are the retinol-binding protein (RBP) [Cowan et al., 1990], which transports retinol (vitamin A) through the blood to target cells [Newcomer et al., 2000] and the different intracellular fatty acid-binding proteins (FABP) that bind hydrophobic molecules such as fatty acids [Matarese et al., 1990]. Another group of the lipocalin superfamily known as the 'immunocalins' including the α_1-acid glycoprotein and the α_1-microglobulin have drug-binding properties which mediate immunological and inflammatory processes in a protective way [Logdberg et al., 2000]. In humans, the most well-known subgroups of lipocalins are formed by the "classical lipocalin" (i.e. LCNs), the FABPs, and the RBPs**.** Most of the lipocalins are found in literature under multiple synonyms indicating the various roles in biological processes. The several lipocalins based on their chromosomal localizations, it was suggested that they have evolved by in situ tandem duplication forming gene clusters in which each gene has obtained a distinct spatial expression and regulation [Suzuki et al., 2004].

4.1.2 Lipocalins in hepatic disease initiation and progression

As outlined above, lipocalins have been studied widely as possible non-invasive, biochemical markers for many diseases. In addition, they have already been extensively used as markers for clinical cases of inflammatory diseases, lipid abnormalities, cancer, kidney injury, and liver functions. Several members of the lipocalin superfamily such as the retinol-binding protein (RBP), Complement C8, lipocalin 13 (LCN13), FABP1, LCN2, and others have been associated with hepatic injury including acute and chronic inflammation, insulin resistance as well as failures in lipogenesis, fatty acid oxidation and nutrient metabolism.

The human complement C8 is mainly produced in liver cells and has been classified in the lipocalin family as an acute-phase protein due to the fact that its production is strongly associated with pro-inflammatory cytokines such as IL-1β, IL-6, and Interferon gamma (IFN-γ) in the hepatoma cell lines HepG2 [Scheurer et al., 1997]. RBP is another lipocalin that is considered a acute phase protein that is elevated soon after the hepatic necrosis. The serum concentrations of RBP have been considered as a great diagnostic tool to predict the hepatic recovery and outcome of patients after acute necrosis [Horn et al., 1999] while it has also been found to be increased in obese children with non-alcoholic fatty liver disease (NAFLD) that correlated with the activity of alanine transaminase (ALT) suggesting that this lipocalin is a contributor to the pathogenesis of NAFLD suggesting serum RBP as a novel marker to predict the disease [Boyraz et al., 2013]. A wide set of experiments has demonstrated that LCN13 reduces hepatic lipid accumulation by both

inhibiting hepatic lipogenesis and enhancing β-oxidation and further that LCN13 deficiency is likely to contribute to fatty liver disease in obese mice [Cho et al., 2011; Sheng et al., 2011]. Therefore, also LCN13 is potentially a novel useful diagnostic marker for formation of fatty liver. Another interesting group of lipocalins that are grouped as FABP contains also several members that were already associated with hepatic steatosis. Independently of obesity, liver fat was initially associated with mRNA expression of the FABP4 and FABP5 [Westerbacka et al., 2007]. Additionally FABP1 was finally reported to protect from lipotoxicity of free fatty acids and to mediate the trafficking of fatty acids in the liver [Guzman et al., 2013]. LCN2 is one members of the lipocalin family with various associations in hepatic conditions regarding injury, inflammation, lipid homeostasis and mitochondrial malfunctions described below.

4.2 Lipocalin 2

The main subject of interest, Lipocalin-2 was discovered by Kjedsen's group in 1993 as a 25 kDa protein that was associated with human neutrophil gelatinase [Kjeldsen et al., 1993]. The protein was isolated from exocytosed material obtained from phorbol myristate-stimulated human neutrophils. Based on the high primary sequence similarity of this new protein with the sequences of the deduced rat a_2-microglobulin and the mouse lipocalin 24p3, this neutrophil gelatinase associated lipocalin (NGAL) was recognized as a novel member of the lipocalin family [Kjeldsen et al., 1993]. As many other lipocalins, NGAL has many synonyms depicted in Table 4-i.

Species	Synonym	Feature	References
Human	Neutrophil gelatinase associated lipocalin (NGAL)	25-kDa protein purified from exocytosed material from phorbol myristate acetate-stimulated human neutrophils	[Kjeldsen et al., 1993]
	(Human) Neutrophil Lipocalin (NL or HNL)	Purified from the granules of human neutrophils	[Xu et al., 1994]
	25kDa α_2-micro globulin – related protein	Homology to an α_2-microglobulin-related protein from rats	[Triebel et al., 1992]
	Siderocalin	Demonstration that LCN2/NGAL binds bacterial catecholate-type ferric siderophores	[Goetz et al., 2002]
Mouse	Lipocalin 2	Chromosomal assignment of LCN2 to human chromosome 9q34	[Chan et al., 1994]
	Oncogene 24p3 protein	Expression in breast cancer	[Slamon et al., 1987]
	Uterocalin	Expression of this lipocalin in the uterus	[Liu et al., 1997]
	24 kDa super-inducible protein (Sip24)	Fibroblast growth factor inducible protein in BALB/c 3T3 cells	[Davis et al., 1991]
Rat	Neu-related lipocalin (NRL)	Expressed in neu-initiated breast cancers	[Stoesz et al., 1995]
	α_2u-globulin, α_2-microglobulin-related protein	Male rat liver protein under complex hormonal control, present in the urine of mature male rats and absent from the urine of female rats	[Roy et al., 1966; Kurtz et al., 1977; Drickamer et al., 1981]

Table 4-i: Synonyms of LCN2/NGAL in: human, mouse and rat **(Source: Asimakopoulou and Weiskirchen, 2015).**

In accordance with the approved gene symbols of the HUGO Gene Nomenclature Committee guidelines (HGNC) (http://www.genenames.org/genefamilies/lipocalin), here the name lipocalin 2

(LCN2) will be used when referring to this protein in this dissertation. In 1994, the group of Kjeldsen achieved the molecular cloning of the full-length human LCN2 cDNA and in recombinant expression of this lipocalin in *E. coli* [Bundgaard et al., 1994].

In the same year, the gene encoding LCN2 was assigned by in situ hybridization to human chromosome 9 on the HSA9q34 area, where most of the known human lipocalins are clustered [Chan et al., 1994]. Over the last years LCN2 has been reported to be expressed in several tissues including liver, kidney, pancreas, and lungs. More analytically sources of LCN2 in humans as published are depicted in Table 4-ii.

Source of LCN2 in humans	Literature
Supernatant of activated Neutrophils	Kjeldsen et al., 1993
Bronchus, stomach, adipose tissue,small intestine, pancreas, kidney, prostate gland, and thymus.	Friedl et al., 1999
Adenocarcinomas of lung, colon and pancreas.	Friedl et al., 1999
Inflamed epithelia in bowel	Nielsen et al., 1996
Mammary adenocarcinomas	Stoesz et al., 1998
Urothelial carcinomas	Monier et al., 2000
Normal liver and Hepato-carcinomas	Zhang et al., 2012

Table 4-ii: Sources of LCN2 in human tissues

Lipocalin 2 in iron transport **-** One of LCN2's main features is the ability to bind iron. That was first indicated by Goetz et al [Goetz et al., 2002] proven to be the result of an iron molecule bound on the enterochelin, which is *E. coli's* siderophore. Yang et al., supported this finding by reporting that LCN2 plays a critical role in delivering iron to the cytoplasm in which it regulates iron-associated genes mediating many cellular iron-dependent reactions [Yang et al., 2002]. Additionally, the Goetz group reported that LCN2 has the ability to bind bacterial ferric siderophores, suggesting that LCN2 mediates the antibacterial iron-depletion strategy of the innate immune system by sequestering iron giving the synonym name Siderocalin to LCN2 [Goetz et al., 2002]. Not long after, Flo and coworkers using mice knock out for LCN2 proved their sensitivity in bacterial infection compared to WT animals. The absence of secreted LCN2 enhanced bacterial growth while LCN2 presence, sequestered the iron bound on siderophore, limiting the bacterial growth [Flo et al., 2004]. For more than a decade, numerous studies reporting the elevated expression of LCN2 in bacterial infection cases gave the unarguable role of LCN2 in the immune system to limit bacterial growth by sequestrating the iron-laden siderophore [Flo et al., 2004; Berger et al., 2006].However, several other experimentation classified LCN2 as a factor that is upregulated in many other conditions such as infection, intoxication, inflammation and other forms of cellular stress.

Lipocalin 2 in cellular stress **-** Regarding liver conditions, there are many experimental and clinical findings in which altered hepatic expression of LCN2 was reported (Table 4-iii). Jiang et al., showed that LCN2 was significantly upregulated by anaemia and hypoxia in murine liver and serum [Jiang et al., 2008]. LCN2 was also proposed as a possible biomarker of early liver damage that occurred during ethanol consumption in mice [Bykov et al., 2007]. At the same period, Sunil and coworkers reported that endotoxemia-induced by intraperitoneal injection of lipopolysaccharide (LPS) to mice (at 1 mg/kg body weight) or rats (at 5 mg/body weight) resulted in an early upregulation of LCN2 that was already evident 4 hrs post infection and persisted for 24-48 hrs [Sunil et al., 2007]. This report further demonstrated that the injection of LPS was also effective in inducing LCN2 expression in the lung, suggested that LCN2 plays a critical role in restoring liver and lung tissue homeostasis after endotoxemia [Sunil et al., 2007]. More reports showed that different tissues including heart, kidney and mainly liver are capable to upregulate expression of LCN2 after an acute and long-term exposure to X-rays [Roudkenar et al., 2007]. After these first reports numerous studies about hepatic inflammation and damage were initiated aiming to understand the regulation of LCN2 and the underlying molecular pathways. Borkham et al., demonstrated a remarkable upregulation of LCN2 in mice after administration of carbon tetrachloride (CCl_4), LPS, Concanavalin A or after bile duct ligation that are all suitable experimental models for acute or chronic liver injury suggesting LCN2 as a reliable indicator for liver damage and that LCN2 evolves hepato-protective effects during phases of acute liver injury [Borkham-Kamphorst et al., 2013]. Shortly before, Labbus et al. showed the intense upregulation of LCN2 in inflammatory responses, indicating the role of LCN2 to restore liver homeostasis after appropriate insult [Labbus et al., 2012]. That result was supported by Lai et al who reported enhanced expression of LCN2 during liver regeneration using a partial hepatectomy model [Lai et al., 2013].

Lipocalin 2 in AKI and HCC **-** The strong association of LCN2 in acute kidney injury (AKI) became the centre of attention when Mishra and co-workers for the first time suggested that LCN2 is a promising and sensitive biomarker of ischemic and nephrotoxic renal injury [Mishra et al., 2003; Mishra et al., 2004; Mishra et al., 2005].Additionally the association of human LCN2 with AKI patients post-liver-transplantation was proved [38, Niemann et al., 2009]. Moreover, LCN2 further plays a significant role in the formation of hepatic cancer, ovarian cancer, lung adenocarcinomas, and breast cancer [Bartsch et al., 1995; Furutani et al., 1998; Friedl et al., 1999; Liu et al., 1995]. Recently, LCN2 was proved to be a diagnostic marker with high sensitivity and specificity for increasing lobular inflammation, ballooning and fibrosis that are the pathogenetic changes during formation of hepatocellular carcinoma (HCC) [El Moety et al., 2013].

During the last years, LCN2 has also been widely studied in obesity and other metabolic dysregulation conditions. Several studies have proved the strong correlation of LCN2 to insulin

resistance [Yan et al., 2007], obesity, obesity-related metabolic complications and cardiovascular diseases [Auquet et al., 2011; Wang et al., 2007] as well as to mitochondrial oxidation and adipocyte metabolism [Zhang et al., 2014].

Species	Model/Disease	Treatment	LCN2 Expression	Conclusions	Refs
Mouse	Anaemia and hypoxia	Anaemia was induced by phlebotomy, iron deprivation, or phenylhydrazine treatment	Upregulation of LCN2 during anaemia and hypoxia	LCN2 has a physiological role during increased iron utilization and mobilization from stores	[Hvidberg et al., 2005]
WT and Lcn2$^{-/-}$ mice	Acute liver injury	Administration of LPS or Concanavalin A and bile duct ligation.	Highly elevated hepatic LCN2 expression	LCN2 has an hepato-protective role and it's a reliable biomarker of acute liver injury	[Borkham-Kamphorst E et al., 2013]
WT and Lcn2$^{-/-}$ mice	Inflammatory liver injury	LPS stimulation	Dramatic upregulation of LCN2	LCN2 has essential function in liver homeostasis	[Labbus et al., 2013]
Human	Patients with chronic liver disease	Clinical samples: 25 controls, 25 HCC patients, 25 HCC patients with hepatitis C	LCN2 elevated in HCV and in combination of combined HCC and HCV	LCN2 associated with increasing liver inflammation, ballooning & fibrosis. LCN2 - diagnostic marker for progression of HCC	[El Moety et al., 2013]
Rat	Acute and chronic liver injury	Administration CCl_4 or bile duct ligation	High expression of LCN2 in cultured hepatocytes isolated from injured rats	LCN2 expression shows clear correlation to liver damage and resulting inflammatory responses; Possible diagnostic value as an early biomarker of liver inflammation	[Borkham-Kamphorst E et al., 2011]
Human	Severely obese women with NAFLD	Clinical samples: Liver histology of 59 obese women and LCN2 serum ELISA measurements	Upregulated expression in NAFLD women	LCN2 is related to NAFLD	[Auguet et al., 2013]
Mouse	Fatty liver Shionogi	Genetic development of NASH	Increased LCN2 expression in NASH mice	LCN2 important for pathogenesis of NASH	[Semba et al., 2013]
Human	NAFLD Chinese patients	Clinical samples: LCN2 serum ELISA measurements in 436 patients with NAFLD and 467 controls	Elevated levels of circulating and serum LCN2	Contribution of LCN2 in the progression of NAFLD	[Ye et al., 2014]
Rat	Hepatic steatosis	HFD, and liquid LDC administration (diet high fructose)	Upregulated LCN2 in rats with NAFLD	Correlation of LCN2 and NAFLD and hepato-protective role of LCN2, correlation of LCN2 to oxidative stress and mitochondrial dysfunction	[Alwahsh et al., 2014]

***Abbreviations used: CCl_4, carbon tetrachloride; HCC, Hepatocellular carcinoma; HCV, Hepatitis C virus; HFD, High fat diet; LDC, Lieber-DeCarli diet; LCN2, Lipocalin 2; LCN2$^{-/-}$ Lipocalin 2 knock out; LPS, Lipopolysaccharide; ; MCD, Methionine and choline deficient diet; NAFLD, Non-alcoholic fatty liver disease; NASH, Non-alcoholic steatohepatitis; PLIN5, Perilipin 5; PPAR-γ, Peroxisome proliferator-activated receptor γ; WT, wild type.**

Table 4-iii: Selected experimental and clinical findings associated with altered hepatic LCN2 expression* **(Source: Asimakopoulou and Weiskirchen, 2015)**

Species	Model/Disease	Treatment	LCN2 Expression	Conclusions	Refs
Human	NAFLD patients	Clinical samples: urine from 65 consecutive patients	Significant upregulation of urinary LCN2	Correlation of urinary LCN2 with NAFLD-related hepatic injury, body mass index, insulin resistance and lipid profiles	[Tekkesin et al., 2012]
WT and Lcn2$^{-/-}$ mice	Hepatic steatosis	HFD feeding	Highly expressed LCN2 in WT mice with NAFLD; lack in LCN2 resulted in significantly potentiated diet-induced obesity, dyslipidemia, fatty liver disease and insulin resistance	LCN2 is a key regulator of glucose, lipid homeostasis and insulin resistance	[Guo et al., 2010]
WT and Lcn2$^{-/-}$ mice	Hepatic steatosis	HFD and Rosiglitazone administration	LCN2 deficiency cancels Rosiglitazone's activity	LCN2 regulates PPARγ which regulates hepatic lipogenesis	[Jin et al., 2011]
WT and Lcn2$^{-/-}$ mice	NAFLD	MCD diet and LCN2 transfection/infection in primary hepatocytes	LCN2 upregulation in NAFLD, upregulation of PLIN5 after LCN2 restoration	LCN2 mediates hepatic lipid droplet formation via regulation of PLIN5	[Asimakopoulou et al., 2014]
Rat	Hepatic Irradiation damage	Rats received a single percutaneous irradiation dose (25 Gray)	LCN2 serum levels increased significantly within 6 hrs	LCN2 is a marker for the early phase of radiation-induced liver damage	[Sultan et al., 2013]
Rat	Toxic liver injury	Data taken from the toxicogenomics database DrugMatrix	LCN2 is correlated to liver fibrogenesis	LCN2 is a marker of hepatic fibrogenesis in rats induced by different toxic treatment	[AbdulHameed et al., 2014]
Hepatocyte specific $^{-}$ and global Lcn2$^{-/-}$ mice	Bacterial infection and partial hepatectomy	Bacterial infection with *Klebsiella pneumoniae* or *Escherichia coli* or partial hepatectomy	Strong upregulation of hepatic LCN2 after bacterial infection and partial hepatectomy	Hepatocytes are the major cell type responsible for LCN2 production after bacterial infection or partial hepatectomy. Hepatocyte-derived LCN2 plays an important role in inhibiting bacterial infection and promoting liver regeneration	[Xu et al., 2014]
Mouse	Partial hepatectomy	Mice were subjected to partial hepatectomy	LCN2 expression is dramatically induced in livers and sera of mice after partial hepatectomy, whereas liver LCN2-receptor expression was decreased	LCN2, although massively induced in mice after partial hepatectomy, is not relevant in murine hepatic regeneration	[Kienzl-Wagner et al., 2014]

***Abbreviations used: CCl_4, carbon tetrachloride; HCC, Hepatocellular carcinoma; HCV, Hepatitis C virus; HFD, High fat diet; LDC, Lieber-DeCarli diet; LCN2, Lipocalin 2; LCN2$^{-/-}$ Lipocalin 2 knock out; LPS, Lipopolysaccharide; ; MCD, Methionine and choline deficient diet; NAFLD, Non-alcoholic fatty liver disease; NASH, Non-alcoholic steatohepatitis; PLIN5, Perilipin 5; PPAR-γ, Peroxisome proliferator-activated receptor γ; WT, wild type.**

Table 4-iv: Selected experimental and clinical findings associated with altered hepatic LCN2 expression*** (Source: Asimakopoulou and Weiskirchen, 2015) (cont.)**

Species	Model/Disease	Treatment	LCN2 Expression	Conclusions	Refs
Mouse	Acetaminophen intoxication, IL-22 induced endotoxemia	Mice were injected with combinations of Acetaminophen and IL-22	LCN2 is induced after Acetaminophen-induced hepatotoxicity and LCN2 mRNA expression is further increased after application of IL-22	LCN2 is a prototypical gene that is up-regulated by the IL-22/STAT3 axis	[Scheiermann et al., 2013]
Mouse	Human colon cancer cells were injected in nude mice	A human colon cancer cell line was genetically manipulated to overexpress LCN2 and subcutaneously or intrasplenically injected into mice	Cells were genetically modified to artificially overexpress LCN2. Respective cells substantially inhibited liver metastasis compared to unmodified colon cancer cells.	LCN2 is a candidate metastasis suppressor	[Lee et al., 2006]
Mouse	Implantation of tumors in nude mice	Mice were injected with LCN2-overexpressing hepatocellular carcinoma cells	Hepatocellular carcinoma cells (Chang liver or SK-Hep1 cells were genetically modified to artificially overexpress LCN2	LCN2 is a suppressor of proliferation, migration, invasion and colony forming efficiency in cells expressing LCN2 is markedly reduced. Tumor growth is suppressed in the presence of LCN2. LCN2 modulates MMP-2 protein expression.	[Lee et al., 2011]
Human	Hepatitis C-induced fibrosis/cirrhosis	18 patients with mild and 24 patients with severe fibrosis/cirrhosis	Urine LCN2 levels (normalized to urine creatinine) were higher in patients with severe fibrosis/cirrhosis showing a positive correlation with urine MMP-9/MMP-2 activity ratios	Urinary LCN2 is a marker of hepatic fibrosis that correlates to urine MMP-9 activity	[Kim et al., 2010]
Human	Acute-on-chronic liver failure, acute liver failure, chronic hepatic failure	Very small cohort of patients with acute-on-chronic liver failure, acute liver failure (n=8) and chronic hepatic failure (n=14)	Baseline LCN2 serum concentrations were significantly increased among acute-on-chronic liver failure and acute liver failure	Serum LCN2 may be useful to discern acute from chronic hepatic failure and to monitor the course as well as the severity of the disease	[Roth et al., 2013]
Rat and Mouse	Turpentine oil- induced sterile abscess/acute phase response	Rats and Mice were injected with 5 mL/kg (rats) or 10 mL/kg turpentine oil	LCN2 was strongly upregulated after 6 hrs in serum (in ELISA) and 12 hrs in liver protein extracts (Western blot)	Confirming previous reports that LCN2 is an acute phase protein	[Sultan et al., 2012]

***Abbreviations used: CCl_4, carbon tetrachloride; HCC, Hepatocellular carcinoma; HCV, Hepatitis C virus; HFD, High fat diet; LDC, Lieber-DeCarli diet; LCN2, Lipocalin 2; $LCN2^{-/-}$ Lipocalin 2 knock out; LPS, Lipopolysaccharide; ; MCD, Methionine and choline deficient diet; NAFLD, Non-alcoholic fatty liver disease; NASH, Non-alcoholic steatohepatitis; PLIN5, Perilipin 5; PPAR-γ, Peroxisome proliferator-activated receptor γ, WT, wild type.**

Table 4-v: Selected experimental and clinical findings associated with altered hepatic LCN2 expression* **(Source: Asimakopoulou and Weiskirchen, 2015) (cont.)**

4.2.1 Lipocalin 2 in fatty liver disease

Fat accumulation in the liver is an abnormal condition that has raised multiple questions from the aetiologies to the progression process and the possible restoration mechanisms. Fatty liver disease (FLD) describes a reversible situation in which the liver presents either simple fat accumulation (steatosis) or fat accumulation accompanied with hepatic inflammation (steatohepatitis). LCN2 has concerned the interest of many researchers and clinicians that are trying to understand the dynamic process through which fatty liver disorders develop. Despite the fact that LCN2 had been widely associated with obesity, insulin resistance and metabolic abnormalities, its relation with FLD has also been studied during the last years resulting in some interesting findings that suggest that LCN2 is a promising therapeutic target for NAFLD.

After analysing the liver histology profile of severely obese women with normal histology, simple steatosis and non-alcoholic steatohepatitis (NASH), Auquet and colleagues observed that hepatic LCN2 gene expression is significantly higher in severely obese women with NAFLD and that LCN2 expression is further induced under inflammatory conditions that place the liver in danger [Auquet et al., 2013]. An interesting animal model of NASH is the fatty liver Shionogi (FLS) mice. This model was used to define the difference in LCN2 expression in NASH mice when compared to mice with simple steatosis suggesting a prominent role of LCN2 in the pathogenesis of NASH because of the upregulated LCN2 expression under NASH conditions in areas surrounding the inflammatory cell infiltrates [Semba et al., 2013]. Ye and co-workers after observing higher levels of serum LCN2 in NAFLD Chinese patients suggested that the higher circulating serum LCN2 levels possibly contribute to the progression of the investigated disease [Ye et al., 2014]. Upregulation of LCN2 was observed in rats-models of hepatic steatosis suggested relation with oxidative stress formation and mitochondrial dysfunction [Alwahsh et al., 2014]. The immunofluorescence staining of those models have shown that LCN2 positivity in the liver was restricted to myeloperoxidase-containing cells that are characteristic for neutrophils suggesting an hepato-protective role of LCN2 supporting previous results [Borkham-Kamphorst et al., 2013; Alwahsh et al., 2014].

In one more experimental study performed in mice fed on an HFD, the expression of the LCN2 gene was analyzed in various tissues. In comparison to normal control mice, *Lcn2*$^{-/-}$ mice showed increased hepatic gluconeogenesis, decreased mitochondrial oxidative capacity, impaired lipid metabolism, and increased inflammatory sites under these conditions. Therefore, they demonstrated that LCN2 is one of the key regulators of energy metabolism, glucose and lipid homeostasis, and formation of insulin resistance [Guo et al., 2010]. The same group investigated the role of LCN2 in peroxisome proliferator-activated receptor gamma (PPAR-γ) activation by evaluating the insulin sensitization and fatty acid homeostasis of the PPAR-γ–agonist, Rosiglitazone, after administration of HFD [Jin et al., 2010]. Deficiency of LCN2 reduced by far the effect of Rosiglitazone in increasing body weight, fat deposition, and liver lipid accumulation.

The presented data of this study indicated that LCN2 appears to be a strong regulator of the PPAR-γ which regulates hepatic lipogenesis and suggests that LCN2 is a possible drug target in antidiabetic medicine [Jin et al., 2010].

4.2.2 Lipocalin 2 in the diagnosis of hepatic disease

Many of the reported studies in rodents and humans about LCN2 have shown that this lipocalin is of great importance and linked to the pathogenesis of hepatic disease including infection, inflammation, organ injury, lipid homeostasis, insulin resistance and gluconeogenesis (Figure 4-iii). Several studies have demonstrated the significant positive correlation of enhanced LCN2 expression to several sources of inflammation suggesting this protein as a versatile biomarker for screening and diagnosis of hepatic injury [Borkham-Kamphorst et al., 2013; Roth et al., 2013]. Moreover, the demonstration that the application of a single dose irradiation on liver results in an intense increase of LCN2 in serum LCN2 within the first 6 hrs suggests LCN2 as an candidate biomarker suitable for detection of early phase hepatic damage induced by radiation [Sultan et al., 2013]. The measurement of both LCN2 and its receptor (LCN2R or NGALR) that are both overexpressed in human HCC have been suggested to be relevant for the prognostic classification [Kim et al., 2010; Zhang et al., 2012]. Additionally the measurement of LCN2 as a parameter for liver lipid metabolism and its critical regulator role for PPAR activation is also well established [Jin et al., 2011].

In summary, the data of all these studies strongly imply that LCN2 is a sensitive and specific biomarker for hepatic inflammation, hepatic cancer, and lipid abnormalities. LCN2 is and will be for the upcoming years ‘under the microscope’ as research so far has suggested promising therapeutic uses of LCN2 in diagnosis and treatment of disease.

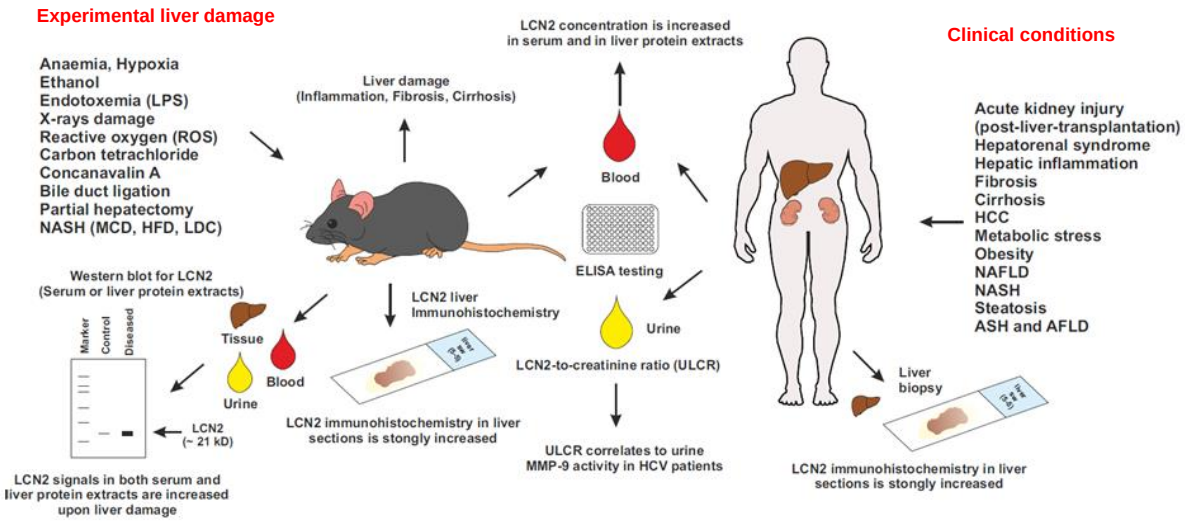


Figure 4-iii: Diagnostic measurement of LCN2 in human specimen. Several clinical conditions or liver damage induced experimentally are connected with significant expression of LCN2. Many reports based on experimentation on rodents led to the outcome that after the induced anaemia, hypoxia, or the application of hepatotoxins (EtOH, LPS, CCl_4, Concanavalin A), and X-rays that lead to reactive oxygen species formation, remarkably increase expression of hepatic LCN2. Moreover experimental induced liver fatty models [induced by feeding of fat rich diets (HFD, LDC) or lack of methionine and choline (MCD)] or clinical conditions leading to liver malfunction are associated as well with increased expression of hepatic LCN2. Clinical condition The levels of LCN2 in serum, urine or liver protein extracts can be measured by quantitative ELISA, Western blot analysis and staining of liver sections with antibodies specific for LCN2. In particular, the measurement of LCN2 by ELISA technique is a fast and robust diagnostic option to detect an early increase of LCN2 in patients suffering from fatty liver diseases (NAFLD, NASH, and ASH) in which the liver insult correlates with LCN2 expression. **(Modified after Asimakopoulou and Weiskirchen, 2015)**

4.3 The liver

The liver is a vital organ and the largest gland in the body of any vertebrate. It has an outstanding variety of essential functions in the human body including digestion, metabolism, glycogen storage, blood protein synthesis, hormone production, decomposition of red blood cells and detoxification.

4.3.1 Functions and anatomy of the liver

Liver is the ‘chemical factory’ of the body. As the biggest metabolic organ and largest gland (secretes bile) in the body it fulfils essential functions in digestion via the metabolism of fats, proteins and carbohydrates (fatty acid synthesis, amino acid breakdown, glycogen storage). Moreover, liver participates in detoxification of excessive amounts of alcohol and drugs. Other important functions of the liver is the embryonic haematopoiesis, the formation of cellular blood components (a procedure taken up by the bone marrow before birth) and the production of blood clotting factors and proteins (albumin). In the liver, blood passes through spaces called sinusoids (low pressure vascular channels) where bacteria, dead or foreign matters are removed by phagocytosis (from the Kupffer cells) giving liver a main role in immunology. Additionally, this ‘chemical factory’ of the body can process certain hormones (thyroid and steroid hormones) while

it serves as a storage for vitamins (A, D, K, E and B_{12}) and minerals [Löffler et al., 1998; Faller et al., 2004].

The liver is found in the upper right-hand portion of the abdominal cavity. It lies beneath the diaphragm and on top of the stomach and intestines, towards the right kidney. The liver has a red-brown colour. This multifunctional organ with roles in metabolism and digestion has an unusual dual-blood supply. The two distinct sources of blood are: a) the hepatic artery from where oxygenated blood flows in every minute and b) the hepatic portal vein where from, nutrients absorbed by the intestine, flow in the liver. The liver consists of four lobes, the right and left lobe as the main larger lobes and the smaller caudate and quadrate lobe. Every lobe is made up of thousands lobules. Every lobule is connected to small ducts that connect to bigger ones to finally form the main hepatic duct which transports the bile produced in the gallbladder and small intestine (duodenum) by liver cells.

The liver in order to carry out all its functions it has different cell types, with different responsibilities, as shown in Figure 4-iv. Parenchymal and non-parenchymal cells reside inside or outside of the sinusoid, which is the space in liver where the blood flows through, instead of capillaries. The hepatocytes are parenchymal cells that constitute 70-80% of the hepatic mass [Löffler et al., 1998]. Hepatocytes are cuboidal, epithelial cells where most of the metabolic procedures storage, digestion, bile production) take place. They are responsible for protein synthesis (albumin, lipoprotein, prothrombin,) for fatty acid synthesis and roles in lipid metabolism and the inflammation procedure. Other parenchymal cells are the cholangiocytes that are responsible for the composition and release of the bile [Tietz et al., 2006]. The non-parenchymal cells compose 30-40% of the total liver cells. The sinusoidal endothelial cells, Kupffer cells, co-live with the hepatocytes in the sinusoid, separated from each other by the space of Disse. The Kupffer cells are lined onto the sinusoidal wall and they are an immune response tool. They serve as macrophages that are in contact with the blood flow breaking down old, red blood cells and foreign molecules [Pocock et al., 2006]. Externally to the sinusoid there are the non-parenchymal cells hepatic stellate cells. They are also called perisinusoidal cells as they line in the space of Disse (perisinusoidal space) attached to the hepatocytes [Kmieć et al., 2001]. These cells store fat and vitamin A and they are the main cells for fibrosis events as responsible for synthesis of collagen and extracellular matrix [Benyon et al., 2000; Löffler et al., 1998].

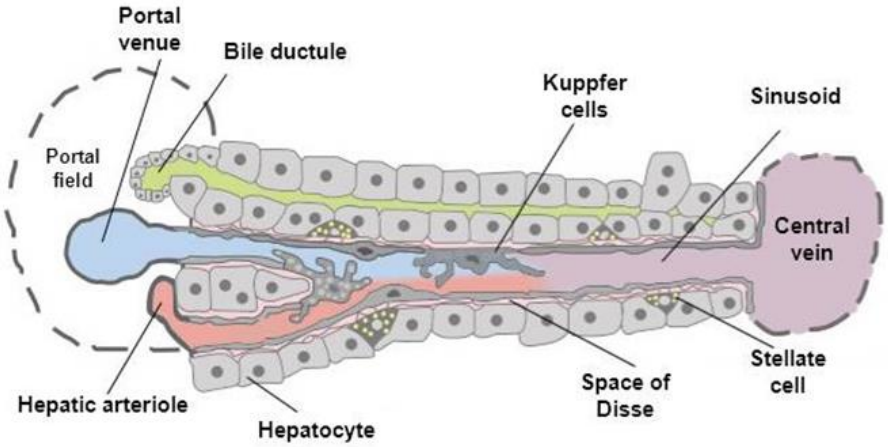


Figure 4-iv: The structure of the hepatic lobule. Microscopically, the liver consists of many hepatic plates composed of hepatocytes. The plates of each lobule usually are organized around a central venule which is the actual connection to the hepatic vein. Each hepatic lobule has oxygenated blood running in through the hepatic artery branches, while branches of the hepatic portal vein peripherally bring in nutrients absorbed by the stomach and intestine. Between the hepatic plates there are hepatic sinusoids that carry blood from the hepatic artery and portal venule to the central vein. **(Modified figure taken from Frevert et al., 2005).**

4.3.2 Hepatocytes in fatty liver disease

Hepatocytes are key cells for many procedures such as, regulating energy balances, protein synthesis and storage, metabolism of carbohydrates, metabolism of fats with the formation and secretion of bile, synthesis of cholesterol and phospholipids and conversion or detoxification of exo- and endogenous for the liver substances.

Moreover hepatocytes has become the last years the aim of attractions for studies based on metabolism of fats and hepatic injury models. The liver is the number one organ in general metabolism. Endogenous and exogenous compounds are taken up by hepatocytes and modified them in other forms maintaining the homeostasis of the liver. The liver is the main organ, where carbohydrates and proteins are converted into fatty acids and triglycerides that are later exported and stored in adipose tissue. Hepatocytes are responsible for fatty acid uptakes and storage of lipids and triglycerides. Another critical function of hepatocytes is to synthesize and secrete lipoproteins such as very low density lipoproteins (VLDL) [Bouma et al., 1988]. The participation of the hepatocytes in all this paths has set it as useful tool to represent liver behaviour to study cases of inflammation and steatosis (lipid accumulation) models such as chronic or acute liver damage and fatty liver diseases. In examples of laboratory induced acute and chronic hepatic damage hepatocytes has been representative of liver damage and inflammation [Borkham-Kamphorst et al., 2011; Semba et al., 2013; Zhao et al., 2009]. In models of fatty liver disease such as NASH where inflammation follows after steatosis hepatocytes tend to give the most answers in the question of fatty acid uptake, inflammatory markers regulation, oxidative stress, lipid

metabolism and in general liver homeostasis [Csak et al., 2011; Zhao et al., 2009; Liu et al., 2011]. Except all the above significant functions of the hepatocytes, another hint that favoured this study is that, experimental liver injury induces rapidly a sustained LCN2 production by injured hepatocytes [Borkham-Kamphorst et al., 2011].

4.4 NAFLD-NASH

Fat accumulation in the liver is an abnormal condition that has raised multiple questions from the aetiologies to the progression process and the possible restoration mechanisms. FLD describes a reversible situation in which the liver presents either bland fat accumulation (steatosis) or fat accumulation accompanied with hepatic inflammation (steatohepatitis).

Two most common phenotypes of FLD are the alcoholic fatty liver disease (AFLD) and NAFLD. ALFD is a form of dangerous fat accumulated in the liver that is the result of excessive and chronic consumption of alcohol. Epidemiological studies have shown that AFLD appears in a frequency that is much lower than NAFLD. NAFLD nowadays is known as one of the most common types of chronic liver disease. In the Western countries, it affects up to 30% of the population [Baumeister et al., 2007; Bellentani et al., 2010]. NAFLD is mainly characterized by a generalized hepatic excessive fat accumulation that reaches more than 5% of the total liver weight [Bellentani et al., 2010]. NASH is a progressive form of the NAFLD condition linked to events of lobular inflammation, injury or/and fibrosis occur that follow after steatosis [Larter and Yeh 1998]. The "two-hit" hypothesis proposed by Day et al.,[Day et al., 1998] in relation to the pathogenesis of NAFLD/NASH is widely accepted. According to this hypothesis the first hit involves lipid accumulation in the hepatocytes [Qureshi et al., 2007; Seki et al., 2002] making the liver sensitive to factors (environmental and genetic) which will cause the second hit that will cause hepatic injury, inflammation and fibrosis. NASH may progress to advanced stages of hepatic fibrosis and cirrhosis, and when liver failure occurs it can cause death.

4.4.1 Diagnosis of NAFLD

Up to now, despite the high prevalence of NAFLD in the general population, no clear common etiology has been suggested. Moreover, so far the only reliable method in diagnosis NAFLD with high sensitivity is the histological examination of liver tissue obtained by the invasive procedure of a needle biopsy [Fierbinteanu- Braticevici et al., 2010]. Through the last years, alternative non-invasive methods in diagnosis that are less risky for the health of and minor painful for the patient have been proposed for the diagnosis of FLD. So far the mostly used biomarker is ALT which is most often increased in patients suffering from FLD but still not globally accepted as a reliable diagnostic marker for this disease [Barr et al., 2010; Mayers 2009].

4.4.2 NASH models and MCD diet

Nowadays, several NASH animal models have been developed. These appear promising for Researchers who investigate the mechanism of the transition from simple steatosis in NAFLD to the inflammatory and progressive injury condition of steatohepatitis in NASH. Some genetic models such as knock out mice for acyl-CoA oxidase-ACOX (responsible for the 1st step of peroxisomal b-oxidation of long chain fatty acids) or null mice for methionine adenosyltransferase-MATO (involved in the synthesis of Phosphatidylcholine which is required for hepatic triglycerides as VLDL) and mice lacking either leptin or the leptin receptor, develop severe steatosis. However, all these models can not represent NASH 100% as they fail in causing one or more metabolic abnormalities related with NASH such as inflammation, continuous steatosis (they become steatosis resistant), insulin resistance, obesity or hyperglycaemia. Moreover there are the nutrition NAFLD/NASH models such as the widely used HFD and MCD. HFD is broadly used over-nutritional model for rodents in research. HFD given to mice for more than 10 weeks caused steatosis however HFD had to be administrated for more than 50 weeks to develop histological steatohepatitis [Ito et al., 2007]. The long feeding periods set it as not practical for NASH investigation. MCD is a diet better established in rodents for inducing NASH. The use of MCD diet induces rapidly steatohepatitis in rodents. As mentioned above for the MATO-null mice the luck of methionine and phosphatidylo-choline synthesis leads to impaired VLDL secretion and impaired mitochondrial β-oxidation [Yao et al., 1988; Anstee et al., 2006; Krahmer et al., 2011] The administration of the MCD diet leads to triglyceride accumulation which causes steatosis in rodents in just a few days while three weeks after MCD administration steatohepatitis has been established with increased ALT levels [De la Pena et al., 2005; Ip et al., 2004].

4.4.3 The mouse as experimental animal in NASH

The use of mice in the elucidating of NASH has been valuable. Animal models of NAFLD/NASH provide critical information either in investigating the pathogenesis of NAFLD/NASH, but also for examining the therapeutic effects of treating agents. The animal models developed to research NAFLD/NASH need to reflect both the histopathology and pathophysiology of the human NAFLD/NASH. The mice models developed so far have been more representing in total more the human conditions than other models. Till now no animal model has reflected 100% the human NASH symptoms, however, the mice models of NAFLD have provided phenotypically consistent tools to estimate the NAFLD/NASH pathogenesis.

4.4.4 Aim of the study

The aim of this study was to analyse the role of LCN2 in liver homeostasis after a nutritional model of NASH in mice. NASH is widely known to disturb liver homeostasis by inducing fat formation and liver damage. Specifically this study focused on the function of LCN2 in the metabolism of the lipids that accumulated after the diet administration and the role of LCN2 in the inflammation induced by the development of NASH. Mice WT and *Lcn2*$^{-/-}$ developed NASH after 4 weeks of a MCD diet. *In vitro* experimentation to support the *in vivo* findings was performed on hepatocytes, from both WT and *Lcn2*$^{-/-}$ mice, fed on normal chow diet. In both *in vivo* and *in vitro* experiments markers of lipid metabolism and inflammation were analysed.

5 Experimental Methods

The composition of all the solutions used in the experimental methods, are mentioned in alphabetic order in section **10.2** *Solutions and buffers* in the Appendix in the end of the dissertation.

5.1 Animal model

Male mice of C57BL/6 genetic background were housed (4-5 mice per cage) in an animal facility maintained at a constant temperature of 20 °C, a relative humidity of 50%, and with a 12-hr on/off light cycle. The animals had free access to mouse chow and drinking water, supplemented with 1% glucose. WT mice (n= 14) and previously generated *Lcn2*$^{-/-}$ mice [Berger et al., 2006] (n= 12) were fed ad libitum (n= 4-8/group), for 4 weeks on a normal diet of standard mouse chow containing methionine and choline, or a MCD diet (MP Biomedicals) to induce non-alcoholic steatosis. Body weight was monitored weekly. Food intake was assessed twice a week by subtracting the amount of chow remaining in a cage from the amount of chow supplied at the start of a given period, and dividing that number by the number of mice in the cage. All animals used in this study received human care, and all animal protocols were in full compliance with the guidelines for animal care approved by the German legislation on protection of animals and approved by the government of the state North Rhine-Westphalia.

5.2 High Fat Diet animal model

As an alternative induction of steatosis, C57BL/6 WT mice at the age of 8 weeks were treated in the same as above animal facilities with unlimited access to drinking water and they were fed a HFD for 16 weeks (Research Diet Services BV) as published before [de Wit et al., 2008]. As control, mice were fed standard chow diet (SSNIFF).

5.3 Blood sampling, serum analysis

Blood sampling, for baseline hematological analyses and liver function tests, was carried out under isoflurane anesthesia before the animals were sacrificed. Blood samples (400-800 µl) were obtained from the Caudal Vena Cava using 27x3/4 G needles and standard 1 mL plastic syringes (Beckman Dickinson) washed with EDTA (100 mM pH 8.0) to avoid immediate blood clotting in syringe. The blood was placed in Microvette CB 100/200 capillary blood collection tubes for serum test (Starstedt). The blood samples were let undisturbed at room temperature (RT) for the blood to clot at 4^{o}C overnight. After clotting the clot was removed by centrifuging at 3,000 *g* for 10 min in a refrigerated centrifuge. The serum (supernatant) was transferred in new sterile Eppendorf tubes and the serum was then analyzed for aspartate transaminase (AST), ALT, total protein, total bilirubin, glucose, triglycerides, and total cholesterol using standard biochemical assays.

5.4 Liver steatosis and inflammation scoring

Mice were sacrificed under isoflurane (Forene®) anaesthesia (Abbott), and whole livers were resected. A part of the liver was fixed in 4% buffered paraformaldehyde (PFA) or Methacarn for 24 hrs and afterwards embedded in paraffin while a second part was snap frozen in liquid nitrogen after it was covered with Tissue TEK OCT solution (Sakura) and kept at -80 ^{o}C. The embedded in paraffin and also snap frozen tissues were sliced into 5 μm standard sections. To evaluate steatosis in liver, frozen cryosections were stained with the lipophilic stain Oil Red O [Koopman et al., 2001] following standard procedures (*see section: Oil Red O staining of neutral lipids on liver sections*). For steatosis and further histological evaluation paraffin embedded standard liver sections were stained with either Haematoxylin and Eosin (H&E) or Sirius Red solution (Sigma-Aldrich) using standard procedures. H&E is one of the principal stains in histology. Hematoxylin is a dark blue stain that binds negatively charged substances such as DNA/RNA. On the other hand Eosin is a red or pink stain that binds to positively charged substances such as amino acids-proteins and intracellular membranes. Moreover, Sirius red collagen stain is a method used for collagen determination with collagen stained red in a pale yellow background. Based on the Oil red O and H&E-stained sections, histological scoring of steatosis and inflammation was performed according to guidelines used in the scoring of nonalcoholic fatty liver disease in humans [Kleiner et al., 2005]. In this system, steatosis is gradually scored as follows: grade 0 = steatosis <5%, grade 1 = steatosis 5%-33%, grade 2 = steatosis >33%-66%, and grade 3 = steatosis >66%. According to the same guidelines, for lobular inflammation: grade 0 = no foci, grade 1 = < 2 foci per 200x field, grade 2 = 2-4 foci per 200x field, and grade 3= > 4 foci per 200x field. Moreover Sirius Red-stained sections were analyzed to determine collagen levels as a measure of fibrosis. Stained tissues were examined using a mono and color light microscope [Nikon Eclipse E80i (Nikon)] equipped with 10x, 20x and 40x objective lenses.

5.5 Isolation of primary hepatocytes and cell culture

Hepatocytes were isolated from livers of 8-14 week old WT and *Lcn2*$^{-/-}$ male mice using the collagenase method of Seglen [Seglen et al., 1976]. Hepatocytes as non-adherent cells were cultured on collagen-coated 6 well dishes in HepatoZYME-SFM medium (Gibco) supplemented with 1% L-glutamine, 1% penicillin/streptomycin (Lonza) and 200 μg/mL bovine serum albumin (BSA) and incubated at 37 ^{o}C in incubator conditions of 5% CO_2 and 100% humidity. The dishes were coated with 1 mL of 0.05 mg/mL collagen in 0.1% Acetic acid the day before for 1 hr, washed 3x with phosphate-buffered saline (PBS) and kept in RT covered with parafilm membrane. For staining the wells included microscopy glasses previously washed overnight with 25% hydrogen chloride (HCl), washed with sterile dH_2O and stored in 70% ethanol (EtOH) at 4 ^{o}C. Before use, the PBS was discarded and dishes were let to dry under the cell culture hood

for 10-15 min. After treatment (e.g. fatty acid or Rosiglitazone stimulation, infection or transfection; see below), hepatocytes were subjected to RNA or protein extraction as described below. Cells seeded on cover slips were washed 3x with PBS (pH 7.4), fixed with 4% PFA in PBS for 20 min, and kept in 1 mL PBS at 4°C until used in experiments.

5.6 Stimulation with fatty acids or Rosiglitazone

Hepatocytes cultured for 24 hrs on collagenase-coated 6 wells dishes with and without cover slips, as described above, were stimulated by the addition of unsaturated oleic acid or saturated palmitic acid (both from Sigma Aldrich) to final concentrations of 0.5 mM and 1 mM. When both fatty acids were used simultaneously for a combination treatment, the final total concentrations of unsaturated oleic acid and saturated palmitic acid together were 1 mM and 2 mM. Control hepatocyte cultures were incubated in standard medium or in medium containing the vehicle in which the fatty acids were emulsed. As an agonist of PPAR-γ, Rosiglitazone was chosen. For stimulation, the hepatocytes were incubated for 24 hrs with 10 µM Rosiglitazone (Abcam) and the control ones with vehicle (0.1% DMSO).

5.7 Adenoviral vector preparation

For construction of the adenoviral vector expressing murine LCN2, pCMV-SPORT6-mLCN2 was digested with *SalI* and *HindIII* and the resulting ~0.8-kbp fragment was cloned into the adenoviral shuttle vector pShuttleCMV (Stratagene). The integrity of the resulting vector, pShuttle-CMV-mLCN2, was confirmed by restriction digestion and sequence analysis. The pShuttle-CMV-mLCN2 was linearized with *PmeI*, dephosphorylated, and transferred into the adenoviral backbone vector pAdEasy-1 (Stratagene) following the manufacturer's procedures. One recombinant clone, designated AdEasy-CMV-mLCN2, was validated by restriction digestion and sequence analysis. For generation of infectious adenoviral particles, AdEasy-CMV-mLCN2 was linearized with *PacI* and transfected into 293A cells following the manufacturer's procedures. The resulting adenoviral particles, designated Ad-CMV-mLCN2, were isolated using the Adeno-X-Maxi purification kit (Clontech) following the manufacturer's protocol. Viral particles were amplified by repeated infection of 293A cells, purified by CsCl gradient centrifugation, and desalted on Centri•Pure P50 gel filtration columns (Emp Biotech.). Final viral particle titers were determined by photometric analysis. The luciferase-based vector AdEasy-CMV-Luc was employed as a control [Borkham-Kamphorst et al., 2014].

5.8 Infection of primary hepatocytes

For adenoviral infections, hepatocytes (4 x 10^5 cells/well) were seeded on collagenase-coated cover slips in 6-well plates in HepatoZYME SFM medium supplemented with 2 mM L-glutamine, 1% penicillin/streptomycin, 50 µg/mL gentamycin, and 1 mg/mL BSA. The next day, cells were infected by incubation for 4.5 hrs with 1 x 10^{10} viral particles (Ad-CMV-mLCN2 or Ad-CMV-Luc). After the addition of fresh medium, infected cells were incubated for another 48 hrs prior to use in experiments. Normal uninfected hepatocyte cultures were always examined in parallel with infected hepatocytes as a control. If adenoviral infections were performed for the purpose of protein extract preparation, 1.2 x 10^6 hepatocytes / well were plated in 6-well plates and infected in 2 mL medium including 2 x 10^9 viral particles / mL.

5.9 Plasmid DNA preparation (small prep)

The expression constructs pCMV-SPORT6-mLCN2 (encoding full-length murine LCN2; IMAGp998L208764Q) and pCMV-SPORT6-mPLIN5 (encoding full-length murine PLIN5; IRAVp968B0772D) used in transfection experiments (see below) were both obtained from ImaGenes GmbH (Source BioScience LifeSciences). A small scale plasmid DNA preparation was applied to prove the identity of the cloned DNA. In the tube containing the clones with the ordered construct 200 µl of LB medium was added, mixed and then transferred in a new sterile tube (clone stock kept at 4 ^oC). Then dilutions were made in Eppedorf tubes with LB medium of 1:10^3, 1:10^5, 1:10^7 and 1:10^9 ratio and vortexed well. Afterwards 20 µl of each dilution was applied to separate petri dishes containing LB-agar and ampicillin. With a sterile glass pen passed above a Bunsen burner, the cells were applied evenly in the petri dishes. The dishes were thereafter placed in incubator at 37 ^oC overnight. The next day, from the petri dish area that single colonies were easier observed, a single bacterial colony was inoculated into 3 mL LB medium containing the appropriate antibiotic in a 15-mL tube and incubated overnight at 37°C under vigorous agitation. Then 1.5 mL of bacterial culture was transferred into a microfuge tube and centrifuged at 12000 *g* for 30 sec. The medium was removed by aspiration and the bacterial pellet was resuspended in 100 µl of ice cold Solution I under vigorous vortexing, and straight after 200 µl of Solution II (freshly prepared) were added, mixed, incubated for 2 min on ice and neutralized with 150 µl of ice cold Solution III, vortex and centrifugation followed at 12000 *g* for 5 min. The supernatant was transferred to a new 1.5 mL tube and 500 µl of phenol and chloroform ($CHCl_3$) (1:1) was added, then vortexed vigorously for 2 min to remove the contaminating proteins, and centrifuged for 5 min. Then the supernatant was transferred to a new tube and the DNA was precipitated with 1 mL of absolute EtOH for 2 min at RT, followed by centrifugation for 10 min. The pellet was washed with cold 70% ethanol and spinned down. The supernatant was removed and air dried. The pellet was dissolved in 20 µl TE. For restriction

analysis with restriction enzymes (*HindIII and EcorI*), 3 μl of 1 μg DNA was added to 7 μl of restriction mix (1 μl restriction buffer, 1 μl RNAse, 3 Units restriction enzyme, and TE until final total volume 7 μl). After 1 hr of incubation at 37 °C the samples were subjected to electrophoresis in an agarose gel to prove the presence of expected sizes from the known sites of the vectors including the plasmid plus the purity of the product. After the first plasmid preparation and purification the plasmids were sent for sequencing to prove the presence of the plasmid of interest before further experimentation. The sequencing was performed by Eurofin MWG Genomics with 300 ng/μl sample.

5.10 Plasmid preparation (large prep)

On the first day, the plasmid amplification was performed with placing a single colony from the overnight agar dish culture into a 250 mL of LB medium containing the appropriate antibiotic 250 μl ampicillin (final conc. 100 mg/mL) in a loosely capped 1L flask. The flask culture was incubated overnight at 37 °C (12 - 16hr) with vigorous shaking, 200 - 250 rpm. The day after, the amplified cells were harvested. 200 - 250 mL of the culture were poured into a GSA bottle. Centrifugation followed for 15 min at 3000 rpm in a JA13-Rotor at 4 °C. The upper phase was discarded and the pellet was dried with inversing the bottle. Then, the pellet was resuspended with 100 mL STE buffer and re-centrifuged again for 15 min at 3000 rpm in a JA13-Rotor at 4°C. In the next steps the alkaline lysis was performed. The supernatant was discarded and 10 mL Solution I were added to resuspend well the precipitate. Then 1mL of Lysozyme – Solution (final conc. 10 mg/mL) was added and let on ice for 10 min incubation. 20 mL Solution II were added, mixed and let at RT for 10 more min. Next 15 mL Solution III were added and shaked vigorously till there were no longer two distinguishable liquid phases. The bottle was incubated on ice for 10 min. A white precipitate was formed. Centrifugation for 15 min at 4 °C and 6000 rpm followed. The supernatant was filtered through bandages while transferred in a new 250 mL GSA bottle.

In the new bottle 25 mL Isopropanol were added, mixed well and let for 10min in RT (isopropanol precipitation). The nucleic acids were recovered by centrifugation at 5000 rpm for 15 min at RT in a Sorval GS3 or equivalent rotor. The supernatant was discarded and the bottle was inverted to let the Isopropanol to evaporate for a few seconds. The pellet and walls were washed with 70% EtOH at RT (3-5mL).The EtOH was drained off by centrifugation for 5 min 10000 rpm. The supernatant was removed extensively with a pipette, and the tube was then dried by inverting it for a few min in RT. Then 2 mL TE (pH 8.0) were added and mixed well with a pipette to dissolve the pellet. Afterwards the purification of the Plasmid DNA with Polyethylene Glycol (PEG) followed with transferring the dissolved, in TE pellet, in a new polypropylene, 14 mL tubes and adding 2 mL of 5 M LiCl. It was mixed well and centrifuged for 10 min, at

4 °C and 10000 rpm. The supernatant was poured in a new 14 mL tube containing 6 mL of isopropanol and then mixed well (isopropanol precipitation). After 10 min of incubation at RT the solution was centrifuged at 10000 rpm for 10 min at 4 °C. The supernatant was discarded and the pellet was washed RT 70% EtOH (3 – 5 mL). Centrifugation for 5 min 10.000 rpm to drain of the EtOH followed. The supernatant was discarded and the tube was inverted till the EtOH was evaporated. Finally the pellet was solved in 500 µl TE (intense pipetting) and transferred into a 1.5 mL sterile tube. RNAse-A solution 10 mg/mL was prepared and 20 µl were added in the tube. The tube was let at 37 °C for 30 - 40 min. Afterwards 520 µl of 1.6M NaCl/13% PEG solution were added, short vortex and centrifugation for 10min at 4°C and 15000 rpm followed. The supernatant was removed carefully with a pipette and 400 µl of TE pH 8.0 were added. The tube was let at 37 °C for 30 min to 1 hr until the pellet was dissolved. As soon as the pellet was dissolved 400 µl Phenol were added and vortexed vigorously for 1 minute for the two phases to mix well. Then centrifugation for 5 min at 15.000 rpm followed. The upper phase was collected and transferred in a new 1.5 mL tube with 200 µl of phenol and 200 µl of $CHCl_3$ and vortexed vigorously for 1 min. Another centrifugation in RT for 5 min and 15.000 rpm followed. The upper phase was collected and transferred in a new tube containing 400 µl of $CHCl_3$ and vortexed for 1 min. Centrifuged at RT for 5 min and 15.000 rpm followed and the upper phase was transferred in a tube again with 100 µl of 10 M ammonium acetate and 1 mL of absolute ethanol. After incubation for 10 min at RT, centrifugation at 4 °C for 5 min in 15000 rpm followed. The supernatant was carefully removed with a pipette and the pellet was then washed with 200 µl cold 70% EtOH and centrifuged at 4 °C for 5 min and 15000 rpm. The ethanol was discarded and 500 µl TE, pH 8.0 were added. The plasmid was let at 37 °C on a thermomixer until the pellet was dissolved (30 min – 1 hr). Meanwhile during this time vortex and pipetting helped the dissolving procedure. Finally when the pellet was completely dissolved with a Photometer and a clean glass cuvette the DNA was quantified. For the DNA quantification 2 µl sample were diluted in 998 µl dH_2O (1:500 dilution) and added it in the glass cuvette to be measured, with water as control, in CARY 50 Scan UV Visible Spectrophotometer (Varian). The plasmid was then stored at -20 °C.

5.11 Rubidium competent cells

An overnight 5 mL (LB medium with no antibiotics) culture of the desired strain XL1-Blue bacteria was prepared. The next day 1 mL of the overnight culture was added to a flask with 100 mL YT medium and let grow with shaking at 225 rpm at 37 °C till they reach OD_{600} = 0.5 (grow duration 2 - 4 hrs). Every hr the optical density (OD) of 1 mL of the culture was measured in the spectrophotometer. After reaching the desired OD, the culture was transferred into two 50 mL conical falcons and chill on ice for 20 min being careful not to contaminate the caps, and after spinning down the cells at 4°C at 3000 rpm for 10 min. From then on, every step was

performed on ice so that the pores that would be created on the bacteria would not close. The supernatant was discarded and each pellet was resuspended in 25 mL of TFB I (50 mL/100 mL culture) gently by hand and incubated on a shaker on ice for 10-20 min. Afterwards the cells were spinned again at 4 °C, 3000 rpm for 10 min and the supernatant was discarded. Each pellet was gently resuspended in 2 mL of TFB II (4 mL/100 mL culture) and incubated on ice for 30 min (incubation on ice could be skipped if the aliquots were made quickly to be placed in -80 °C). Aliquots of 200 µl competent bacteria were made and frozen at -80 °C in autoclaved labelled cryotubes.

5.12 Transformation of competent cells

A vial of competent cells (XL1-Blue) was thawed on ice. After addition of 100 ng plasmid DNA and tapped smoothly .The vial was then incubated for 30 min on ice. Straight after, the tube was heated at 42°C for 2 min (Heat shock). Then immediately the tube was transferred on ice for 5 min. LB medium, 600 µl to 1 mL (without antibiotic) was added and briefly mixed. The samples were incubated at 37 ^{o}C and 225 rpm for 1 hr. Afterwards dilutions of 1:1, 1:10, 1:100 and 1:1000 were made and 20 – 100 µl were added in agar plates containing Ampicillin (50 mg/mL). The cells were spread with a sterile glass stick to an even surface. Finally the inverted dishes were incubated overnight at 37 °C incubator.

5.13 Transfection of primary hepatocytes

For transfections, hepatocytes (4 x 10^5 cells/well) were seeded on collagenase-coated 6-well plates in 2 mL HepatoZYME SFM (Life technologies) supplemented with 2 mM L-glutamine and 1% penicillin/streptomycin. One day prior to transfection, cells were transferred to medium without antibiotics and allowed to reach 70-80% confluence. Cells were transfected by the addition of 2 µg DNA plus 4 µl Lipofectamine® 2000 transfection reagent (Life technologies) in OptiMEM medium (Life technologies). At 6 - 8 hrs post-transfection, the medium was exchanged for standard HepatoZYME medium containing antibiotic and the cells were incubated overnight at 37 °C before harvesting.

5.14 RNA isolation of primary hepatocytes

For isolation and purification of total RNA from hepatocytes the PureLink RNA Mini kit system (Life Technologies) was used, according to the manufacturer's instructions. In summary, the cells were washed 3x with ice cold PBS and 150 µl of buffer containing 1% (v/v) β-Mercaptoethanol were added in each well. Cells were scraped off using RNase free tissue cell rubber scrapers. Cells were then homogenized using 27x3/4 G needles and standard 1-mL plastic syringes (Becton Dickinson). Then the manufacturer's instructions of the Purelink RNA Mini kit

system were followed. The RNA was finally eluted in 30 mL RNase free dH_2O. The concentration of the total RNA was measured and the RNA was stored at -80 °C.

5.15 RNA isolation from liver sections

The liver tissue as soon as it was extracted was placed in 1.5 mL tube with 1 mL of QiaZol Lysis Reagent (Qiazen) and stored in -80 ^{o}C. For the RNA extraction the sample was thawed on ice. The thawed sample was emptied in a sterile Polystyrene tube 13 mL (Sarstedt) where it was homogenized for 30 sec with Dispersing drive Ultra Turrax T 25 basic, and then poured back in the initial 1.5 mL tube. The sample was then incubated in RT for 5 min and then 200 μl of Chloroform were added in the sample. Slight-shake followed for 15 sec (inversions of tubes). After 3 min incubation in RT the sample was centrifuged for 15 min at 4^{o}C and 12000 *g*. Without disturbing the middle white phase the upper phase was transferred in a new sterile 1.5 tube. Then isopropanol of the same volume with the upper phase (1:1) was added and after vortex and 10 min incubation in RT, centrifugation at 4 ^{o}C and 12000 *g* for 10 min followed. The supernatant was carefully discarded without disturbing the pellet. Then 1 mL 75% EtOH was added and after vortexing the sample was centrifuged at 4^{o}C and 7000 *g* for 5 min. After the centrifugation the supernatant was carefully discarded and the pellet was let to dry under the hood for 30 min to 1 hr. When the pellet was dried 100 - 200 μl of RNase free water from the PureLink RNA mini kit (Life Technologies) was added and incubated at RT for 30 min or on ice at 4 ^{o}C for the pellet to dissolve.

After the RNA quantification followed and 100 μg of the sample was transferred in new sterile 1.5 mL tubes (the rest sample was placed in -80^{o}C for later use). In the tube containing the sample and RNase free water (total volume 87.5 μl) 12.5 μl MIX 1 (1.25 μl 10 X DNAse buffer, 2.5 μl DNAase and 8.75 μl RNase free water) were added, mixed and incubated for 10 min at RT. Then 357 μl MIX 2 (350 μl lysis buffer and 7 μl DTT 2M) were added and the solution was shaked well. Pure EtOH, 100%, 250 μl was added in the tube and mixed. Then 700 μl of the probe were transferred to the RNA extraction tubes from PureLink RNA mini kit and the tube was then spinned for 30 sec in 12000 *g* at RT. After spin the membranes were transferred in new caps and 500 μl of Wash buffer II were added and spinned for 30 sec in 12000 *g* at RT. The resulting flow-through was discarded and 500 μl of Wash buffer II were re-added and centrifuged for 5 min in 12000 *g* at RT to dry the membrane. The excess liquid was discarded and the membrane was centrifuged under same conditions for 1 min. Then the membranes were transferred in new sterile recovery tubes and 50-100 μl of RNase free water was added in the middle of the membrane and incubated at RT for 1 min. Finally the membranes were centrifuged for 1 min in 12000 *g* at RT and the RNA was then quantified and stored in -20 ^{o}C.

5.16 Complementary DNA (cDNA) synthesis

Purified RNA was quantified and 1 µg samples were reverse –transcribed in a final volume of 25 µl using Superscript II reverse transcriptase and random hexamer primers (all from Life Technologies). The procedure for the cDNA synthesis included adding 1 µg of the RNA sample in a 500 µl reaction tube. Then 16 µl of the first Mix containing 1 µl random primers (250 ng), 1 µl dNTP mix (10 mM each) and sterile dH_2O (14 - $Volume_{RNA}$ µl) were added. The mixture then was heated in the Polymerase chain reaction (PCR) device at 65 ^oC for 5 min and then quickly chilled on ice. After a short spin the second mix containing 4 µl of First strand buffer and 2 µl of Dithiothreitol (DTT) 0.1 M. The samples were incubated in the PCR device at 25 ^oC for 2 min. Finally 1 µl of SuperScript II reverse transcriptase was added and placed back to the PCR device where it was incubated at 42 ^oC for 50 min. Afterwards, the reaction was inactivated at 70^oC for 15 min. Thereafter the samples were stored at 4 ^oC for short period or at -20 ^oC for long term.

5.17 PCR for cDNA synthesis check up

For the verification of successful cDNA synthesis a standard PCR for the house gene Glyceraldehyde 3-phosphate dehydrogenase (GAPDH) was performed. For a 25 µl reaction volume 1 µl cDNA sample (produced by 1 µg RNA) was placed in a 500 µl reaction tube. 24 µl master mix containing, 1 µl forward primer (10 nmol), 1 µl reverse primer (10 nmol), 0.5 µl dNTP mix (10 mM each), 2.5 µl Buffer 10x (without Mg^+), 2 µl Mg^+, 0.25 µl TaqMan polymerase and 16.75 µl sterile dH_2O, were added in the same reaction tube and incubated in the PCR device under a standard PCR program including the initial denaturation at 94°C for 5 min in the first cycle and 30 seconds for every other cycle (30 cycles) which included annealing at 57 °C for 30 sec, and elongation at 72 ^oC for 1 min in all cycles (10 min for the last cycle). After the 30 cycles the temperature reached the preservation temperature of 4 ^oC. In the end the PCR products samples were subjected to electrophoresis in an agarose gel to prove the presence of the amplified product.

5.18 Quantitative real time PCR (qRT-PCR)

For the preparation of the samples for the qRT-PCR 5 µl of cDNA (preserved as 5x diluted) were placed in a 98 well PCR-plate and add 20 µl of the Master mix containing: 6.5 µl sterile dH_2O and 12.5 µl SYBR GreenTM qPCR SuperMix (Life Technologies). The primer pairs for specific mouse mRNAs amplification were designed using the Universal Probe Library tool (Roche) and are listed in Supplementary table 10-i. For amplification of target gene sequences, samples were incubated with all necessary reagents at 50 °C for 2 sec, denatured at 95 °C for 10 min, and amplified in 40 cycles of 95 °C for 15 sec followed by 60 °C for 1 min. All samples were placed and analyzed in double. Relative levels of target mRNA were calculated using the comparative

CT method [Schmittgen et al., 2008] and normalized to the mRNA expression of the housekeeping gene, GAPDH. The final mRNA quantities were expressed as the normalized quantity of target mRNA relative to the normalized quantity of the housekeeping gene mRNA.

5.19 Protein extraction

Total protein, from cultured hepatocytes, or from samples of freshly extracted total liver tissue that had been snap-frozen in liquid nitrogen, was prepared using RipaC buffer containing 20 mM Tris–HCl (pH 7.2), 150 mM NaCl, 2% (v/v) NP-40, 0.1% (w/v) SDS, 0.5% (w/v) sodium deoxycholate and the Complete™-mixture of proteinase inhibitors (Roche). The cell samples were passes 10 x through a 27x3/4 G needle and standard 1-mL plastic syringe (Becton Dickinson). For liver tissue homogenisation with a tissue grind pestle (Kimble & Chase) was initially used. For protein extraction both cells and tissue were sonicated in an UltraSonic processor (Hielscher) 3x for 1 min each time on ice at 100% amplitude. The samples (cells and tissue) homogenised in RipaC were incubated on ice for 30 min and then centrifuged in 10000 rpm and at 4 ^{o}C for 10 min. The protein extract (supernatant) was transferred in new 1.5 mL tubes and stored at -80 ^{o}C.

5.20 Protein quantification (DC assay)

For the protein quantification of cell lysates or extracted tissue the DC protein Assay kit from BIO RAD was used. Protein quantification standards for the standard curve were prepared of final concentrations 0 μg/μl, 0.6 μg/μl, 0.9 μg/μl, 1.2 μg/μl, 1.5 μg/μl, 1.8 μg/μl, 2.1 μg/μl and 2.4 μg/μl with BSA and RipaC buffer. In a 96-well micro-titer plate 5 μl of the sample were added twice in a 96-well plate. Then 25 μl of Reagent A* (20 μl Reagent S and 1 mL Reagent A) were added in every sample and standard and in the end 200 μl of Reagent B from the kit were added on top. Incubation was performed in a dark room for 15 min in a smooth shaker and then the absorbance was measured in Victor X3 - Multimode Plate Reader at 690 nm.

5.21 SDS-PAGE and Western blot analysis

Equal amounts of total protein (20 μg/lane for hepatocyte lysates and 100 μg/lane for whole liver tissue extracts) were mixed with Nu-PAGE™ LDS electrophoresis sample buffer containing DTT 1M, as a reducing agent. Samples were heated at 87 °C for 10 min before fractionation on 4 - 12% Bis-Tris gels in MES (2-(N-morpholino) ethanesulfonic acid) or MOPS (morpholinopropanesulfonic acid) running buffer (both by Roth). Proteins were electroblotted onto a Protran membrane (GE Healthcare), and equal protein loading was confirmed by Ponceau S (Sigma Aldrich) staining.

For Western blotting, membranes were first blocked by incubation in Tris-buffered saline supplemented with 1% Tween20 (TBST) containing 5% (w/v) non-fat milk powder (Roth).

Primary antibodies were diluted in 2.5% (w/v) non-fat milk powder in TBST prior to application to the membrane. Primary antibodies were visualized with anti-mouse-, anti-rabbit anti-rat IgG or anti-goat IgG secondary antibodies (all from Santa Cruz) and the SuperSignal chemiluminescent substrate (Thermo Scientific) under the Lumi imager™ (Roche). All antibodies used in this study are listed in the Supplementary table 10-ii.

5.22 Immunohistochemistry

Liver tissue sections were deparaffinised and rehydrated with xylene and decreasing graded ethanol, whereas antigen retrieval was engendered by heating the sections in 10 mM sodium citrate buffer (pH 6.0) in a microwave for 20 min. Slides were blocked for non-specific binding with 5% FCS (fetal calf serum) made in 1% BSA/PBST (BSA/Phosphate-Buffered Saline supplemented with Tween 20) at RT for 1 hr. Primary antibodies polyclonal rabbit anti-PLIN5 (Novus Biologicals) polyclonal rabbit anti-MPO (Hycult Biotech), and monoclonal rat anti-CD45 (Beckman Dickinson) were applied on the tissues in dilution 1:50 in blocking solution and incubated at 4 °C overnight for the detection of PLIN5, and CD45. An immunoglobulin (IgG) was used as a negative control. The day after, the sections were incubated with biotinylated secondary antibodies (Vector Laboratories), followed by avidin-conjugated peroxidase (Vector Laboratories) and 3.3′-diaminobenzidine substrate (DAKO). The sections were counterstained with haematoxylin and microscopy images were taken at a magnification of 200x and 400x using the Nikon Eclipse 80i microscope (Nikon) equipped with the NIS Elements Vis software (version 3.22.01).

5.23 Immunofluoresence-histochemistry

Liver tissue cryosections were let to thaw and air-dried for 1 hr at RT. The tissues then were fixed by dipping the slides in 4% PFA for 25 min. Then the sections were washed and rehydrated with dipping the slides in PBS 3x 5 min each time. The slides were blocked for non-specific binding with 10% donkey serum in PBS supplemented with 0.3% Triton X at RT for 1 hr. For the detection of Myeloidperoxidase (MPO) in liver tissues of mice fed on MCD diet, primary, polyclonal antibody, rabbit anti-MPO (Hycult Biotech), was applied in dilution 1:100 in antibody dillution solution (1% BSA/PBST) and incubated at 4 °C overnight for the detection of MPO. A tissue section of tonsilitis (a severe case of neutrophil infitration) was used as a positive control, treated as above whereas an IgG was used as a negative control. The primary antibody, polyclonal rabbit anti-Plin5 (Novus Biologicals), was used in dilution 1:50 to detect PLIN5 expression in liver tissue of mice fed on HFD. The day after, the slides were washed 3x with PBS and incubated at RT for 1 hr with Alexa 555-donkey anti-rabbit secondary antibody that had been conjugated to ALEXA Fluor (Life Technologies) and diluted to 1:200 in antibody dilution buffer. The stained slides were washed 3x with PBS and counterstained with 100 ng/mL 4', 6-

diamidino-2-phenylindole (DAPI) (Life Technologies) in PBS, for 10 min at RT to visualize nuclei. Slides were washed twice with PBS and a 3rd wash with dH_2O water. Afterwards they were mounted with PermaFluor aqueous mounting medium (Thermo Scientific) and analyzed under a Nikon Eclipse E80i fluorescence microscope.

5.24 Immunofluorescence in primary hepatocytes

Hepatocytes cultured on collagenase-coated cover slips as described above were fixed for 20 min in 4% PFA. The fixed cells were washed 3x with PBS, permeabilized on ice by the addition of 0.5 mL/well of pre-cooled 0.1% Na-citrate/0.1%TritonX solution, and incubation of 2 min. Permeabilized cells were washed 3x with PBS and blocked by incubation with 0.5 mL 50% FCS/0.5% BSA in PBS for 1 hr at 37 ^{o}C on a shaker. Blocked cells were washed 3x with PBS and incubated with primary antibodies overnight at 4 ^{o}C in a moist dark chamber. Goat anti-human LCN2 or rabbit anti-mouse PLIN5 primary antibodies were diluted 1:50 and 1:100, respectively, in 1% BSA in PBS. Non-specific goat IgG and rabbit IgG were used as negative controls. The next day, slides were washed 3x with PBS and incubated at RT for 1 hr with the appropriate secondary antibodies that had been conjugated to ALEXA Fluor (Life Technologies) and diluted to 1:500 in 1% BSA in PBS. The stained slides were washed 3x with PBS and counterstained with 100 ng/mL DAPI (Life Technologies) in PBS, for 10 min at RT to visualize nuclei. Slides were washed with PBS, mounted with PermaFluor aqueous mounting medium (Thermo Scientific) and examined using a Nikon Eclipse E80i fluorescence microscope.

5.25 Cell quantification

After the immune fluorescence staining of MPO in liver tissue the images were transformed in 8-bit grayscale data. Then the MPO positive cells were quantified with the help of the Image J, a Java-based image processing program developed at the National Institutes of Health [Version 1.49p 28 Feb. 2015].

5.26 Oil Red O staining of neutral lipids on liver sections

Frozen tissue sections were let in RT to thaw and dry for 1 hr. The tissues then were fixed by dipping the slides in 4% PFA for 25 min. Then the sections were washed and rehydrated with dipping the slides in dH_2O water 3x 5 min each time. Then the slides were incubated in working Oil Red O staining solution [Neyzen et al., 2006] at RT for 30 min. Stained slides were repeatedly washed in dH_2O water followed by counterstaining of nuclei (blue colour) with dipping the slides in undiluted DAKO REAL haematoxylin solution (DAKO). Slides were mounted using PermaFluor aqueous mounting medium (Thermo Scientific). Stained slides were examined using a Nikon Eclipse E80i microscope equipped with 10x, 20x and 40x objective lenses.

5.27 Oil Red O staining of neutral lipids on hepatocytes

Cultured hepatocytes were fixed on collagenase-coated slides in 4% PFA for 20 min and the slides were incubated in working Oil Red O staining solution [Neyzen et al., 2006] at RT for 30 min. Stained slides were repeatedly washed in dH_2O water followed by counterstaining of nuclei (blue colour) with 2 mL undiluted DAKO REAL haematoxylin solution (DAKO). Slides were mounted using PermaFluor aqueous mounting medium (Thermo Scientific). Stained slides examined using a Nikon Eclipse E80i microscope

5.28 Nile red staining on primary hepatocytes

An alternative neutral lipid staining method, ultra-pure Nile Red reagent (ENZO Life Sciences) was applied to collagenase-coated slides with fixed hepatocytes using a previously published protocol [Listenberger et al., 2007]. Briefly, Nile red working solution was applied on slides for 10 min at RT in the dark. The slides were afterwards washed with PBS and counterstained for 1 min with DAPI working solution 100 ng/mL in PBS for 10 min. Coverslips were mounted on the glass slides as mentioned before and the cells were examined using a Nikon Eclipse E80i microscope in the green fluorescent channel. The green channel was chosen instead of the red to increase contrast.

5.29 Triglyceride assay

Liver tissue samples were homogenized in 5% (v/v) nonyl phenoxypolyethoxylethanol (NP-40) in water. The homogenized tissue was afterwards heated at 100 ^{o}C and cooled down for 5 min to solubilize all triglycerides (the heating – cool down procedure was repeated twice). The triglycerides were quantified with the use of the Triglyceride Quantification kit, by Abcam according to the manufacturer's instructions and the colorimetric absorbance measurements were taken on the Victor X3 - Multimode Plate Reader at 490 nm.

5.30 Free fatty acid assay

Liver tissue samples were homogenised in 1% Triton X in pure $CHCl_3$ and vacuumed for 3-4 hrs at 50 ^{o}C for the $CHCl_3$ to be removed and the lipids to dry. The free fatty acids were later quantified with the use of the Free Fatty acid Quantification kit, by Abcam according to the manufacturer's instructions and the colorimetric absorbance measurements were taken on the Victor X3 - Multimode Plate Reader at 490 nm.

5.31 Myeloperoxidase (MPO) activity quantification assay

Liver tissue samples were homogenized in 4 volumes of 0.1% (v/v) NP-40 in PBS. The homogenized tissue was afterwards centrifuged at 13000 *g* for 10 min and the supernatant was collected. The MPO activity was quantified with the use of the MPO activity quantification kit,

by Abcam, according to the manufacturer's instructions and the colorimetric absorbance measurements were taken on the Victor X3 - Multimode Plate Reader at 450 nm.

5.32 RNA and DNA quantification

The concentration and purity of RNA was determined by measuring the absorbance at 260 nm using a spectrophotometer. For single stranded RNA, C_{RNA} in mg/mL = OD_{260} x dilution factor x 40. The ratio of pure RNA for OD_{260}nm and OD_{280}nm was between 1.8 and 2.2. The concentration and purity of DNA was determined by measuring the absorbance at 260 nm using a spectrophotometer. The concentration of double stranded DNA C_{DNA} in mg/mL = OD_{260} x dilution factor x 50. The ratio of OD_{260}nm and OD_{280}nm was accepted when between 1.8 and 2.0 [Barbas et al., 2007].

5.33 Statistical analysis

Statistical analyses were performed using the Student's t-test for comparison of individual groups. Results are expressed as the mean ± standard deviation (SD). For *in vitro* experiments, results are the mean ± SD of 3 independent trials each performed in triplicate. For *in vivo* experiments, results are the mean ± SD involving at least 4 animals per group. Probability values of < 0.05 were considered statistically significant. All statistical analyses were performed using Excel Analysis 2010 and Windows XP software.

6 Lipocalin 2 regulates PLIN5 expression and intracellular lipid formation in the liver

The initial aim of this study was to unravel how LCN2 participates in the lipid homeostasis in the liver. To this end it was known that in the liver, LCN2 triggers protective effects following acute or chronic injury, and that its expression is a reliable indicator of liver damage. Additionally, there was the interesting observation from a previous report, that *Lcn2*$^{-/-}$ hepatocytes accumulated lipid droplets after induced liver injury while the WT didn't. However, little is known about LCN2's functions in the homeostasis and metabolism of hepatic lipids or in the development of steatosis.

6.1 Introduction

Lipocalin 2 is a protein mainly associated, with injury and inflammation sites. However, there are studies suggesting that LCN2 has important roles in intracellular lipid metabolism and the maintenance of liver homeostasis [Guo et al., 2010; Borkham-Kamphorst et al., 2011]. Guo et al., showed that LCN2 protein is highly abundant in normal adipose tissues [Guo et al., 2013] and more recently, it was demonstrated that IFN-γ and TNF-α can induce LCN2 secretion by cells within white adipose tissue depots, and that STAT1 and NF-κB can bind directly to the human LCN2 gene promoter in human fat cells [Zhao et al., 2014]. Experimenation with primary hepatocytes of *Lcn2*$^{-/-}$ mice has revealed abnormal lipid droplet accumulation and increased apoptosis [Borkham-Kamphorst et al., 2013]. These observations imply that LCN2 has essential functions in the control of hepatic lipid homeostasis.

A family of proteins associated with lipid droplet formation and triacylglycerol storage [Brasaemle 2007] is the Perilipins. They constitute a highly conserved family of five proteins (PLIN1-PLIN5). Perilipins are also known as PATs, an acronym derived from the first three family members identified: perilipin 1 (PLIN1), adipocyte differentiation-related protein (ADRP or PLIN2), and tail-interacting protein-47 (TIP47or PLIN3) [Greenberg et al., 1991; Heid et al., 1996 and Diaz et al., 1998]. PLIN4 is also known as S3-12, while PLIN5 was originally called oxidative tissue-enriched PAT (OXPAT), or alternatively LSDP5 (lipid storage droplet protein 5) or MLDP (myocardial lipid droplet protein) [Nagase at al., 2001; Wollins et al., 2003; Wollins et al., 2006; Dalen et al., 2007]. Several studies have focused on the essential regulation of the Perilipins in lipid metabolism. In humans and mice, PLIN2 is strongly upregulated during the development of fatty liver and steatosis [Motomura et al., 2006]. *In vitro*, overexpression of PLIN2 promotes the uptake and incorporation of lipids into lipid droplets [Gao et al., 1999; Londos et al., 2005]. Mice fed with a high fat diet (HFD) so that they develop fatty liver show increased PLIN2 expression that depends on activation of PPAR-γ [Motomura et al., 2006]. Conversely, mice

lacking PLIN2 are protected against diet-induced obesity, adipose tissue inflammation, and fatty liver disease [McManaman et al., 2013]. Likewise, expression levels of PLIN3 and PLIN5 are increased in hepatocytes exposed *in vitro* to free fatty acids, suggesting that these two perilipins are also important for hepatic lipid accumulation [Grasseli et al., 2010]. In mouse and human adipocytes, levels of PLIN1 and PLIN4 are tightly correlated to the expression and activation of PPAR-γ, and the promoters of these genes contain PPAR-γ response elements which are well conserved [Dalen et al., 2004]. Taking it all together, the Perilipins appeared to have functions in hepatic lipid accumulation, steatosis and inflammation that could associate with possible functions of LCN2.

To investigate whether LCN2 and the Perilipins cooperate to regulate hepatic lipid accumulation, WT and *Lcn2*$^{-/-}$ mice were fed with a MCD diet as a nutritional model of non-alcoholic steatohepatitis and comparison of the intrahepatic lipid accumulation lipid droplet formation, mitochondrial content, and expression of the perilipin proteins followed. As mentioned above MCD diet is known to induce strong hepatic steatosis in rodents by impaired VLDL secretion due to lack of phosphatidyl-choline synthesis, impaired mitochondrial β-oxidation [Yao et al., 1988, Anstee et al., 2006; Krahmer et al., 2011]. In addition, expression of LCN2 and PLIN5 was analyzed in WT animals that received a high fat diet as an alternative model for hepatic steatosis.

We found that MCD diet accumulated more lipids in the liver of *Lcn2*$^{-/-}$ mice than WT controls, and that the basal expression of the lipid droplet coat protein PLIN-5 was significantly reduced in these animals. Moreover, it's proved in this study that PLIN5 expression is directly linked to the presence of LCN2. As restoration of LCN2 activity in *Lcn2*$^{-/-}$ primary hepatocytes induces strong PLIN5 expression and rescues lipid droplet formation. The presented data indicate that LCN2 is a key regulator of hepatic lipid homeostasis that operates, at least in part, by inducing PLIN5. LCN2 may therefore represent a novel therapeutic drug target for the treatment of liver diseases associated with elevated fat accumulation and steatosis.

6.2 Results

Does LCN2 participate in lipid metabolism in fatty liver disease? Initially in order to test whether LCN2 is involved in disease-associated fat accumulation in the liver and whether it has essential functions in the control of hepatic inflammation and lipid metabolism, WT and *Lcn2*$^{-/-}$ mice were subjected to a MCD diet. The MCD diet contains high sucrose and fat but lacks methionine and choline, an amino-acid and a nutrient critical for hepatic β-oxidation, VLDL production, and the stimulation of hepatic lipogenesis. Prolonged feeding of WT mice on the MCD diet, results in severe hepatic lipid accumulation within a short timeframe [Anstee et al., 2006; Pickens et al., 2010; Pickens et al., 2009]. These conditions lead to, oxidative stress and altered cytokine and adipo-cytokine secretion profiles development that contribute to liver injury characterized by increased ALT levels, hepatic steatosis, lobular inflammation, ballooning degeneration of hepatocytes, and increased PPAR-γ expression [Larter et al., 2008].

Macroscopic appearance of the liver after 4 weeks of MCD or control diet showed a pale color to the whole liver as a result of the MCD diet (Figure 6-iA). MCD has been characterized with sharply decreased caloric intake [Kirsch et al., 2003] so as expected the feeding of WT and *Lcn2*$^{-/-}$ mice on an MCD diet for 4 weeks led to a drastic decrease in body weight in both groups (Figure 6-iB). The mean decrease in body weight did not really differ between MCD-fed WT and MCD-fed *Lcn2*$^{-/-}$ mice.

However the total liver weight and the liver-to-body weight ratio were higher in MCD-*Lcn2*$^{-/-}$ mice than in MCD-WT controls (Figure 6-iC) suggesting a more enlarged fatty liver for the MCD-*Lcn2*$^{-/-}$ mice. It's been shown before in other experimental animals, that MCD administration causes enlargement and a more yellowish color to the liver [Ye et al., 2013].

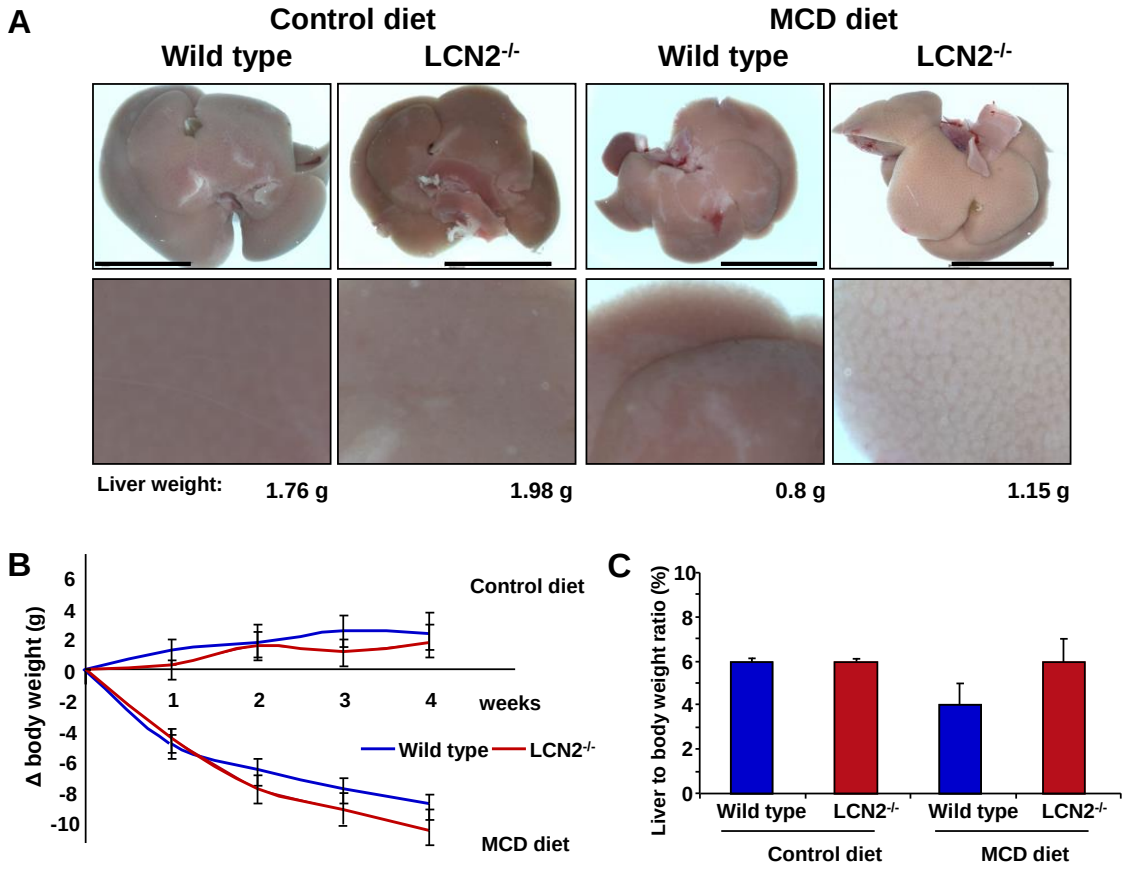


Figure 6-i: MCD diet leads to sharp alterations of the body weight. (A) Macroscopic appearance representative livers from WT and *Lcn2*$^{-/-}$ mice (scale bars: 10mm) after 4 weeks of control and MCD diet. In the lower panel higher magnification of the livers above which denotes a rougher surface and paler color for the MCD treated mice. The bottom line shows the weight in grams of the respective livers on top. (B) Weekly measurements of the changes to the body weight of WT or *Lcn2*$^{-/-}$ mice (n=4-8/group) fed on control or MCD diet for 4 weeks. Results are the mean body weight change in grams (g) relative to the starting body weight. (C) Quantitation of the liver-to-body weight ratios of the mice in (A) Data are the ratio of the mean total liver weight to mean total body weight expressed as a percentage. Although no statistically significant differences between groups were obtained, the data suggest that, unlike control animals, MCD-*Lcn2*$^{-/-}$ mice maintain a constant liver-to-body weight ratio. (**Source: Asimakopoulou et al., 2014).**

Afterwards histological examination of liver sections in WT and *Lcn2*$^{-/-}$ mice and blood biochemical analysis were performed. It was found that, even on a normal diet, *Lcn2*$^{-/-}$ mice exhibited spontaneous mild steatosis (Figure 6-iiA, 6-iiB), decreased total bilirubin, and higher serum concentrations of GPT/ALT and GOT/AST than control animals (Figure 6-iii). After administration of MCD diet, both WT and *Lcn2*$^{-/-}$ mice developed prominent steatosis that was characterized by apparent elevated levels of intrahepatic fat and increased formation of lipid droplets (Figure 6-iiA, 6-iiB).

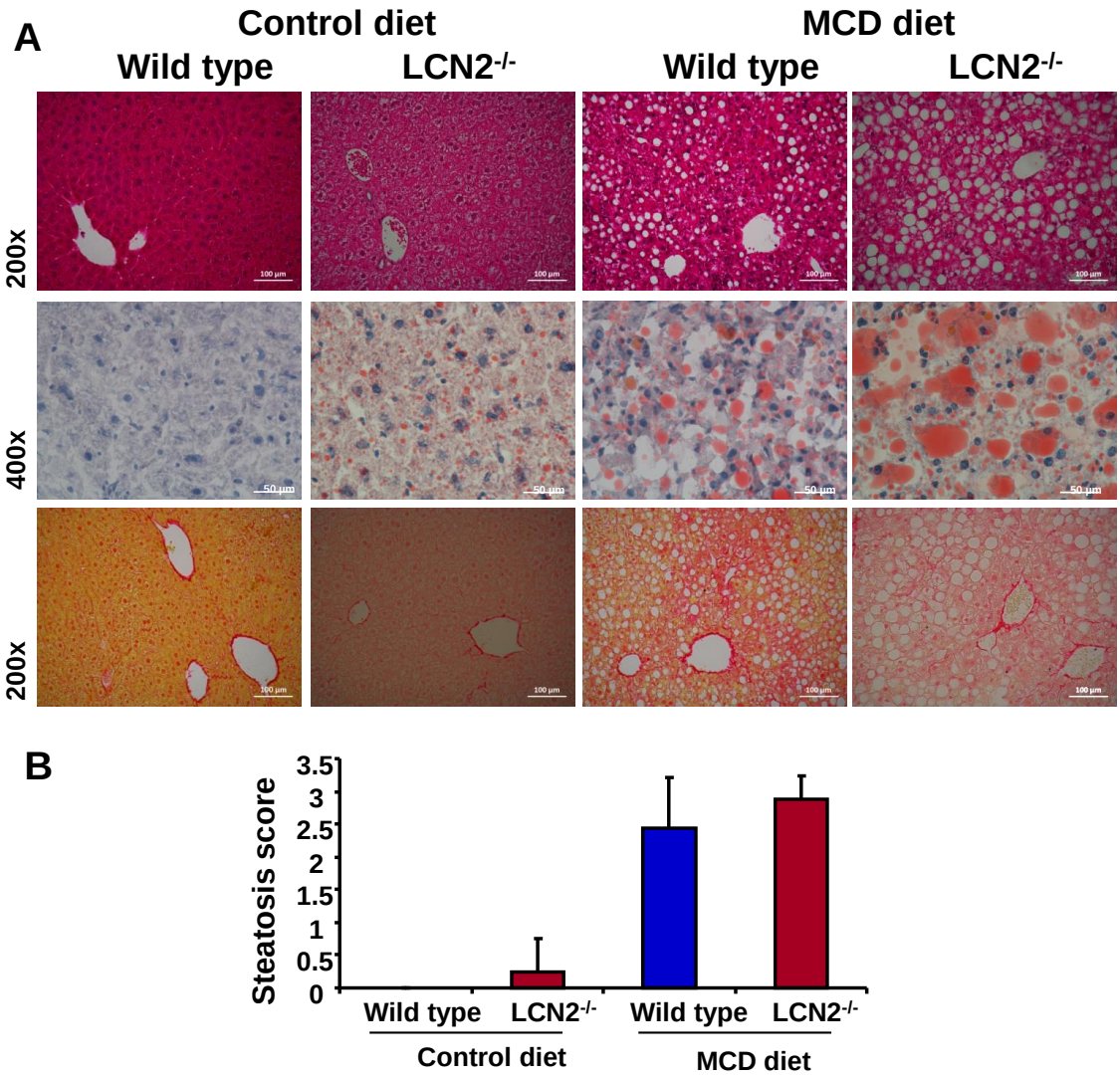


Figure 6-ii: Effects of the MCD diet on livers of WT and *Lcn2*$^{-/-}$ mice. (A) H&E staining (top panels), Oil Red O staining (middle panels), and Sirius Red staining (lower panels) of specimens of the livers in 3.1A. Scale bars: top panels, 100 µm; middle panels, 50 µm; bottom panels, 100 µm. All stainings show the drastic lipid droplet accumulation after the MCD diet. Livers from *Lcn2*$^{-/-}$ mice appear to have slight steatosis even on control diet. Results are representative images taken from individual animals in each group. (B) Scoring of steatosis in liver sections from the mice after 4 weeks of diet. The histological scoring system was adapted from guidelines used in scoring non-alcoholic fatty liver disease in humans [Kleiner et al., 2005]. Results shown are the mean ± SD of WT or *Lcn2*$^{-/-}$ mice (n=4-8/group). **(Source: Asimakopoulou et al., 2014).**

Hepatic fibrosis observed by Sirius red staining was similar in MCD-WT and MCD-*Lcn2*$^{-/-}$ mice (Figure6-iiA). However the MCD-*Lcn2*$^{-/-}$ animals showed greater hepatic damage than controls based on the higher elevations of GPT/ALT and GOT/AST (Figure 6-iii). Enhanced liver malfunction in MCD-*Lcn2*$^{-/-}$ in comparison to the MCD-WT mice was reflected also by the reduced total liver protein and cholesterol (Figure 6-iii). Blood glucose was decreased to a similar

extent in MCD-*Lcn2*$^{-/-}$ and MCD-WT mice, and serum triglycerides were significantly higher in MCD-*Lcn2*$^{-/-}$ mice than in MCD-WT animals (Figure 6-iii).

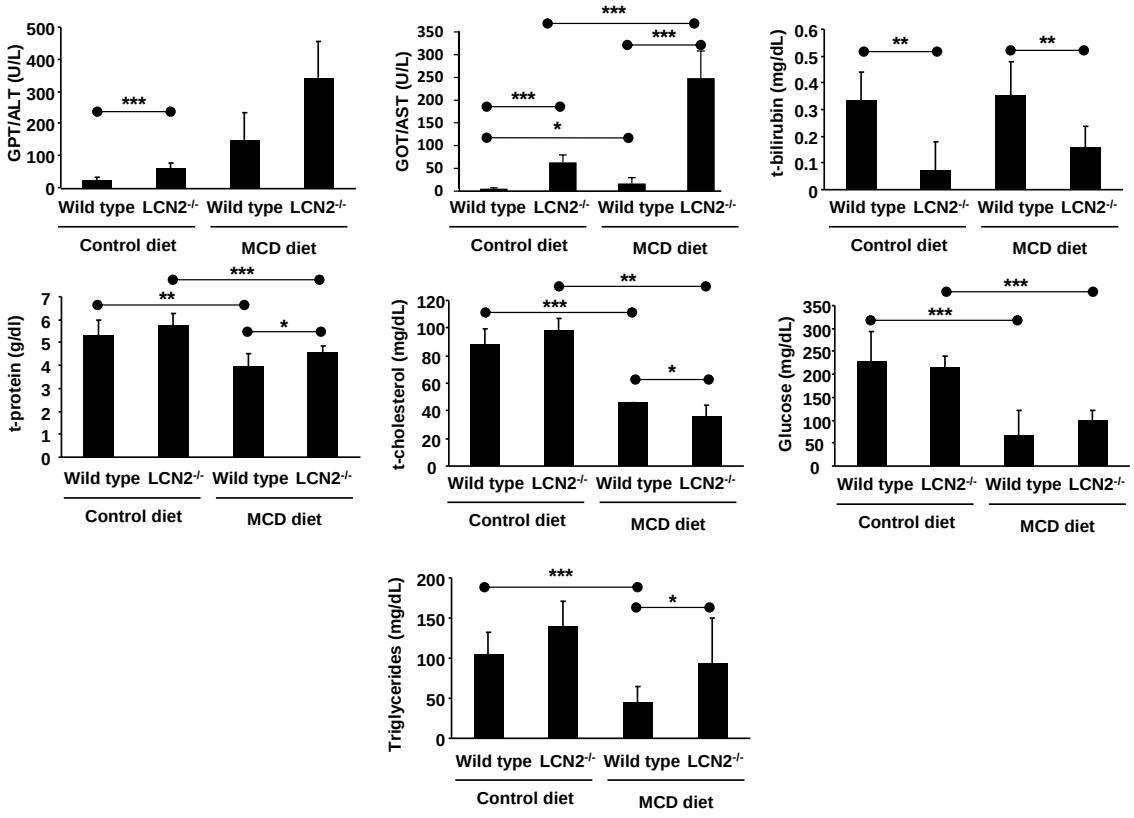


Figure 6-iii: Serum analysis. WT or *Lcn2*$^{-/-}$ mice (n=4-8/group) were fed normal chow or an MCD diet for 4 weeks. Concentrations or activities of the indicated parameters were measured in the serum of sacrificed animals using standard procedures. Results are the mean ± SD. *p ≤ 0.05; **p ≤ 0.01; ***p ≤ 0.001. **(Source: Modified and taken from Asimakopoulou et al., 2014).**

Free fatty acid (FFA) and triglyceride assays were also applied on liver tissue extracts (colorimetric quantification kits, both by Abcam). The results indicate a clear increase of the hepatic FFA levels 2-3 fold after the MCD diet application, as well as total triglyceride levels which were increased 1,5-2 folds in MCD conditions as observed in previous report of induced steatohepatitis [Larter et al., 2008]. Interestingly the *Lcn2*$^{-/-}$ mice, tended to higher levels of FFA and triglycerides than the WT mice not only in MCD diet but also in control diet (Figure 6-iv) suggesting the increased susceptibility of lipid formation in absence of LCN2.

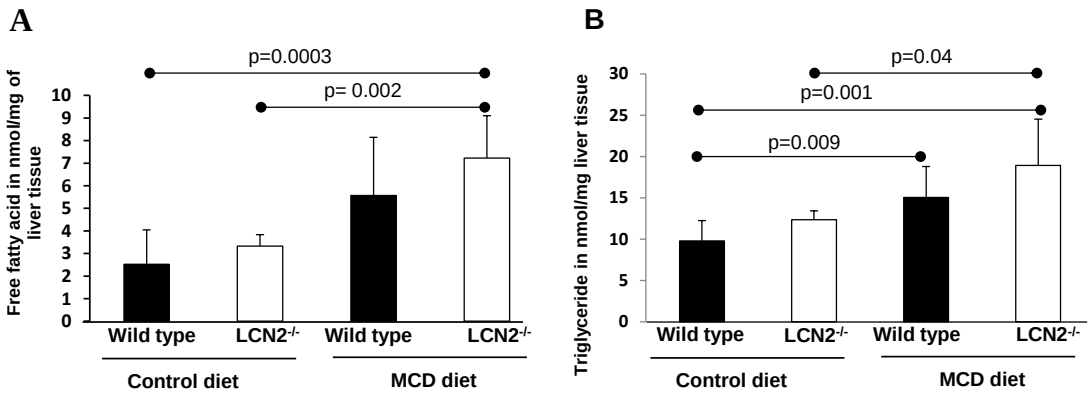


Figure 6-iv: Free fatty acid and triglyceride quantitation. Liver tissue from WT and *Lcn2*$^{-/-}$ mice, after being fed with control or MCD diet for 4 weeks, were homogenised and the Free fatty acid and Triglycerides were quantified. Results are the Results are the mean ± SD, (n=4-8 per group) each analyzed in duplicate.

In total the above data revealed the first confirmation that the MCD diet inflicts greater liver damage in the absence of LCN2.

Does LCN2 correlate with the Perilipins upon MCD diet? After the first hints of LCN2 participation in the liver homeostasis during MCD diet clarification was needed on how LCN2 is correlated to the steatosis development upon MCD diet. As mentioned above the PAT protein family is a group of proteins closely associated with lipid droplet formation, fact that gives a hint of a possible co-operation with the LCN2 within the event of steatosis development during experimental NASH induction. Analysis of the perilipin proteins in total liver extracts revealed a remarkable decrease in the expression of PLIN5 in the absence of LCN2, whether or not the animals had been fed with the MCD diet (Figure 6-vA). In contrast, PLIN2 protein was already increased in livers of *Lcn2*$^{-/-}$ mice on the normal chow diet compared to WT mice. On the MCD diet, WT mice showed by far, greater increase in PLIN2 protein than the *Lcn2*$^{-/-}$ mice did, while PLIN3 protein was strongly expressed in both MCD-WT and MCD-*Lcn2*$^{-/-}$ mice. Most strikingly, MCD-WT mice showed dramatically higher levels of LCN2 than WT mice fed normal chow, consistent with results from other experimental models of liver injury models reflecting a strong inflammatory response similar to that documented [Borkham-Kamphorst et al., 2011]. The observed changes of liver protein expression in MCD-*Lcn2*$^{-/-}$ mice were most likely the result of regulation at the transcriptional level since qRT-PCR analysis revealed parallel differences in mRNA levels of all these genes except PLIN3 (Figure 6-vB-E). qRT-PCR analysis of PPAR-γ expression showed that livers of *Lcn2*$^{-/-}$ mice had slightly lower mRNA levels of this nuclear receptor than WT controls when fed either normal or MCD chow (Figure 6-vA F).

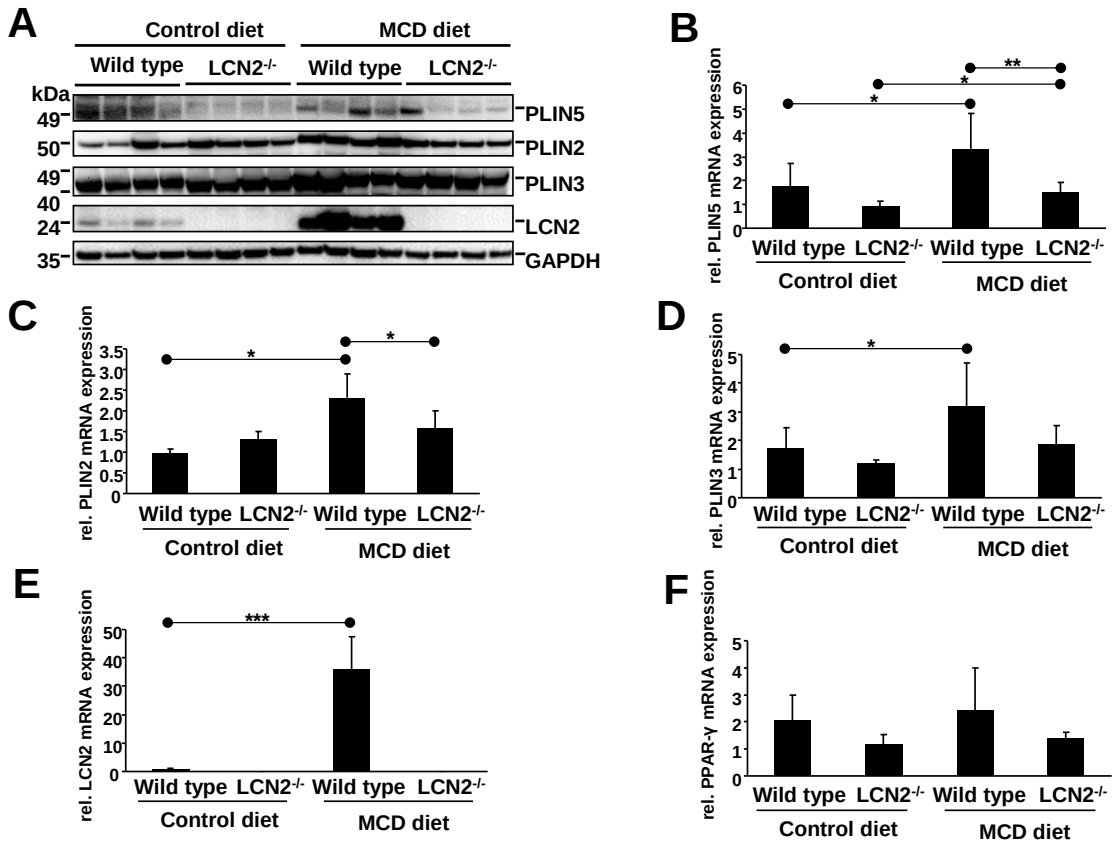


Figure 6-v: Effects of a MCD diet on the protein expression and mRNA level of genes correlated to lipid metabolism. (A) Western blot analysis to detect PLIN5, PLIN2, PLIN3 and LCN2 protein in liver extracts from WT or Lcn2$^{-/-}$ mice that were fed normal chow or an MCD diet for 4 weeks (n=4-8 mice/group). GAPDH served as a loading control. (B-F) qRT-PCR analysis of mRNA expression of *Plin5* (B), *Plin2* (C), *Plin3* (D), *Lcn2* (E) and *Ppar-γ* (F) in liver extracts from WT or *Lcn2*$^{-/-}$ mice that were fed normal chow or an MCD diet for 4 weeks (n=4-8 mice/group). Results are the mean ± SD of qRT-PCR data for n=4-8 mice/group, each analyzed in duplicate. *p ≤ 0.05; **p ≤ 0.01; ***p ≤ 0.001. **(Source: Asimakopoulou et al., 2014).**

Although these differences were not statistically significant, it is tempting to speculate that a decrease in PPAR-γ expression in the absence of LCN2 might trigger the observed hepatic steatosis and elevated total triglycerides. Additionally, immunohistochemical staining of liver sections of both genotypes after control or MCD diet was performed, to conclude that PLIN5 was located in the peripheral rings around the lipid droplets in a significant difference of increased PLIN5 around the lipid droplets of the WT mice (Figure 6-vi), suggesting that the PLIN5 regulation is stronger based on LCN2 expression than the MCD diet-induced lipogenesis itself.

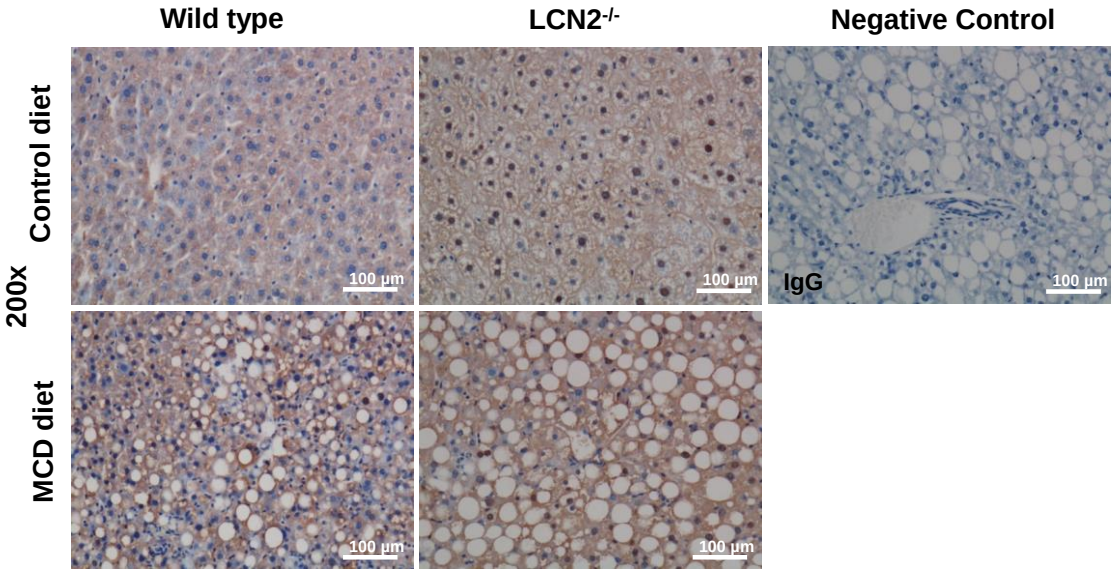


Figure 6-vi: Immunohistochemisty for PLIN5 in the liver tissue. WT and *Lcn2*$^{-/-}$ mice 4 weeks after the administration of control or MCD diet were stained for PLIN5. PLIN5 was found to be located peripherally of the lipid droplets that were formed after the MCD diet. The livers from WT mice revealed a higher expression of PLIN5 (darker brown color around the droplets) than the *Lcn2*$^{-/-}$ mice. Bar scales: 100µm. Results are representative images taken from individual animals in each group.

Can overexpression of LCN2 upregulate PLIN5 expression? The presented findings indicate that the absence of LCN2 is associated with decreased PLIN5 expression in liver extracts triggering next to test if transient overexpression of LCN2 in hepatocytes could enhance PLIN5 expression. To do so, primary hepatocytes from WT and *Lcn2*$^{-/-}$ mice (submitted to just normal chow diet) were isolated and transfected with the empty control vector pCMV-SPORT6 or a construct that drove the expression of the full-length murine *Lcn2* cDNA (CMV-mLcn2). One day post-transfection, with qRT-PCR the expression levels of PLIN5 mRNA were tested and it was found that transient LCN2 expression indeed significantly increased PLIN5 mRNA in both, WT and *Lcn2*$^{-/-}$, hepatocytes (Figure 6-viiA). This alteration in PLIN5 transcription resulted in a corresponding elevation in PLIN5 protein (Figure 6-viiB), establishing a regulatory link between LCN2 and PLIN5 expression. The same stimulatory effect on PLIN5 protein was detected when WT and *Lcn2*$^{-/-}$ hepatocytes were infected with an adenoviral expression vector mediating LCN2 expression (Ad-CMV-mLcn2), but not when cells were mock-infected or infected with a control adenoviral vector expressing luciferase (Ad-CMV-Luc) (Figure 6-viiC). These data support the hypothesis that LCN2 is a modulator of the Perilipins involved in hepatic lipid accumulation.

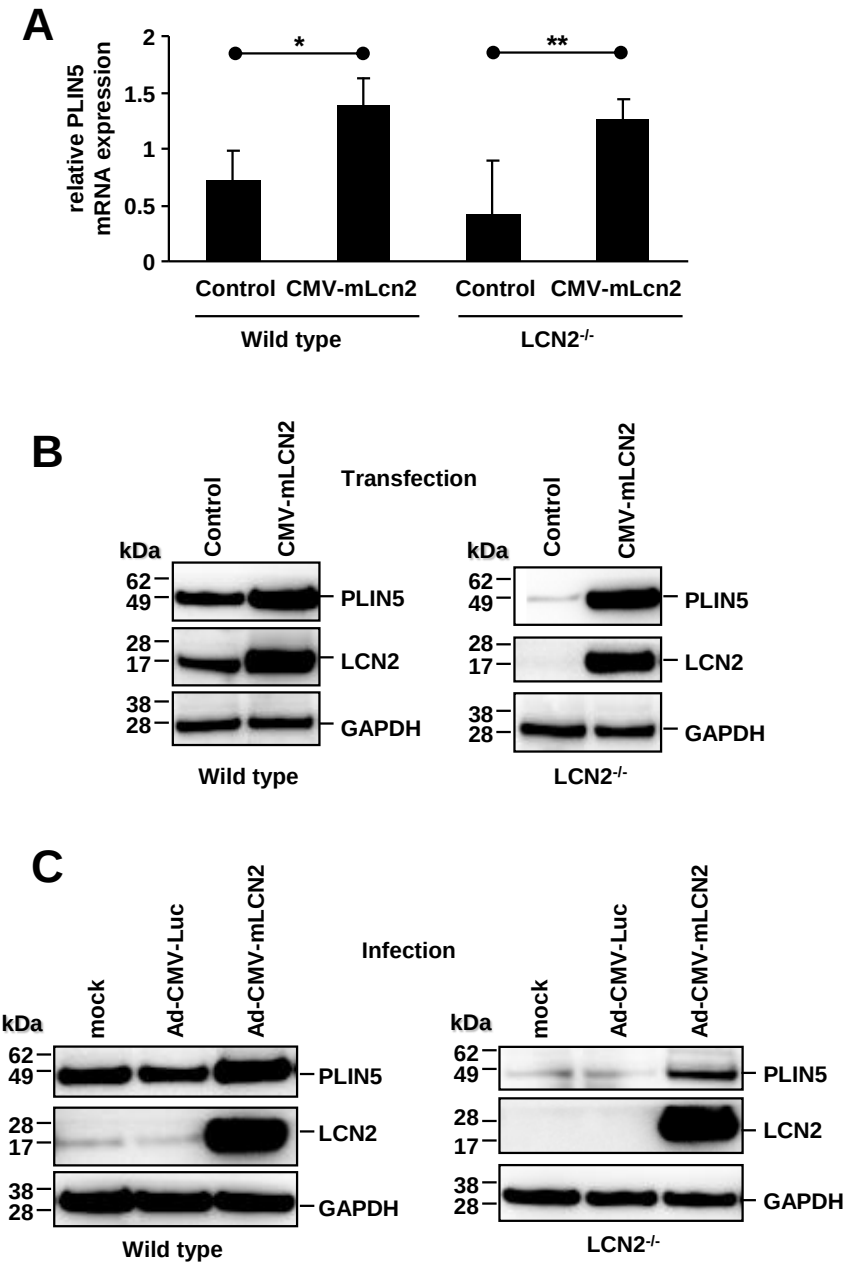


Figure 6-vii: Induction of PLIN5 by LCN2 overexpression in cultured hepatocytes. A) qRT-PCR analysis of PLIN5 mRNA expression in primary hepatocytes that were isolated from WT or *Lcn2*$^{-/-}$ mice ,fed with normal chow, and transfected with empty vector (control) or a construct expressing LCN2 (CMV-mLcn2). RNA was extracted 24 hrs post-transfection. Results are the mean ± SD of triplicates and are representative of 3 independent trials. *$p \leq 0.05$; **$p \leq 0.01$; ***$p \leq 0.001$. (B) Western blot analysis to detect LCN2 and PLIN5 proteins in the cells in (A). Proetin extracts were prepared 48 hrs post-transfection. The transfection results are representative of 3 independent experiments, while the infection was only done once. (C) Western blot analysis to detect LCN2 and PLIN5 proteins in WT and *Lcn2*$^{-/-}$ primary hepatocytes that were left uninfected (mock), infected with control adenoviral vector (Ad-CMV-Luc), or infected with adenoviral vector expressing LCN2 (Ad-CMV-mLcn2). Extracts were prepared 48 hrs post-infection. Results are representative of 3 independent experiments. **(Source: Asimakopoulou et al., 2014).**

Is LCN2 overexpression induced PLIN5 upregulation capable of affecting lipid formation? PLIN5 is critical for the storage of fat in primary hepatocytes [Grasselli et al., 2010]. Since LCN2, as shown above, regulates the expression of PLIN5, next it was tested if the elevated quantities of PLIN5 that are induced by LCN2 overexpression could influence lipid droplet formation or fat deposition in hepatocytes. To this question transfection of WT and *Lcn2*$^{-/-}$ primary hepatocytes was performed with LCN2 expression constructs. These cells were later stained (after cultivation in basal conditions) with the widely known lipophilic stainings Nile Red (Figure 6-viiiA) and Oil Red O (Figure6-viiiB) to detect lipid droplets. Easy to observe, both staining methods revealed that LCN2 overexpression led to increased lipid droplet formation, in both WT and *Lcn2*$^{-/-}$ hepatocytes. Moreover, the size of these droplets appeared to be enlarged in the presence of overexpressed LCN2, suggesting that LCN2 participates in the synthesis or recruitment of lipid droplet membranes.

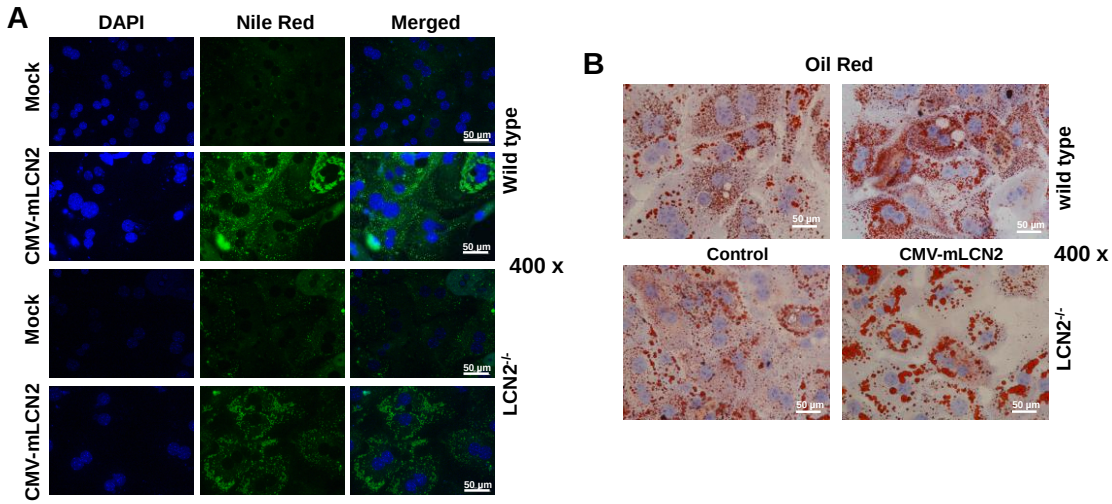


Figure 6-viii: Effect of LCN2 overexpression in hepatic lipid droplets. Overexpression of LCN2 in primary hepatocytes increased the formation of Lipid droplets. (A) Nile Red staining of lipid droplets in WT or *Lcn2*$^{-/-}$ primary hepatocytes that were transfected with empty vector (mock) or vector expressing LCN2 (CMV-mLCN2). Staining was performed 48 hrs post-transfection. To increase contrast, microscope settings were chosen such that Nile Red was displayed in green. Nuclei were visualized using DAPI (blue). Scale bars, 50 μm. (B) Oil Red O staining of lipid droplets in the primary hepatocytes in (A) examined at 48 hrs post-transfection. Scale bars, 50 μm. For (A) and (B), results are representative of 3 cultures/group. **(Source: Asimakopoulou et al., 2014)**

To test if these alterations required LCN2 itself or were solely the consequence of an increase in PLIN5, transfection of WT and *Lcn2*$^{-/-}$ hepatocytes with a construct expressing full-length murine PLIN5 (CMV-mPLIN5) was performed. Interestingly, PLIN5 overexpression alone was sufficient to enhance lipid droplet formation, irrespective of LCN2's presence (Figure 6-ix) Under condition in which the medium was further supplemented with oleic acid after transfection with LCN2 in hepatocytes isolated from Lcn2$^{-/-}$mice, it was demonstrated that LCN2 alone is already sufficient for increasing lipid droplet formation as well (not shown).

As a control for a successful stimulation with oleic acid the elevated expression of Adipose triglyceride lipase (*Atgl*) was proved (not shown).

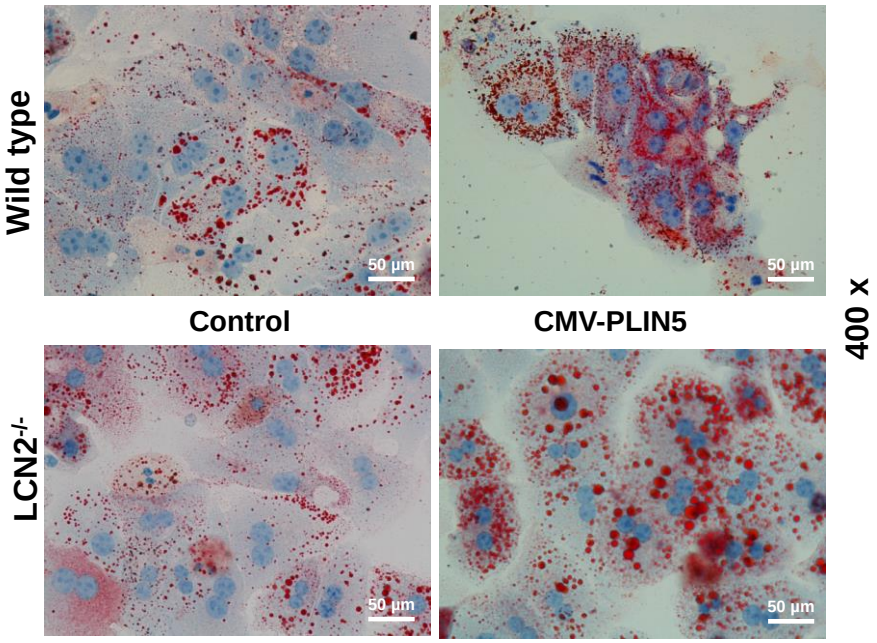


Figure 6-ix: Increase in lipid droplets in primary hepatocytes overexpressing PLIN5. Oil Red O staining of lipid droplets in WT or *Lcn2*$^{-/-}$ primary hepatocytes that were transfected with empty vector (control) or vector expressing PLIN5 (CMV-mPLIN5). Staining was performed 48 hrs post-transfection. Scale bars, 50 µm. Results are representative of 3 cultures/group examined in 3 independent trials. **(Source: Asimakopoulou et al., 2014).**

So far the results show that LCN2's key role in this context is to stimulate PLIN5 expression. To confirm this hypothesis, immunocytochemistry was applied to analyze PLIN5 protein expression in WT and *Lcn2*$^{-/-}$ hepatocytes subjected to transfection or adenoviral infection with LCN2 expression constructs. Again, the data indicated a strict correlation between the presence of LCN2 and vigorous PLIN5 production (Figure 6-x). Intriguingly, it was found that transient transfection of LCN2, at a transfection rate of ~30% of cells, resulted in similarly strong level of PLIN5 expression as adenoviral infection of LCN2, with an infection rate of ~100% of cells. This result demonstrates that LCN2 is indeed a key inducer of PLIN5.

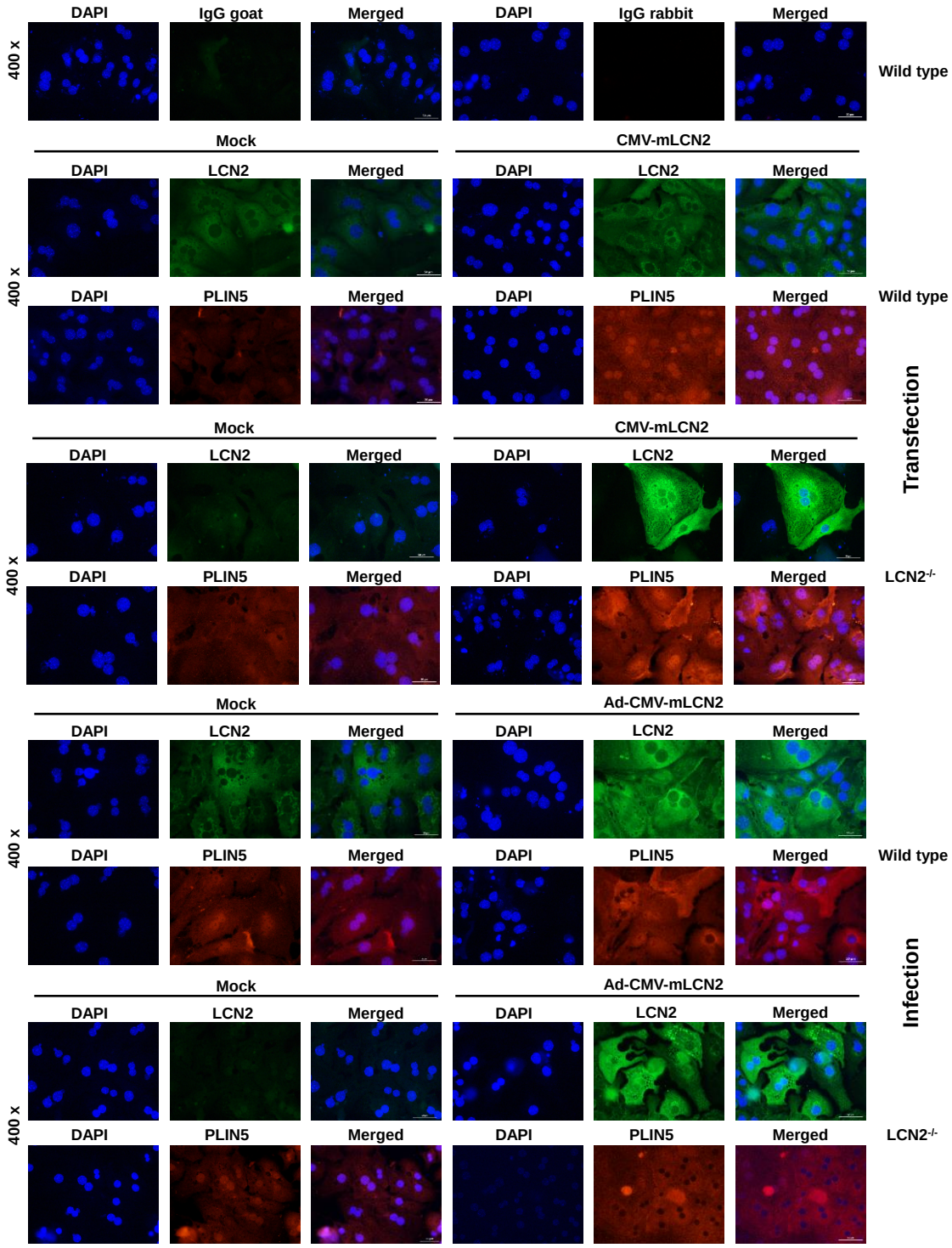


Figure 6-x: Immunocytochemical analysis of PLIN5 induction by LCN2 overexpression in primary hepatocytes. Top panels: Control immune-staining of WT hepatocytes to confirm the specificity of the antibodies used in this analysis. Transfection panels: WT and Lcn2$^{-/-}$ primary hepatocytes were mock-transfected (mock) or transfected with vector overexpressing LCN2 (CMV-mLCN2). Cells were fixed at 48 hrs post-transfection and immunostained with anti-LCN2 (green) and anti-PLIN5 (red) antibodies. Nuclei were counterstained with DAPI (blue). Infection panels: WT and *Lcn2*$^{-/-}$ primary hepatocytes were not infected (mock) or infected with adenoviral vector overexpressing LCN2 (Ad-CMV-mLCN2). Cells were fixed at 48 hrs post-infection and immunostained as for transfections. Scale bars, 50 μm. Results are representative of 3 cultures/group examined in 3 independent trials. **(Source: Asimakopoulou et al., 2014).**

Fatty acid rich environment. Can it affect the PLIN5-LCN2 correlation? Till now, it's clearly proven that LCN2 strongly regulates PLIN5 in basal conditions. But in order to investigate if this LCN2-PLIN5 regulation can be disturbed from sudden fatty acid accumulation, WT and *Lcn2*$^{-/-}$ hepatocytes were stimulated *in vitro* with oleic acid (unsaturated) and stained with Oil Red O to evaluate intracellular lipid accumulation. Loss of LCN2 did not prevent lipid droplet formation in oleic acid-treated cells (Figure 6-xi).

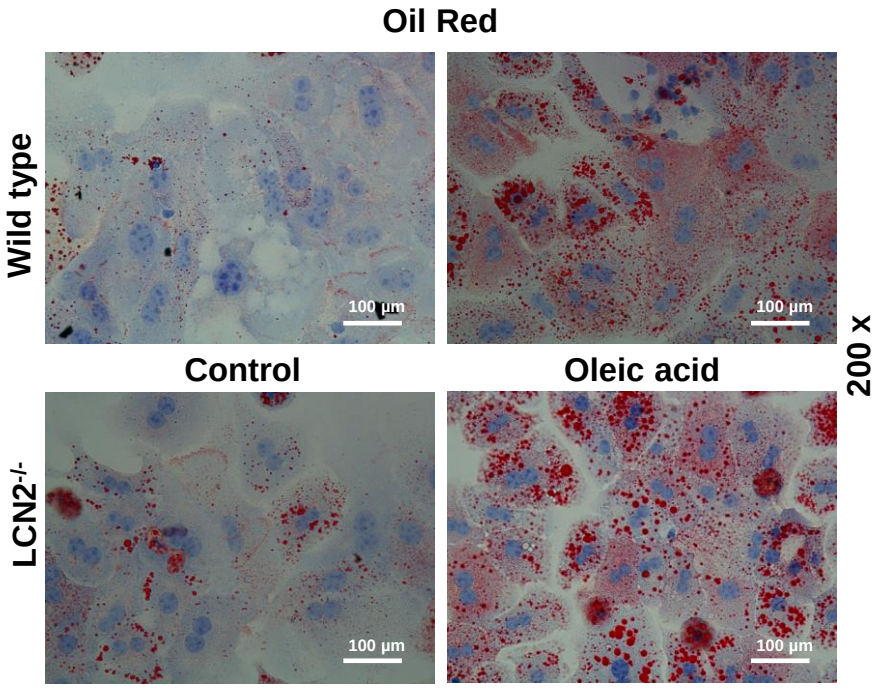


Figure 6-xi: Stimulation of primary hepatocytes with oleic acid. WT or *Lcn2*$^{-/-}$ primary hepatocytes were stimulated in culture with vehicle (control) or 0.1 mM oleic acid for 16 hrs and lipid droplets were visualized by Oil Red O staining. Scale bar, 100 µm. Results are representative of 3 cultures/group. **(Source: Asimakopoulou et al., 2014).**

However, the lipolytic activity in livers of *Lcn2*$^{-/-}$ mice was significantly suppressed in MCD diet as evident by lower expression of lipolysis associated genes including hormone sensitive lipase (HSL), ATGL, monoglyceride lipase (MGL), and hepatic triglyceride lipase (HTGL), respectively (Figure 6-xii).

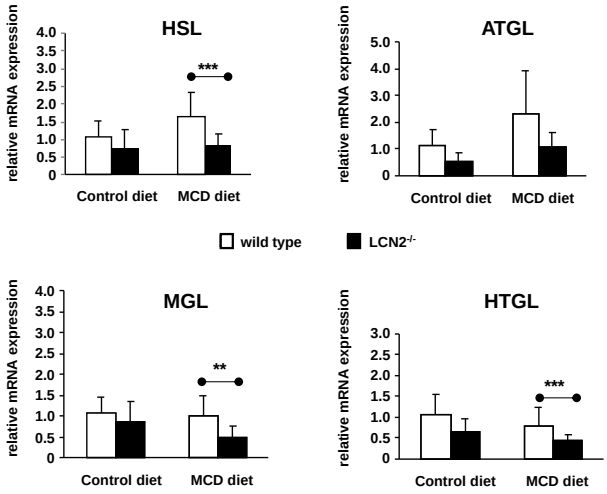


Figure 6-xii: Quantitative analysis of lipolytic markers. Mice were fed with a control or MCD diet for four weeks. Animals were sacrificed, livers extracted and analyzed for expression of HSL, ATGL, MGL, and HTGL by qRT-PCR.. Results are the mean ± SD of qRT-PCR data for *n*=4-8 mice/group, each analyzed in duplicate. *p ≤ 0.05; **p ≤ 0.01; ***p ≤ 0.001 **(Source: Asimakopoulou et al., 2014).**

When levels of PLIN5 and LCN2 proteins were examined in WT and *Lcn2*$^{-/-}$ hepatocytes treated with oleic acid (unsaturated) and/or palmitic acid (saturated) these fatty acids failed to significantly increase PLIN5 or LCN2 protein in WT hepatocytes, or PLIN5 protein in *Lcn2*$^{-/-}$ hepatocytes (Figure 6-xiiiA and Figure 6-xivA). Similarly, oleic acid treatment of WT hepatocytes did not stimulate their expression of *Lcn2* mRNA (Figure 6-xiiiB). Interestingly, there was a tendency that the levels of PLIN5 mRNA in cultured *Lcn2*$^{-/-}$ hepatocytes were lower than those in WT hepatocytes in the presence or absence of free fatty acids (Figure 6-xivB). Under the chosen conditions, no indication for apoptosis or lipotoxic effects was found (Figure 6-xivC). All these results suggest that, at least *in vitro*, LCN2 overexpression can mimic the effects of free fatty acids on lipid droplet formation by stimulating high expression of PLIN5, but that free fatty acids cannot induce PLIN5 in the absence of LCN2.

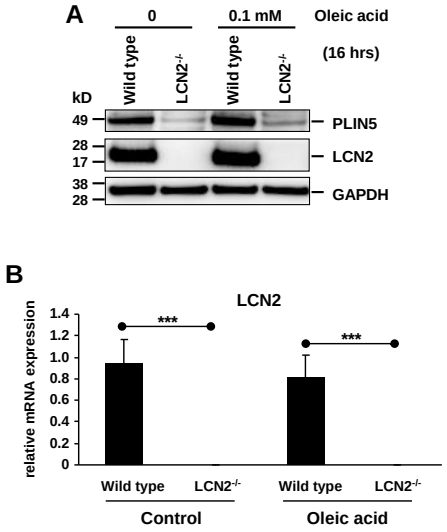


Figure 6-xiii: Induction of PLN5 expression in hepatocytes by stimulation with fatty acids. (A) Western blot analysis to detect PLIN5 and LCN2 proteins in extracts of WT or *Lcn2*$^{-/-}$ primary hepatocytes that were left untreated (0) or stimulated with 0.1 mM oleic acid for 16 hrs. GAPDH, loading control. (B) qRT-PCR analysis of LCN2 mRNA expression in extracts of WT or *Lcn2*$^{-/-}$ primary hepatocytes that were left untreated (control) or stimulated with 0.1 mM oleic acid for 16 hrs. Results are representative of 3 cultures / group. *p ≤ 0.05; **p ≤ 0.01; ***p ≤ 0.001**. (Source: Asimakopoulou et al., 2014).**

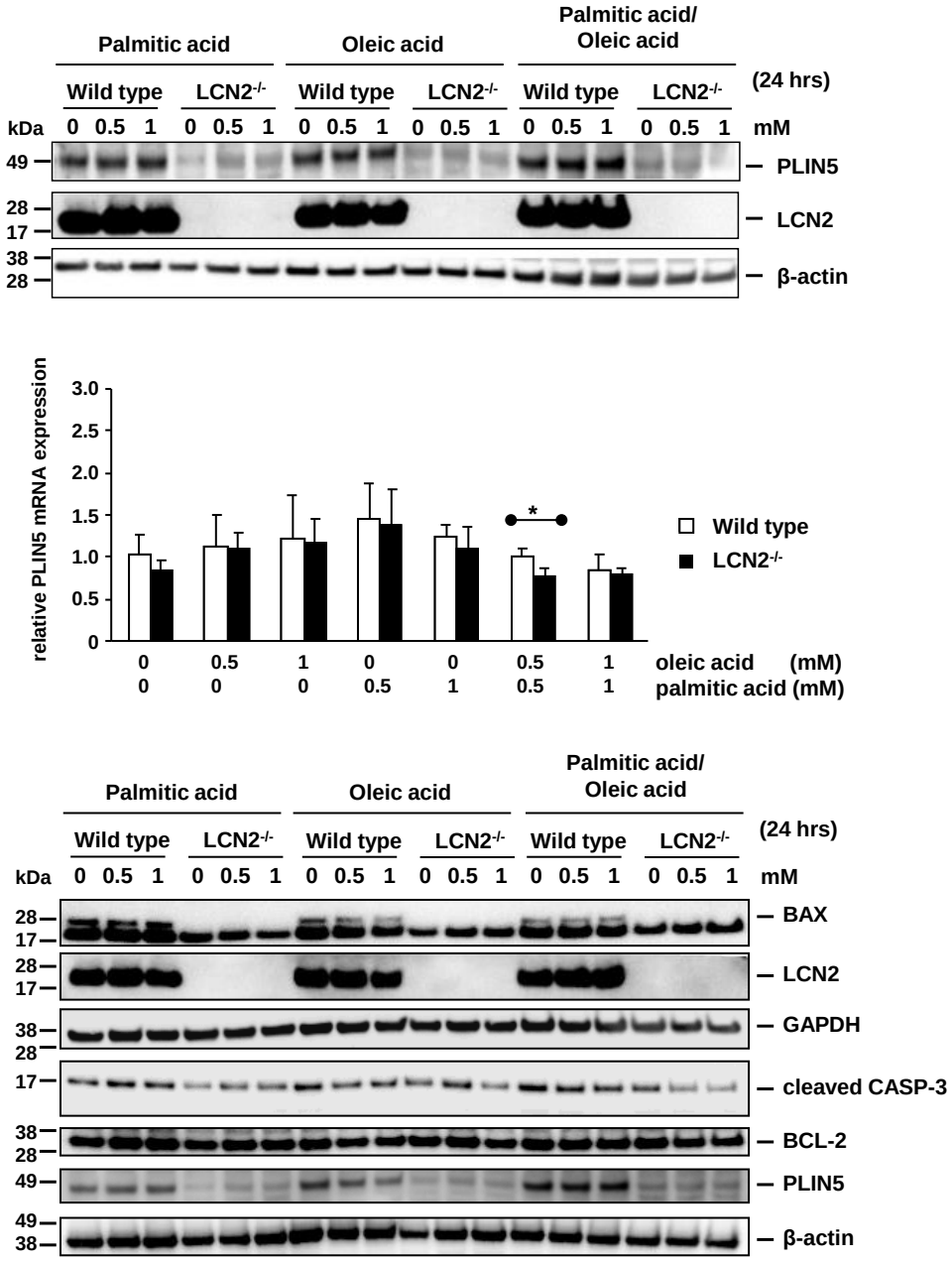


Figure 6-xiv: Induction of PLIN5 expression in hepatocytes by stimulation with fatty acids. (A) Western blot analysis to detect PLIN5 and LCN2 proteins in extracts of WT or *Lcn2*$^{-/-}$ primary hepatocytes that were stimulated for 24 hrs with the indicated concentrations of palmitic acid, oleic acid, or both. β-actin, loading control. Results are representative of 3 cultures/group. (B) qRT-PCR analysis of PLIN5 mRNA in extracts of WT or *Lcn2*$^{-/-}$ primary hepatocytes that were treated with indicated stimuli for 24 hrs. Results are representative of 3 independent experiments.),*p ≤ 0.05; **p ≤ 0.01; ***p ≤ 0.001. (C) For test of potential lipotoxicity of the conditions used, the expression of several genes associated with apoptosis (BAX, BCL-2, cleaved Caspase-3) was analyzed. **(Source: Asimakopoulou et al., 2014).**

Is the observed LCN2-PLIN5 correlation potent? Krahmer et al had already shown that phosphatidylcholine is required to prevent lipid droplet coalescence, which results in lipolysis resistant lipid droplets [Krahmer et al., 2011] suggesting that the formation of lipid droplets upon MCD is due to lipid droplet coalescence and that these droplets are lipolysis resistant in this model. In line with these findings trying to clarify if the LCN2-PLIN5 correlation is potent another nutritional model was used, a HFD diet, widely used for steatosis development. Briefly it is demonstrated that hepatic expression of Lcn2, PLIN5 and PLIN2 is increased in animals that received a HFD (Figure 6-xvB) supporting the initial result. Also immunofluorescence-histochemistry in liver sections for PLIN5 of these animals revealed the upregulation of PLIN5 after the HFD administration similarly to the MCD diet effect (Figure 6-xvC). Oil red staining was applied to prove the HFD induced lipid accumulation in the mouse livers (Figure 6-xvA).

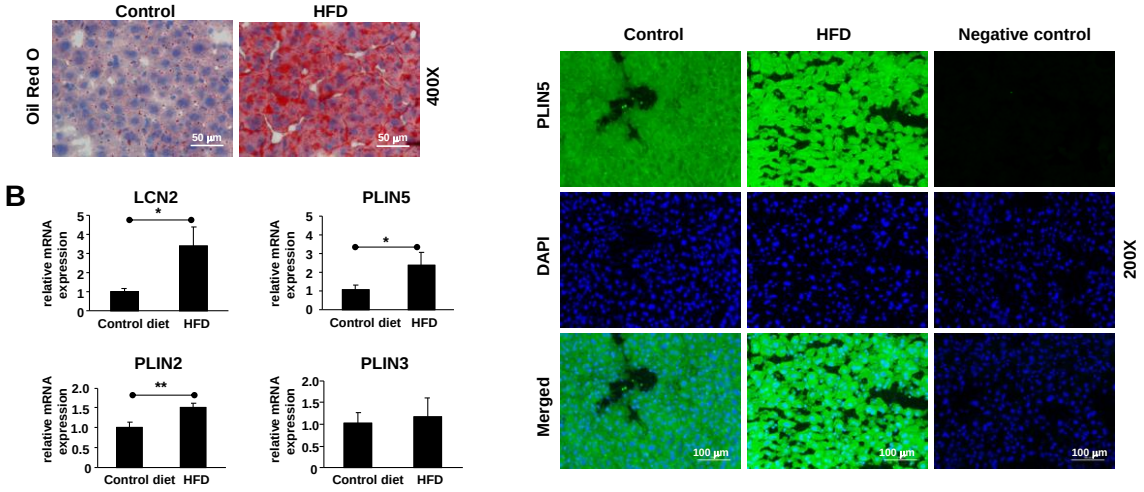


Figure 6-xv: High fat diet. WT animals were subjected to a control or a high fat diet (HFD) for 16 weeks. (A) Compared to control mice that were fed on a standard chow, HFD animals were characterized by hepatic fat accumulation as determined in Oil Red O stain. Space bars represent 50 µm. (B) Expression of *Lcn2*, *PLIN5*, *PLIN2*, and *PLIN3* were analyzed in respective animals by qRT-PCR). Results are the mean ± SD of qRT-PCR data for n=3-6 mice/group, each analyzed in duplicate, *p ≤ 0.05; **p ≤ 0.01; ***p ≤ 0.001. (C) Expression of PLIN5 was determined by immunohistochemistry. Nuclei were counterstained with DAPI. Space bars represent 100 µm. **(Source: Asimakopoulou et al., 2014).**

Can a PPRA-γ agonist affect the expression of LCN2 and PLIN5? Rosiglitazone is PPR-γ agonist reported to downregulate LCN2 [Zhang et al., 2008] and to increase PLIN5 gene expression [Wolins et al., 2006]. To investigate how such an agonist will affect the LCN2-PLIN5 relation, hepatocytes were stimulated with Rosiglitazone. This PPAR-γ agonist failed to suppress significantly LCN2 or upregulate PLIN5 expression, while the expression of ATGL representing a PPAR-sensitive gene [Shi et al., 2013] is strongly inhibited (Figure 6-xvi) suggesting that the LCN2-dependent regulation of PLIN5 is PPAR independent in murine hepatocytes.

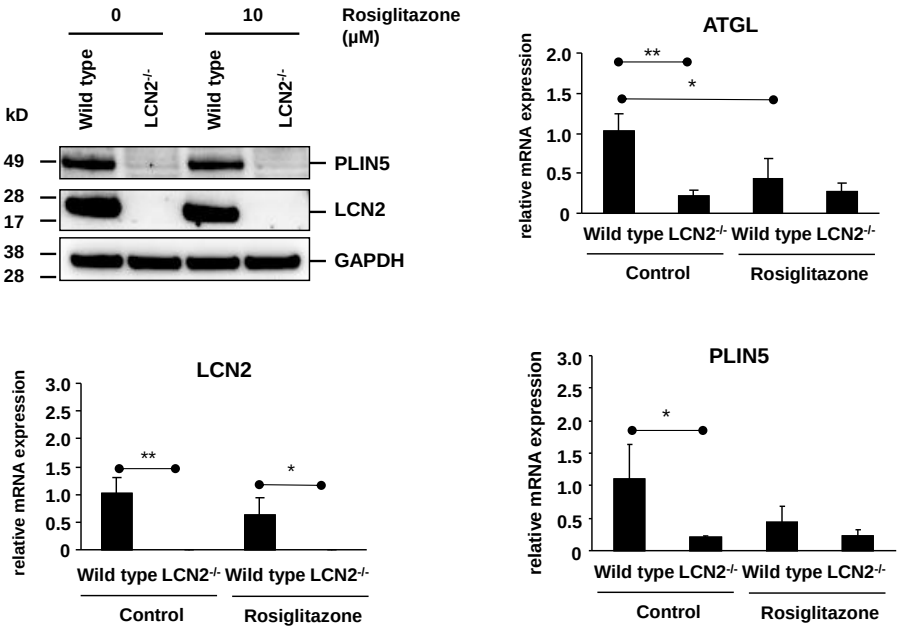


Figure 6-xvi: Effect of Rosiglitazone on LCN2 and PLIN5 expression. WT or Lcn2$^{-/-}$ hepatocytes were stimulated with Rosiglitazone or vehicle (DMSO). 24 hrs later, the cells were harvested and the expression of PLIN5 and LCN2 analysed by Western Blot and qRT-PCR. Results are the mean ± SD of triplicates and are representative of 3 independent trials. *p ≤ 0.05; **p ≤ 0.01; ***p ≤ 0.001. In addition, the expression of ATGL was measured by qRT-PCR. **(Source: Asimakopoulou et al., 2014).**

Is LCN2's expression associated with the mitochondria content? In previous reports, it has been suggested that PLIN5 may also be associated with mitochondria (next to the lipid droplet-associated pool). In a last set of experiments, the hepatic content of mitochondria was tested for possible alterations in animals that lack LCN2 and were fed with MCD by quantitative expression analysis of mitochondrial marker genes that were previously proved to be downregulated [Guo et al., 2010] in brown adipose tissue. This analysis revealed that in complete agreement with this previous study, the expression of *Tfam, Nrf1, CTP1-β, CoxIV, ATP5-β* and *CPT1* were significantly suppressed in Lcn2$^{-/-}$ mice that received MCD diet compared to WT controls, while there was a tendency that respective animals had already lower numbers of mitochondria under normal feeding conditions (Figure 6-xvii). which might point (not firmly at the moment) to not

only a LCN2 association with oxidative metabolism as reported before [Zhang et al., 2014] but also a link of PLIN5 and mitochondrial function as suggested before where PLIN5 was proved to protect mitochondria from excessive FA influx [Wang et al., 2011].

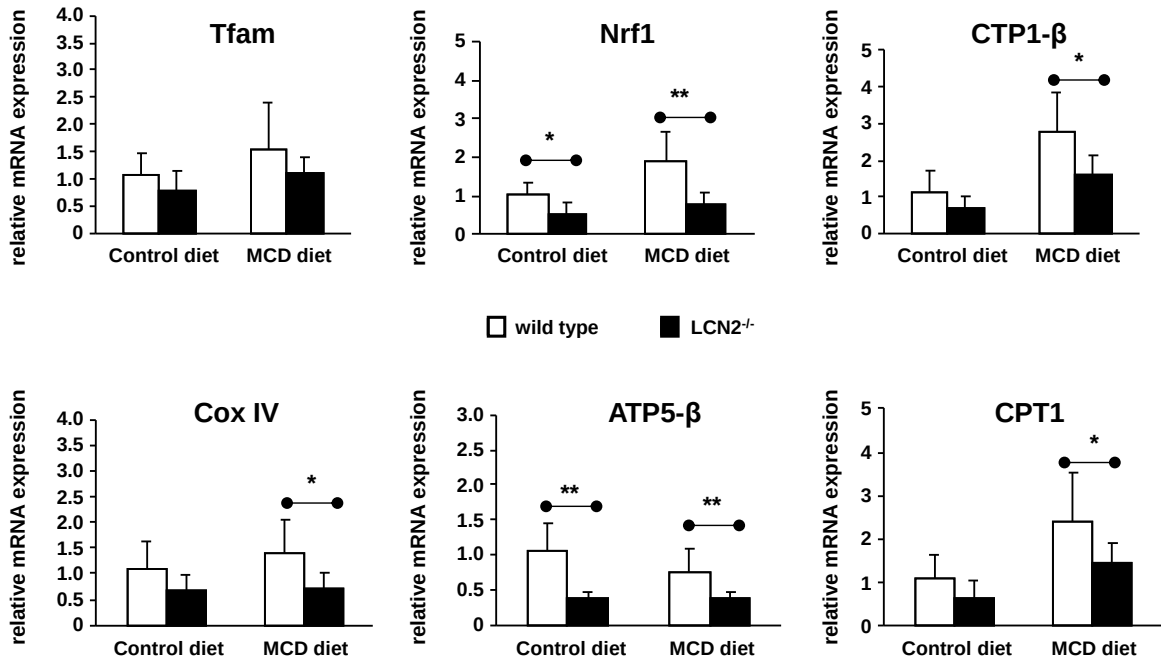


Figure 6-xvii: Expression of mitochondrial marker genes. The hepatic expression of *Tfam*, *Nrf1*, *CTP1-β*, *CoxIV*, *ATP5-β* and *CPT1* was tested by qRT-PCR in livers of animals that received control chow or MCD with the *Lcn2*$^{-/-}$ presenting significantly reduced expression in the majority of the mitochondrial markers.). Results are the mean ± SD of qRT-PCR data for *n*=4-8 mice/group, each analyzed in duplicate, *p ≤ 0.05; **p ≤ 0.01; ***p ≤ 0.001 **(Source: Asimakopoulou et al., 2014)**

Discussion

In this study, the functions of LCN2 in hepatic fat homeostasis were explored using two nutritional models of non-alcoholic steatohepatitis. WT and *Lcn2*$^{-/-}$ mice were subjected to an MCD diet and compared intrahepatic lipid accumulation, lipid droplet formation, and expression of perilipins. Basal expression of PLIN5 was significantly reduced in Lcn2$^{-/-}$ hepatocytes. In a second model of steatosis, WT mice were fed with a HFD.

Lipids accumulated more in *Lcn2*$^{-/-}$ liver and the expression of LCN2 and PLIN5 increased during hepatic steatosis induced by MCD or HFD. These findings fit to a previous report that has demonstrated that *Lcn2*$^{-/-}$ mice develop more severe fatty liver under regular chow diet and high fat diet [Guo et al., 2010]. Moreover this previous report suggested that LCN2 has a fundamental role in adaptive thermoregulation, diet-induced insulin resistance, and lipid metabolism [Guo et al., 2010]. Loss of LCN2 and consequently PLIN5 activities prevented normal intracellular lipid droplet formation both *in vitro* and *in vivo*. Restoration of LCN2 expression in *Lcn2*$^{-/-}$ primary hepatocytes by either transfection or adenoviral vector infection induced PLIN5 expression and restored proper lipid droplet formation. Thus, these data indicate that LCN2 is a key modulator of hepatic lipid homeostasis that controls the formation of intracellular lipid droplets by regulating PLIN5 expression.

Although the lack in LCN2 results in more severe fatty liver, the cultured hepatocytes had more intracellular lipid droplets when transfected or infected with expression vectors for LCN2. This paradoxical might be explained by the fact that presently the biochemical consistency of the lipid droplets observed in this study is unknown and that there is no discrimination between free fatty cytosolic fatty acids and fatty acids that are incorporated in lipid droplets.

It was previously shown that an increase in LCN2 expression correlates with an inflammatory response and has protective effects in models of experimental liver insult [Borkham-Kamphorst et al., 2013]. Elevated LCN2 is reliable marker of liver damage, as evidenced by its marked upregulation in livers of mice subjected to treatment with toxic agents such as carbon tetrachloride, lipopolysaccharide, or Concanavalin A, or that have undergone bile duct ligation surgery [Borkham-Kamphorst et al., 2013]. Other laboratories have demonstrated that LCN2 is a critical selective modulator of PPAR-γ activation and contribute to the metabolic syndrome in nonalcoholic fatty liver disease [Jin et al., 2011 and Milner et al., 2009]. LCN2 thereby functions in lipid homeostasis and energy expenditure, and contributes to the metabolic syndrome in non-alcoholic fatty liver disease in which excess fat accumulates in the liver.

The present work has revealed a new role for LCN2 in the regulation of at least one of the perilipin proteins involved in lipid homeostasis. Each of the perilipins PLIN2, PLIN3 and PLIN5 is expressed in its own distinct time course after exposure to free fatty acids. It's demonstrated here that the control of PLIN5 expression rests on factors in addition to the presence of free fatty acids, and that one of those factors, is LCN2. PLIN3 and PLIN5 are initially upregulated in

response to lipid overload, with PLIN3 having a major function in inducing lipid droplet formation, initializing droplet structure, and directing droplet coating during rapid fat storage [Wolins et al., 2006]. PLIN2 resides on the surface of lipid droplets [Grasselli et al., 2010] and is upregulated after PLIN3 and PLIN5 to promote hepatic fat storage [Chang et al., 2006]. It is shown that WT mice fed the MCD diet exhibited elevated levels of PLIN3 mRNA that correlated with the observed lipid droplet accumulation, and that this increase in PLIN3 expression was compromised in the absence of LCN2. Moreover, an increase in PLIN2 mRNA and protein in livers of MCD-WT mice was observed, reflecting a correlation between PLIN2 expression and lipid loading in hepatocytes that is consistent with that reported for other cell populations [Buechler et al., 2001]. Once again, this elevation in PLIN2 mRNA was impaired in the absence of LCN2. However, a lack of LCN2 had no significant effect on protein levels of PLIN3 and PLIN2. In contrast, an absence of LCN2 compromised both mRNA and protein expression of PLIN5 in whole liver and hepatocytes, and consequently led to enhanced lipid accumulation. Thus, LCN2 is an important new regulator of perilipin-mediated lipid storage in the liver.

The mechanism by which LCN2 modulates PLIN5 expression remains a mystery. It might be possible that the lack of LCN2 modulates the expression of some lipolytic markers including HSL, ATGL, MGL and HTGL (Figure 6-xii) but these results also indicate that LCN2 directly affects genes (PLIN5) that are involved in proper lipid droplet formation (Figure 6-vii). These two findings might explain why the size of the lipid droplets that was observed in the *Lcn2*$^{-/-}$ mice is increased when compared to WT controls.

On the other side, it is possible that LCN2 influences hepatocyte uptake of lipids and fatty acids by enhancing the passive diffusion of these hydrophobic substances through the membrane bilayer. Alternatively, LCN2 may participate in a till now unidentified receptor system. It is generally accepted that any uptake of fatty acids in excess of metabolic requirements will lead to the storage of these fatty acids as triglycerides, resulting in hepatic steatosis, lipid peroxidation, and inflammation progressing to steatohepatitis [Bradbury et al., 2006].

Based on these experiments, a model was proposed in which LCN2 is a central mediator in hepatic lipid metabolism that can influence glucose homeostasis and adipogenesis (Figure 6-xviii). A similar role has been proposed for LCN13, which is markedly reduced in mice exhibiting obesity and type-2 diabetes [Cho et al., 2011]. Similarly as for LCN2 overexpression in WT mice, short-term overexpression of LCN13 via adenovirus-mediated gene transfer attenuated hepatic steatosis in mice with either dietary or genetic obesity [Sheng et al., 2011]. Conversely, neutralization of endogenous LCN13 increased lipogenesis and suppressed fatty acid β-oxidation in primary hepatocytes [Sheng et al., 2011]. The presented data in this dissertation reinforced the conclusion that lipocalins have roles far beyond the transport of lipophilic substances, and can act as major regulators of lipid metabolism.

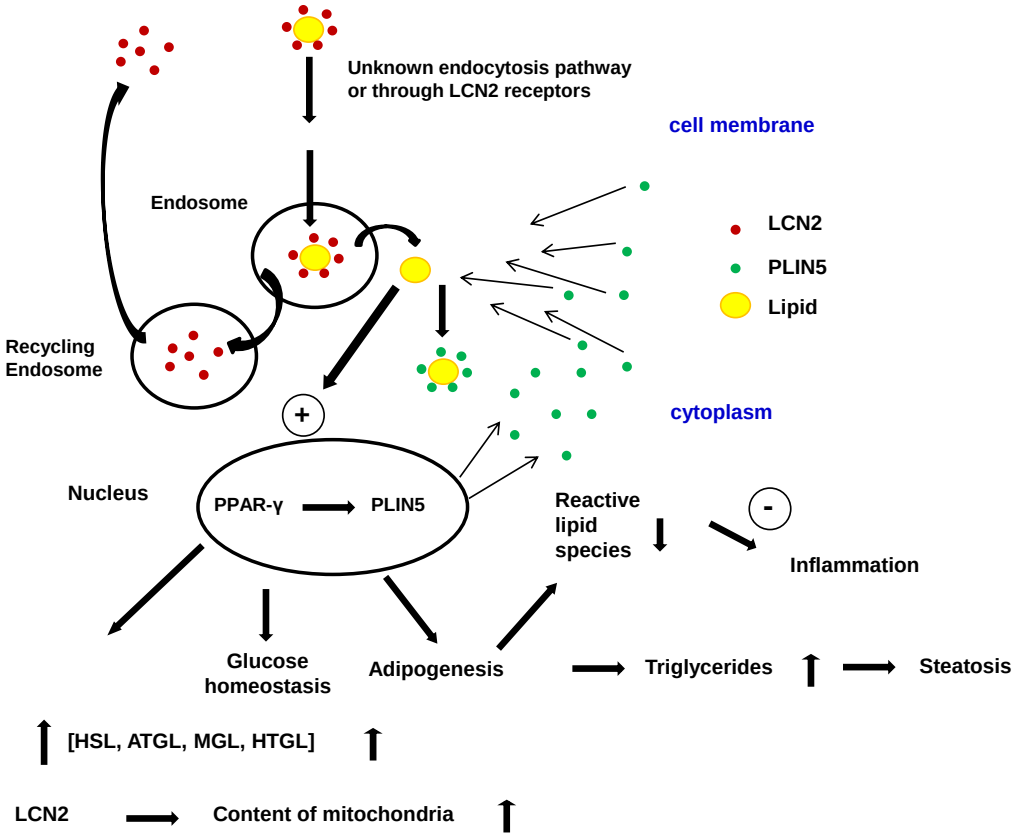


Figure 6-xviii: Model of LCN2 function in the regulation of PLIN5 expression and control of lipid homeostasis. LCN2 is a small protein known to bind to hydrophobic substances such as lipids. It is proposed that LCN2 may import lipids into hepatocytes either via an unknown endocytosis pathway or through unidentified LCN2 receptors. Within the hepatocyte cytoplasm, the LCN2-lipid complex may be compartmentalized into endosomes whose slightly acidified microenvironment may eventually cause LCN2 to dissociate from the lipids. The lipids may be discharged from the endosome into the cytoplasm, where they may be bound to the lipid droplet protein PLIN5 to protect them from degradation. LCN2 may be returned to the cell's exterior by endosome recycling. Hepatocyte PLIN5 production may be upregulated by PPAR-γ, which itself is upregulated by the higher cytoplasmic fat content that results when LCN2 facilitates lipid import. Together, this regulatory network of LCN2, PPAR-γ, and PLIN5 affects lipid metabolism, glucose homeostasis, adipogenesis, and mitochondrial content. In the presence of LCN2, intracellular concentrations of reactive lipid species may be reduced and inflammatory responses suppressed. However, in the absence of LCN2, or when PLIN5 expression is modulated by PPAR-γ, the formation of triglycerides may be increased and eventually lead to steatosis. **(Source: Asimakopoulou et al., 2014)**.

In total the results shown in this study give some hints as to how LCN2 can help to protect the liver against acute injury. PLIN5 regulates oxidative lipid droplet hydrolysis, and is involved in the control of fatty acid flux to protect mitochondria against excessive exposure to fatty acids during stress conditions [Wang et al., 2011]. Specifically, PLIN5 stabilizes lipid droplets by inhibiting their hydrolysis and channels fatty acids to triglyceride stores at the expense of fatty acid oxidation by the mitochondria [Wang et al., 2011].

The proposed scenario resulting from this study wants LCN2 elevation in response to stress to increase concentrations of intracellular PLIN5. This PLIN5 may attempt to maintain cellular integrity by storing fatty acids transiently in the lipid droplet compartment, preventing them from triggering pro-inflammatory cytokine and chemokine production and the activation of ROS-associated pathways [Boden et al., 2008]. For example, hepatocytes are induced to produce large quantities of IL-8 by exposure to pathophysiologic concentrations of palmitic acid. This palmitic acid stimulates an excessive influx of fatty acids into hepatocytes through mechanisms involving NF-κB activation [Joshi-Barve et al., 2007]

It has been previously shown that LCN2 expression correlates with an inflammatory response in the liver, and is controlled by the NF-κB pathway in hepatocytes [Borkham-Kamphorst et al., 2011]. A speculation rises, that an increase in intracellular fatty acid concentration in hepatocytes may first trigger the expression of cytokines and chemokines that subsequently activate the NF-κB pathway. LCN2 is then expressed and subsequently stimulates PLIN5 expression in concert with other factors. In primary cardiomyocytes, PPAR-γ agonist treatment for example has been shown to induce PLIN5 mRNA expression [Wolins et al., 2006], and LCN2 modulates PPAR-γ activation associated with control of lipid homeostasis and energy expenditure [Shi et al., 2013]. Conversely, a deficit in PPAR-γ activity induces steatosis and reduces serum triglycerides [Rogue et al., 2014 and Seber et al., 2006]. Although there was no statistically significant difference observed in PPAR-γ levels in the *Lcn2*$^{-/-}$ hepatocytes, a suggestion that a decrease in PPAR-γ expression associated with loss of LCN2 function might trigger the observed hepatic steatosis and elevated serum triglycerides in the MCD-*Lcn2*$^{-/-}$ mice can be made.

The lipid droplet formation is a complex process in which many factors are essential and the MCD model does not necessarily mimic all the biochemical requirements that control lipid droplet formation and coalescence that was in detail reported elsewhere [Krahmer et al., 2011]. Although the content of phosphatidylcholine was not analyzed in this study, the finding that *Lcn2*$^{-/-}$ mice have already more lipid droplets than WT mice when fed with a regular chow suggest that phosphatidylcholine alone is not responsible for the observed alterations during hepatic steatosis in the knock out animals. Moreover, the demonstration that some lipolytic and mitochondrial markers are suppressed in *Lcn2*$^{-/-}$ mice requires additional future experimentation in order to understand the pathophysiological role that is induced by lack of LCN2.

In conclusion, it's here shown that LCN2 is a critical regulator of lipid uptake that influences the expression of the key perilipin PLIN5 in a PPAR independent manner as well as the formation of lipid droplets in primary hepatocytes. These findings support recent proposals that lipid droplets can be considered a potential therapeutic target in diseases associated with fatty livers [Anderson et al., 2008; Goh et al., 2013]. A deeper understanding of the roles of LCN2 and PLIN5 in the pathogenesis of steatosis and hepatic inflammation could yield important fundamental data on mechanisms leading to hepatic fat accumulation. Consequently, this knowledge could lead to new avenues of therapy and prevention of human diseases, such as NASH and NAFLD that are associated with increased hepatic lipid uptake.

There are recent advances in understanding the role of PLIN proteins in lipid droplet formation and the pathogenesis of liver diseases [Okumura et al., 2011 and Li et al., 2012]. PLIN1 has the ability to bind lipid droplet, PLIN2 coats lipid storage droplets, while PLIN3 failed to be associated with amount of lipid droplets in liver and the function of PLIN4 is still unknown [Okumura et al., 2011]. It is here shown that PLIN5 is upregulated during hepatic steatosis. In addition, other laboratories have shown that the expression of this perilipin family member is modulated by PPARα in the liver, heart and skeletal muscle and by PPARγ in epididymal adipose tissue [Dalen et al., 2007; Yamaguchi et al., 200; Wolins et al., 2006]. In this study it's suggested that PLIN5 is maybe the most important perilipin that in conjunction with LCN2 controls lipid droplet homeostasis and potentially impacts lipolysis and mitochondrial balance.

7 Lipocalin-2 (NGAL/LCN2), a "HELP-ME" Signal in hepatic inflammation

In this second part of the study, investigation of the role of LCN2 in inflammation induced by MCD diet (nutritional model of NASH), fed to WT and *Lcn2*$^{-/-}$ mice was carried out. The hepatic LCN2 and inflammatory cytokines and chemokines (IL-6, IL-1β, TNF-α, CCL2 and CCR2) as well as the transcription factors STAT1 and STAT3 expression were compared between the two genotypes. Additionally, histology inflammation score and immunohistochemistry stainings with leukocytes and neutrophil granulocyte markers were performed. It was found that while both, WT and *Lcn2*$^{-/-}$, developed inflammation after 4 weeks of MCD diet, the WT presented enhanced leukocyte and neutrophil recruitment than the *Lcn2*$^{-/-}$ mice. Moreover, the WT mice fed with MCD diet, presented a remarkably stronger expression of phosphorylated forms of STAT1 and STAT3. These results indicate that the biological activity of LCN2 in experimentally-induced liver injury acts in a protective way ('HELP-ME' signal) to liver homeostasis as it enhances the recruitment of the first cells responsible for the immune defence against injury.

7.1 Introduction

LCN2 has been proved to protect against bacterial growth by sequestering siderophores making iron inaccessible to the bacteria [Goetz et al., 2002 and Flo et al., 2004], a characteristic which was confirmed when *Lcn2*$^{-/-}$ mice were reported to favour bacterial infections [Berger et al., 2006]. The rodent homologue of LCN2 (24p3) was initially localised in mouse urine after viral infection (Simian virus 40) in the kidney [Hraba-Renevey et al., 1989], while the human homologue, NGAL was purified from stimulated neutrophils [Kjedsen et al., 1993]. LCN2 has been attributed several functions, as mentioned before in Chapter 3, however the cellular mechanisms still need to be defined.

Hints have been given of LCN2 correlation in inflammation pathways [Sunil et al., 2007]. Injured hepatocytes have been proved to be the main source of hepatic LCN2 [Borkham-Kamphorst et al., 2011]. More specifically, hepatic LCN2 expression is drastically upregulated during inflammation and in response to cellular stress and evolves protective effects during acute and chronic injury models. It had been recently reported that LCN2 is induced during experimental liver injury showing that the pro-inflammatory cytokine IL-1β induces the LCN2 expression in hepatocytes in those models [Borkham-Kamphorst et al., 2011]. Moreover, after administration of the hepatoxin CCl_4 increased liver damage was found in *Lcn2*$^{-/-}$ mice in comparison with WT. The *Lcn2*$^{-/-}$ animals presented increased expression of inflammatory cytokines and chemokines such as IL-1β, IL-6, TNF-α and MCP-1/CCL2, leading to continuous activation of STAT1 and STAT3

pathway suggesting a protective role for LCN2 in liver damage [Borkham-Kamphorst et al., 2013]. Several recent studies suggested that LCN2, functions as a recruiter of inflammatory cells in cases of inflammation in astrocytes, hind paws and injured spinal cord [Lee et al., 2011; Jha et al., 2014 ; Rathore et al., 2011]. However, there are also studies indicating the role of LCN2 in the progression of kidney disease in both mice and human [Rinella et al., 2004]. Trying to clarify further the role of LCN2 in inflammation WT and *Lcn2* $^{-/-}$ mice were fed with a MCD diet-used widely to induce NASH . Next the expression of inflammation markers in both genotypes was analysed. In the present study it's shown, that the WT animals showed extreme LCN2 upregulation after the MCD diet and that they recruited significantly more neutrophils and leukocytes than the *Lcn2*$^{-/-}$ mice. The WT mice appeared to have wider leukocytes and neutrophil infiltrates while the active forms of STAT1 and STAT3 expression were significantly higher in the WT mice. Moreover, conduction of inflammation score based on liver tissue, agreed with the above experimentation. The present study provides solid information that LCN2 serves as a 'HELP-ME' signal inducing recruitment of the first-line immune defence cells (neutrophil granulocytes) preventing the liver of further damage development in a MCD model of NASH.

7.2 Results

MCD is a nutritional model of fatty liver disease for rodents resulting in liver injury similar to human NASH, including steatosis, inflammation and fibrosis [Brunt et al., 1999; Pickens et al., 2010; Pickens et al., 2009; Larter et al., 2008]. Livers of WT and *Lcn2*$^{-/-}$ mice fed on normal chow diet for 4 weeks appeared normal while WT and *Lcn2*$^{-/-}$ mice on MCD diet showed extensive steatosis with the formation of clear lipid droplets and infiltrating inflammatory cells (Figure 7-iA). However, the WT mice presented more focal and clear lobular inflammatory infiltration than the *Lcn2*$^{-/-}$ with more and wider areas of neutrophil and leukocyte accumulation. Moreover, inflammation score by a blinded pathologist, based on the H&E stained tissue sections, showed enhanced inflammatory response after the MCD diet for 4 weeks was higher in the WT mice (0.43±0.53 *vs.* 0.13±0.35) compared to the *Lcn2*$^{-/-}$ Figure 7-iB).

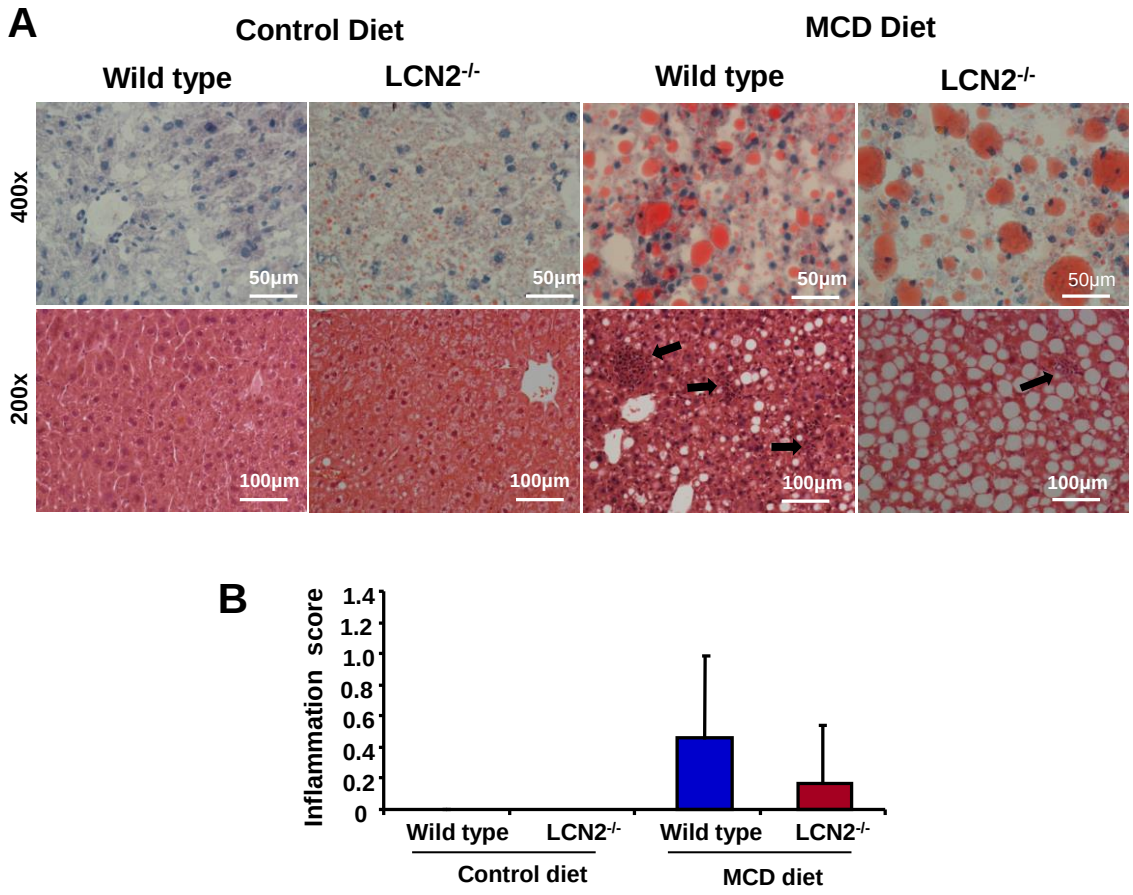


Figure 7-i: Inflammation effect after four weeks of MCD diet administration. (A) Representative Oil Red O staining (top panels) and H&E staining (lower panels) of hepatic specimens of both, WT and *Lcn2*$^{-/-}$ mice, after MCD or normal-control diet. (Bar scales: 100 μm). Lipid accumulation is observed as well as the formation of inflammation infiltrates (indicated with black arrows) as results of the MCD diet mechanism. The WT representative individual samples show significantly more and bigger areas of accumulation of inflammatory cells. Results are representative images from individual animals from each group. In (B), for all the WT and *Lcn2*$^{-/-}$ animals fed on chow or MCD diet for 4 weeks, an histological inflammation score based on H&E stained tissue sections was performed, enhancing the outcome of the stainings in (A). Results shown are the mean ± SD of WT or *Lcn2*$^{-/-}$ mice (n=4-8/group). **(Source: Asimakopoulou et al., 2015).**

To study further and in more detail the inflammatory effect after the MCD diet, liver sections were immune-stained with CD45 (cluster of differentiation 45) antibody as the leukocyte-common antigen After the MCD diet, it's clear that in the WT animals more leukocytes recruited than the *Lcn2*$^{-/-}$ mice (Figure 7-iiA).The protein level of CD45 was also tested with the WT mice showing increased expression of CD45 in control and MCD diet (Figure 7-iiB). Additionally the mRNA expression levels of the common-leukocyte marker agreed with the already results (Figure 7-iiC).

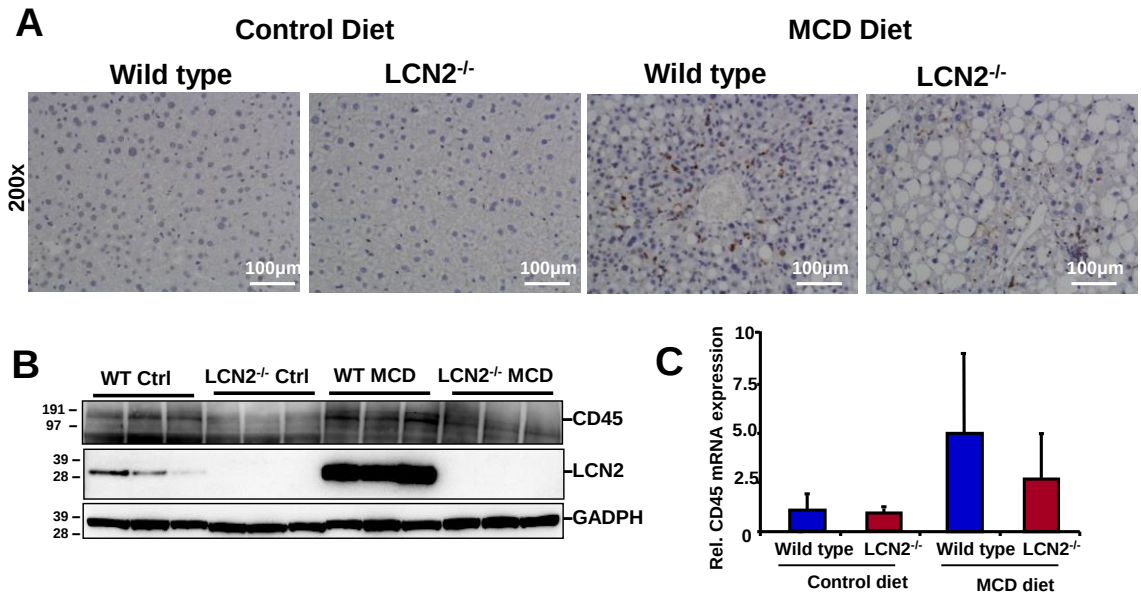


Figure 7-ii: MCD diet induces the formation of inflammatory infiltrations. With immunohistochemical staining (A) Leukocytes were detected on 5 μm liver tissues with CD45 (cluster of differentiation 45) antibody in both WT and *Lcn2*$^{-/-}$ after 4 weeks of normal chow diet or MCD, indicating a burst out of leukocytes infiltration in the WT mice after the MCD diet in comparison to the *Lcn2*$^{-/-}$ mice. Scale bars: 100μm. Results are representative images from individual animals from each group. (B) Western blot on liver lysates of the same mice revealed significantly enhanced expression of CD45 not only in MCD conditions but also when fed a normal-control diet. (C) The expression of the leukocyte marker was tested with qRT-PCR. Results shown are the mean ± SD of WT or *Lcn2*$^{-/-}$ mice (n=4-8/group). **(Source: Asimakopoulou et al., 2015).**

Moreover, immunostaining of liver tissues from animals of both genotypes with MPO antibody that is mostly abundantly expressed in neutrophil granulocytes was performed. Interestingly, the WT animals fed on MCD diet, presented much higher infiltrated neutrophils than the *Lcn2*$^{-/-}$ mice (Figure 7-iiiA). The staining followed by quantification of the MPO expressing cells clearly show that MCD diet induces inflammation with WT animals recruiting remarkably up to 5-fold more inflammatory cells than the *Lcn2*$^{-/-}$ suggesting that the expression of LCN2 affects expression of proteins related to inflammation (Figure 7-iiiB). Another method used to prove the levels of neutrophil infiltration was the MPO activity assay by a colorimetric kit from Abcam. The quantification revealed that the MPO activity is significantly increased in the WT mice after MCD diet in comparison with the *Lcn2*$^{-/-}$ mice (Figure 7-iiiC), which supports the previous experimentation.

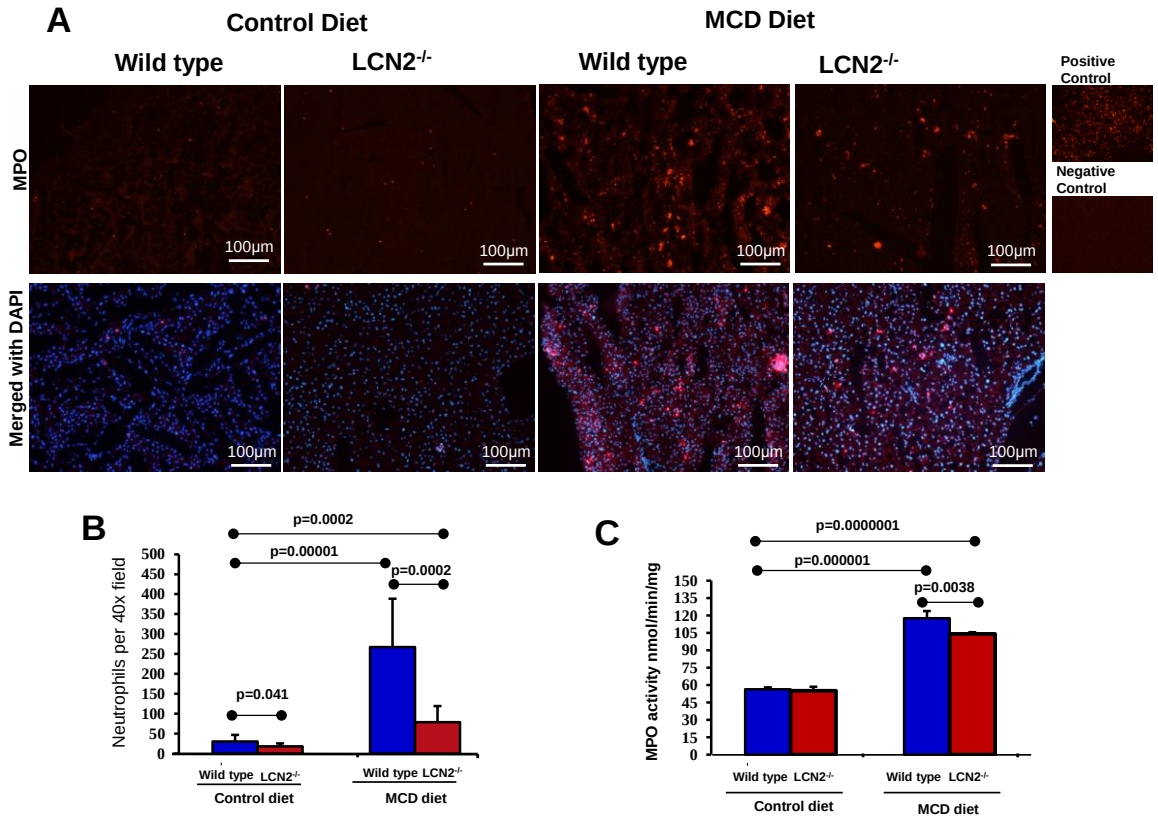


Figure 7-iii: MCD diet enhances the recruitment of neutrophils granulocytes. (A) Immunohistochemical staining with MPO antibody, neutrophils were detected in liver tissues of WT and *Lcn2*$^{-/-}$ after 4 weeks on normal or MCD diet. (Top panel) visualisation of MPO expression. (Lower panel) Merged pictures of MPO staining with counterstained nuclei with DAPI. Results are representative images from individual animals from each group. Scale bars: 100µm. (B) Five different areas of MPO stained tissue of each sample of 40x magnification were used for quantification of the neutrophil granulocytes. Results shown are the mean ± SD. (C) The MPO activity was measured by a colorimetric assay, enhancing the previous results for MPO significantly greater accumulation in the WT animas after MCD diet for 4 weeks. Results shown are the mean ± SD (n=4-5 per group). *p ≤ 0.05; **p ≤ 0.01; ***p ≤ 0.001. **(Source: Asimakopoulou et al., 2015)**

Western blot analysis of animals subjected to the MCD diet showed an interesting upregulation of the transcription factors, STAT1 and STAT3 protein levels for the WT animals compared to the *Lcn2*$^{-/-}$ ones. The same difference was observed when the activated-phosphorylated forms of those proteins pSTAT1 and pSTAT3 were tested (Figure 7-ivA). The activation of the STATs in tissue damage agrees with previous studies [Lang et al., 2005; Ernst et al., 2008 and Wang et al., 2011]. The pro-inflammatory cytokine IL-1β also presented an upregulated protein expression in WT animals (Figure 7-ivA). STAT proteins are known to be induced by several cytokines [Wang et al., 2011]. The mRNA expression of cytokines, chemokines and transcription factors was tested with qRT-PCR The analysis revealed that the MCD diet leads to intense upregulation of the mRNA of CCL2, CCR2, IL-6, IL-1β, TNF-α, STAT3 and STAT1 with the WT animals marking higher levels of mRNA expression in

comparison with the *Lcn2*$^{-/-}$ (Figure 7-ivB). Although the differences between WT and *Lcn2*$^{-/-}$ were not statistically significant, it enhances the previous significant results from protein analysis, H&E staining and immunohistochemistry that LCN2 enhances inflammatory response.

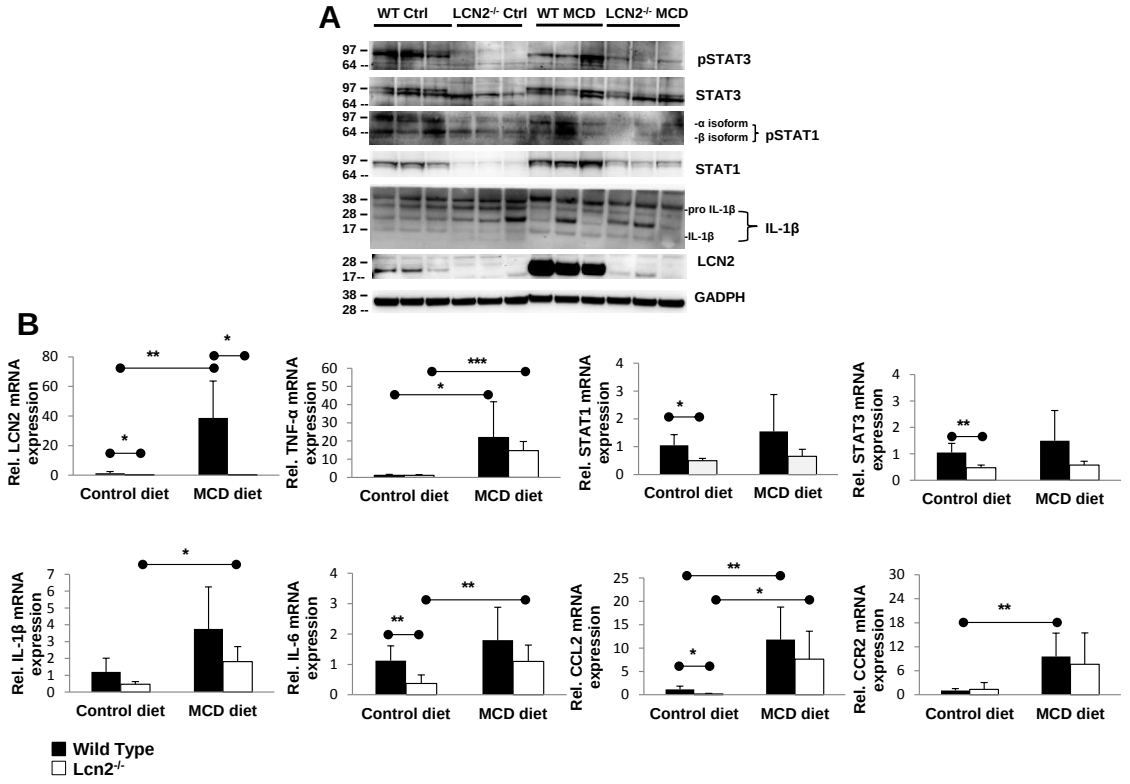


Figure 7-iv: MCD diet affects protein and mRNA expression of genes involved in the inflammation process. (A) Western blot analysis to detect STAT3, STAT1, and their activated / phosphorylated forms pSTAT1, pSTAT3, the proinflammatory cytokine IL-1β, and LCN2 protein in liver extracts from WT and Lcn2$^{-/-}$ mice after 4 weeks of normal chow or MCD diet. GAPDH was used as the loading control. All inflammation markers show a significantly higher expression in the WT animals with great enhancement of the STAT1, STAT3 and their activated / phosphorylated form pSTAT1 and pSTAT3. (B) qRT-PCR analysis of mRNA expression of the inflammation-correlated markers CCL2, CCR2, IL-6, IL-1β, TNF-α, STAT3, STAT1 and LCN2 was performed in liver extracts from the WT and Lcn2$^{-/-}$ mice. Results are the mean ± SD of qRT-PCR data for *n*= (4–8 mice/group), each analysed in duplicate. Values of significance are *p ≤ 0.05; **p ≤ 0.01; ***p ≤ 0.001.

Based on the finding that LCN2 expression correlates with STAT1 and STAT3 expression in hepatic tissue extracts overexpression (not shown) of the pro-inflammatory agent LCN2 in primary hepatocytes was performed to check if the expression of STAT3 and STAT1 will be enhanced. Primary hepatocytes were isolated from WT and *Lcn2*$^{-/-}$ mice and after 24 hrs were, transfected with empty control vector or a CMV-mLcn2 construct or infected with adenoviral vector (Ad-CMV-mLcn2) Primary hepatocytes that served as controls were left untreated or infected with control adenoviral vector (Ad-CMV-Luc) **(**not shown). Both transfection constructs CMV-mLcn2

and adenoviral vector (Ad-CMV-mLcn2) led to the expression of the full-length murine Lcn2 cDNA. Forty eight hrs post transfection the protein levels of STAT1, STAT3, pSTAT1, pSTAT3 and LCN2 were checked to conclude that overexpression of LCN2 itself is not enough to induce the STAT proteins expression (not shown). An overall conclusion of all these results was set on a scheme suggesting that LCN2 co-serves with STATs and cytokine induction to informing with a 'HELP-ME' signal the liver to recruit neutrophils and other leukocytes to resolve inflammation and protect it develop further injury (Figure 7-v).

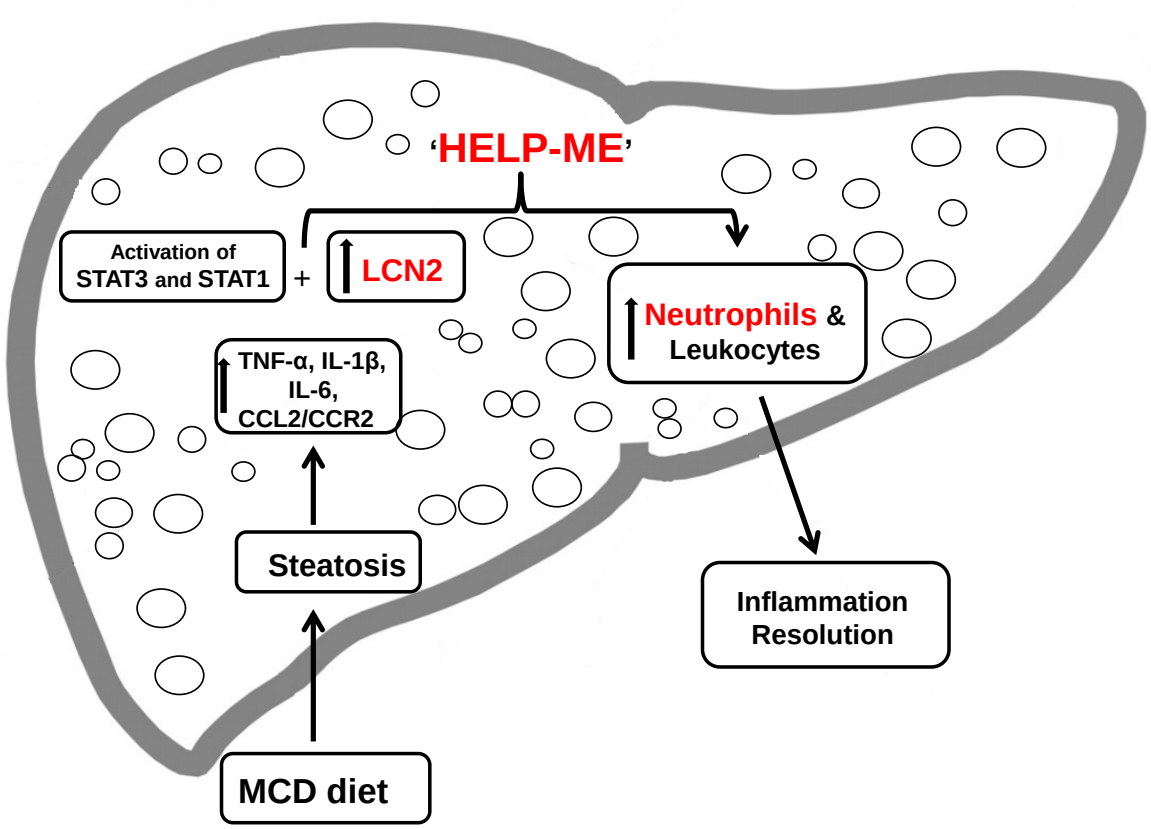


Figure 7-v: Proposed scheme of LCN2 role in hepatic inflammation. Based on the results from the experimentation shown in this chapter LCN2 seems to maintain the liver from further damage if damage has already occurred. In this MCD model steatosis is the first hit to the liver. Secondary factors (unknown) act to development of Inflammation and NASH. At this point the organ reacts with induction of expression of chemokines and proinflammatory cytokines such as, IL-6, IL-1β, TNF-α which further upregulate LCN2 *via* a STAT-dependent pathway. LCN2 seems to be the 'HELP-ME' alarm that induces the recruitment of leukocytes and mainly neutrophil granumocytes to the liver preventing further injury to the organ and to inflammation resolution.

.

7.3 Discussion

This study focused on clarifying the correlation of LCN2 in the inflammation process in Non-alcoholic fatty liver disease. An MCD nutritional model was used on WT and Lcn2$^{-/-}$ male mice for four weeks to induce NASH. The formation of NASH was proven with the steatosis (formation of lipid droplets) and the recruitment of inflammatory cells. LCN2 has recently been reported multiple times to correlate with inflammation [Borkham-Kamphorst et al., 2011; Valapala et al., 2014; Lindberg et al., 2014; Lee et al., 2011; Jha et al., 2014; Rathore et al., 2011].

Inflammation is a reaction of the immune system caused by tissue damage or injury. One of the early stages of the inflammatory procedure is the transmigration of leukocytes through the endothelium and their recruitment at the area of injury [Kubes et al., 1996; Langer et al., 2009]. Additionally, neutrophil granulocytes are large phagocytes that react primarily in case of injury [Swirski et al., 2013]. They are an essential part of the immune system that in case of injury they are the first-responders cells to migrate towards the inflammation-site. The WT animals of this MCD model showed a significant accumulation of inflammatory cells, when compared with the liver tissues of the *Lcn2*$^{-/-}$ mice, a process essential for the resolution of inflammatory processes.

One of the first studies linking LCN2 to inflammatory recruitment was the work of Lee et al., who proved LCN2 to be chemokine inducer in the central nerve system that accelerates cell migration upon inflammation [Lee et al., 2011]. LCN2 has also been reported in mouse models of systemic lupus erythematosus, collagen induced - arthritis and serum-transfer arthritis that *Lcn2*$^{-/-}$ mice presented up to a 50% reduction in inflammation, suggesting that LCN2 regulates immune cell recruitment to the site of inflammation [Shashidharamurthy et al., 2013]. Recently Jha et al., demonstrated that inflammatory cell-derived LCN2 at the sites of inflammation plays important roles in central sensitization and the subsequent nociceptive behaviour in the complete Freund's adjuvant-induced chronic inflammatory pain mouse model [Jha et al., 2014]. Moreover, using flow cytometry Rathore et al., observed reduced influx of neutrophils in *Lcn2*$^{-/-}$ injured spinal cords accompanied by decreased expression of several pro-inflammatory chemokines and cytokines while compared to WT animals, suggesting that LCN2 regulates inflammation in the spinal cord injury [Rathore et al., 2011]. Another report of Liu et al., proved that *Lcn2*$^{-/-}$ mice are characterized by impaired neutrophil function that makes them more sensitive to bacterial infections. They showed that *Lcn2*$^{-/-}$ mice presented low functional competence of neutrophils including migration and function in response upon inflammatory trigger [Liu et al., 2013].

All the above studies show that in various injury models in many tissues, LCN2, when inflammation is about to occur, it clamours a ‘HELP-ME’ signal which is strong enough to regulate the direct inflammatory cells recruitment to the inflammation site to process with resolution and help the organ from excess damage.

Elevation of LCN2 in hepatic injury has been reported before from several research groups [Borkham-Kamphorst et al., 2011; Borkham-Kamphorst et al., 2013; Valapala et al., 2014; Lindberg et al., 2014]. In this study the elevation of LCN2 is confirmed such in protein level as in mRNA after the administration of the MCD diet. It has been previously demonstrated [Borkham-Kamphorst et al., 2013] *via* qRT-PCR analysis the elevation of pro-inflammatory markers in hepatic injury models. Similarly the mRNA of cytokines including IL-6, TNF-α, IL-1β, TFN-α, CCL2, CCR2 in this study clearly indicates the initiation of inflammation processes in the liver caused by the MCD diet.

TNF-α and IL-1β are reported before as inducers of LCN2 [Borkham-Kamphorst et al., 2011; Borkham-Kamphorst et al., 2013; Zhao et al., 2014] and are mainly produced from Kupffer cells during injury. Its upregulated expression after the MCD diet participated in the elevation of LCN2 expression as a first signal of liver damage. Furthermore, IL-6 is a cytokine secreted from macrophages during tissue damage that leads to inflammation. Its expression was increased in mRNA and protein level after MCD diet with the *Lcn2*$^{-/-}$ presenting reduced expression in comparison to the WT. IL-6 has been demonstrated before to enhance neutrophil infiltration and to improve bacterial clearance. These roles of IL-6 were assigned to its ability to activate the transcription of STAT1 and STAT3 transcription factors [Jones et al., 2006]. Moreover, the inflammatory CCL2 and its receptor CCR2 presented a tendency of higher mRNA levels in the WT mice after the MCD diet. CCL2 is also referred to as monocyte chemotactic protein 1. As the name reveals CCL2 participates in monocytes recruitment, and other immunity cells such as dendritic cells to the sites of inflammation [Carr et al., 1994; Mehrabian et al., 1991]. CCL2 and its receptor CCR2 have been given by Lança et al., the role of protectors during inflammation in cancer conditions as they are responsible for the recruitment of type 1 cytotoxic γδ T lymphocytes (another type of white blood cells) [Lança et al., 2013].

The protein elevation of the STAT1 and STAT3 in the WT samples for normal chow diet and MCD as well as their sustained activation-phosphorylation after the MCD treatment is as well of high significance in these results. STAT1 is an agent reported before contributing to inflammation, injury and tumours [Przanowski et al., 2014]. STAT1 and STAT3 have also been proved to regulate inflammatory cells [Yoshimura et al., 2006]. Activation of STAT3 is induced by cytokines like IL-6 [Guobin et al., 2011]. A very interesting study from Xu and colleagues demonstrates that the hepatocyte-derived-LCN2 plays an important role in inhibiting bacterial infection and promoting liver regeneration via the activation of STAT3 signalling pathway by IL-6 [Xu et al., 2015]. Another report associates the STAT1 and STAT3 transcription activators to enhance neutrophil recruitment in inflammation sites after their phosphorylation/activation for IL-6 enhancing the control of inflammation resolution [Jones et al., 2006]. STAT1 has been several times addressed the role of inducer of neutrophils for the clearance of pathogens in the spleen [Pan et al., 2013], and in chronic liver diseases *via* the IFN-γ/STAT1 pathway [Jaruga et al., 2004]. The

sustained activation STAT1 and STAT3 relatively indicate the more intense inflammatory cell recruitment in the liver of WT mice in this model.

After proving with LCN2 overexpression that LCN2 can't itself induce STAT1 or STAT3 expression (not shown), LCN2 seems to act synergistically with the STATs to induce and accelerate the neutrophil and leukocytes recruitment to the sites of injury for the inflammation to be resolved before further damage occurs to the organ.

In conclusion, LCN2 has been reported before in models of hepatic damage, acute and chronic and also models of bacterial infections in several organs to have a protective role against inflammation. LCN2 strongly seems to be the 'HELP-ME' signal that notifies the immune system that inflammation is occurring so the recruitment and release of leukocytes and mainly neutrophils overrun the inflammation site to rescue the organ from further future injury. In the presented model MCD diet induced the inflammatory cell recruitment in the livers of the WT mice in a grade bigger than the *Lcn2*$^{-/-}$ mice did. Moreover, the upregulation of many proinflammatory cytokines, chemokines and the activation of the STAT proteins in the respective mice increases the speculation that LCN2 acts cooperatively to clamour for 'HELP' for inflammation resolution. The performed experimentation with all the previous reports mentioned above assign LCN2 as a reliable biomarker for hepatic inflammation and as a novel drug target for infestations associated with excess inflammatory reactions in liver and other organs.

8 General conclusion and future aspects

Based on the new evidence demonstrated here and from the already existing reported research on LCN2, it's un-doubtful that LCN2 is a multifunctional protein linked to the pathogenesis of several hepatic disorders such as NAFLD, abnormal lipid profile and inflammation. Numerous studies including the present one, propose LCN2 as a reliable biomarker and as a novel drug target.

The deep correlation of LCN2 and cases of lipid metabolism disorders and FLD including NASH, can suggest that this lipocalin can be developed to an early and robust marker that will improve differential diagnosis and prognosis of respective diseases.

In this study the finding that LCN2 modulates expression of PLIN5 that is an important protective factor against hepatic lipotoxicity might be of particular interest. The LCN2/PLIN5 axis will potentially allow identifying novel important drug targets that are helpful in specific treatment of FLD and NASH.

Moreover, the LCN2s function as a neutrophil chemoattractant in the liver in cases of inflammation brings LCN2 closer to be used a drug against harmful stimuli and to prevent patients from risking further their hepatic health.

LCN2 in this MCD nutritional model gave enough information that make more attractive the continuous research on this protein. As a continuation of this project liver tissues from WT and *Lcn2*$^{-/-}$ fed with control or MCD diet for 4 weeks, are being assessed under a full *Proteomics analysis* that will give a bigger spectrum of protein alterations between the two genotypes and also the same samples are going under *Lipidomics analysis* which will reveal the real lipid profile of the livers. These two big experimentations, will widen the spectrum of possible correlation of several proteins with LCN2 and functions that probably will clarify the role of LCN2 in lipid metabolism and not only.

9 References

Alwahsh SM, Xu M, Seyhan HA, Ahmad S, Mihm S, Ramadori G, Schultze FC. Diet high in fructose leads to an overexpression of lipocalin - 2 in rat fatty liver. World J. Gastroenterol. (2014), 20:1807-1821.

Andersen JF, Weichsel A, Balfour CA, Champagne DE, Montfort WR. The crystal structure of nitrophorin 4 at 1.5 A resolution: transport of nitric oxide by a lipocalin - based heme protein. Structure (1998), 6:1315-1327.

Anderson N, Borlak J, Molecular mechanisms and therapeutic targets in steatosis and steatohepatitis. Pharmacol. Rev. (2008), 60:311-357.

Anstee QM, Goldin RD, Mouse models in non - alcoholic fatty liver disease and steatohepatitis research, Int J Exp Pathol. (2006), 87:1-16.

Asimakopoulou A, Borkham-Kamphorst E, Henning M, Yagmur E, Gassler N, Liedtke C, Berger T, Mak TW, Weiskirchen R. Lipocalin - 2 [LCN2] regulates PLIN5 expression and intracellular lipid droplet formation in the liver. Biochim. Biophys. Acta. (2014), 1841:1513-1524.

Asimakopoulou A, Borkham-Kamphorst E, Tacke F, Weiskirchen R. Lipocalin-2 (NGAL/LCN2), a "HELP-ME" Signal in Organ Inflammation. Hepatology (2015), 62: in press.

Asimakopoulou A, Weiskirchen R. Lipocalin 2 in the pathogenesis of fatty liver disease and nonalcoholic statohepatitis. Clin Lipidology. (2015),10:47-67.

Auguet T, Quintero Y, Terra X, Martínez S, Lucas A, Pellitero S, Aguilar C, Hernández M, del Castillo D, Richart C. Upregulation of lipocalin 2 in adipose tissues of severely obese women: positive relationship with proinflammatory cytokines. Obesity [Silver Spring]. (2011), 19:2295-2300.

Auguet T, Terra X, Quintero Y, Martínez S, Manresa N, Porras JA, Aguilar C, Orellana - Gavaldà JM, Hernández M, Sabench F, Lucas A, Pellitero S, Del Castillo D, Richart C. Liver lipocalin 2 expression in severely obese women with non alcoholic fatty liver disease. Exp. Clin. Endocrinol. Diabetes (2013), 121:119-124.

Barbas CF 3rd, Burton DR, Scott JK, Silverman GJ. Quantitation of DNA and RNA. CSH Protoc. (2007).

Barr J, Vázquez - Chantada M, Alonso C, Pérez - Cormenzana M, Mayo R, Galán A, Caballería J, Martín - Duce A, Tran A, Wagner C, Luka Z, Lu SC, Castro A, Le Marchand - Brustel Y, Martínez - Chantar ML, Veyrie N, Clément K, Tordjman J, Gual P, Mato JM. Liquid chromatography - mass spectrometry - based parallel metabolic profiling of human and mouse model serum reveals putative biomarkers associated with the progression of nonalcoholic fatty liver disease. J. Proteome Res. (2010), 9:4501-4512.

Bartsch S, Tschesche H. Cloning and expression of human neutrophil lipocalin cDNA derived from bone marrow and ovarian cancer cells. FEBS Lett. (1995), 357:255-259.

Baumeister SE, Völzke H, Marschall P, John U, Schmidt CO, Flessa S, Alte D. Impact of fatty liver disease on health care utilization and costs in a general population: a 5 - year observation. Gastroenterology. (2007), 134:85-94 .

Bellentani S, Scaglioni F, Marino M, Bedogni G. Epidemiology of non - alcoholic fatty liver disease. Dig. Dis. (2010), 28:155-161.

Benyon RC, Iredale JP. Is liver fibrosis reversible? Gut. (2000), 46:443-446.

Berger T, Togawa A, Duncan GS, Elia AJ, You - Ten, Wakeham A, Fong HE, Cheung CC, Mak TW. Lipocalin 2 - deficient mice exhibit increased sensitivity to Escherichia coli infection but not to ischemia–reperfusion injury. Proc. Natl. Acad. Sci. U S A. (2006), 103:1834–1839.

Beynon RJ, Hurst JL. Multiple roles of major urinary proteins in the house mouse, Mus domesticus. Biochem. Soc. Trans. (2003), 31:142-146.

Boden G. Obesity and free fatty acids. Endocrinol. Metab. Clin. North Am. (2008), 37:635-646.

Borkham-Kamphorst E, Van de Leur E, Zimmermann HW, Karlmark KR, Tihaa L, Haas U, Tacke F, Berger T, Mak TW, Weiskirchen R. Protective effects of lipocalin - 2 (LCN2) in acute liver injury suggest a novel function in liver homeostasis. Biochim. Biophys. Acta. (2013), 1832:660-673.

Borkham-Kamphorst E, Drews F, Weiskirchen R. Induction of lipocalin - 2 expression in acute and chronic experimental liver injury moderated by pro - inflammatory cytokines interleukin - 1β through nuclear factor - κB activation. Liver Int. (2011), 31:656-665.

Borkham-Kamphorst E., C. Schaffrath, E. Van de Leur, U. Haas, L. Tihaa, S.K. Meurer, Y.A. Nevzorova, C. Liedtke, R. Weiskirchen. The anti - fibrotic effects of CCN1/CYR61 in primary portalmyofibroblasts aremediated through induction of reactive oxygen species resulting in cellular senescence, apoptosis and attenuated TGF - β signalling. Biochim. Biophys. Acta. (2014), 1843:902–914.

Bouma ME, Pessah M, Renaud G, Amit N, Catala D, Infante R. Synthesis and secretion of lipoproteins by human hepatocytes in culture. In Vitro Cell Dev Biol. (1988), 24:85-90.

Boyraz M, Cekmez F, Karaoglu A, Cinaz P, Durak M, Bideci A. Serum adiponectin, leptin, resistin and RBP4 levels in obese and metabolic syndrome children with nonalcoholic fatty liver disease. Biomark. Med. (2013), 7:737-745.

Bradbury MW. Lipid metabolism and liver inflammation. I. Hepatic fatty acid uptake: possible role in steatosis. Am. J. Physiol. Gastrointest. Liver Physiol. (2006), 290:G194 - G198.

Brasaemle DL. Thematic review series: adipocyte biology. The perilipin family of structural lipid droplet proteins: stabilization of lipid droplets and control of lipolysis. J. Lipid Res. (2007), 48:2547-2559.

Brunt EM, Janney CG, Di Bisceglie AM, Neuschwander-Tetri BA, Bacon BR. Nonalcoholic Steatohepatitis: a proposal for grading and staging the histological lesions. Am J Gastroenterol. (1999), 94:2467–2474.

Buechler C, Ritter M, Duong CQ, Orso E, Kapinsky M, Schmitz G. Adipophilin is a sensitive marker for lipid loading in human blood monocytes. Biochim. Biophys. Acta. (2001), 1532: 97-104

Bundgaard JR, Sengeløv H, Borregaard N, Kjeldsen L. Molecular cloning and expression of a cDNA encoding NGAL: a lipocalin expressed in human neutrophils. Biochem. Biophys. Res. Commun. (1994), 202:1468-1475.

Bykov I, Junnikkala S, Pekna M, Lindros KO, Meri S. Effect of chronic ethanol consumption on the expression of complement components and acute - phase proteins in liver. Clin Immunol. (2007), 124:213-220.

Carr MW, Roth SJ, Luther E, Rose SS, Springer TA. Monocyte chemoattractant protein 1 acts as a T - lymphocyte chemoattractant. Proc Natl Acad Sci U S A. (1994), 91:3652–3656.

Carson M**.** Ribbons. Methods Enzymol. (1997), 277:493-505.

Chan P, Simon - Chazottes D, Mattei MG, Guenet JL, Salier JP. Comparative mapping of lipocalin genes in human and mouse: the four genes for complement C8 gamma chain, prostaglandin - D - synthase, oncogene - 24p3, and progestagen - associated endometrial protein map to HSA9 and MMU2. Genomics. (1994), 23:145-150.

Chang BH, Li L, Paul A, Taniguchi S, Nannegari V, Heird WC, Chan L. Protection against fatty liver but normal adipogenesis in mice lacking adipose differentiation - related protein. Mol. Cell Biol. (2006), 26:1063-1076.

Cho KW, Zhou Y, Sheng L, Rui L. Lipocalin - 13 regulates glucose metabolism by both insulin - dependent and insulin - independent mechanisms. Mol. Cell Biol. (2011), 31:450-457.

Cianci M, Rizkallah PJ, Olczak A, Raftery J, Chayen NE, Zagalsky PF, Helliwell JR. The molecular basis of the coloration mechanism in lobster shell: beta - crustacyanin at 3.2 - A resolution. Proc. Natl. Acad. Sci. U S A. (2002), 99:9795-9800.

Coles M, Diercks T, Muehlenweg B, Bartsch S, Zölzer V, Tschesche H, Kessler H. The solution structure and dynamics of human neutrophil gelatinase - associated lipocalin. J. Mol. Biol. (1999), 289:139-157.

Cowan SW, Newcomer ME, Jones TA: Crystallographic refinement of human serum retinol binding protein at 2A resolution. Proteins (1990), 8:44-61.

Csak T, Ganz M, Pespisa J, Kodys K, Dolganiuc A, Szabo G. Fatty acid and endotoxin activate inflammasomes in mouse hepatocytes that release danger signals to stimulate immune cells. Hepatology. (2011), 54:133-144.

Dalen KT, Dahl T, Holter E, Arntsen B, Londos C, Sztalryd C, Nebb HI. LSDP5 is a PAT protein specifically expressed in fatty acid oxidizing tissues. Biochim Biophys Acta. (2007), 1771:210-227.

Dalen KT, Schoonjans K, Ulven SM, Weedon - Fekjaer MS, Bentzen TG, Koutnikova H, Auwerx J, Nebb HI. Adipose tissue expression of the lipid droplet - associating proteins S3 - 12 and perilipin is controlled by peroxisome proliferator - activated receptor - gamma. Diabetes (2004), 53:1243-1252.

Davis TR, Tabatabai L, Bruns K, Hamilton RT, Nilsen - Hamilton M. Basic fibroblast growth factor induces 3T3 fibroblasts to synthesize and secrete a cyclophilin - like protein and β2 - microglobulin. Biochim Biophys Acta. (1991), 1095:145-152.

De Wit NJ, Bosch - Vermeulen H, de Groot PJ, Hooiveld GJ, Bromhaar MM, Jansen J, Muller M , van der Meer R. The role of the small intestine in the development of dietary fat - induced obesity and insulin resistance in C57BL/6J mice. BMC Med. Genet. (2008), 1:14.

Dela Peña A, Leclercq I, Field J, George J, Jones B, Farrell G. NF - kB activation, rather than TNF, mediates hepatic inflammation in a murine dietary model of steatohepatitis. Gastroenterology. (2005), 129:1663–1674.

Diaz E, Pfeffer SR. TIP47: a cargo selection device for mannose 6 - phosphate receptor trafficking. Cell (1998), 93:433-443.

Drickamer K, Kwoh TJ, Kurtz DT. Amino acid sequence of the precursor of rat liver α2 micro - globulin. J. Biol. Chem. (1981), 256:3634-3666.

El Moety HA, El Sharkawy RM, El Menem Hussein NA: Lipocalin. A novel diagnostic marker for hepatocellular carcinoma in chronic liver disease patients in Egypt. Int. J. Clin. Med. (2013), 4:440-450.

Ernst M, Najdovska M, Grail D, Lundgren - May T, Buchert M, Tye H, Matthews VB, Armes J, Bhathal PS, Hughes NR, Marcusson EG, Karras JG, Na S, Sedgwick JD, Hertzog PJ, Jenkins BJ. STAT3 and STAT1 mediate IL - 11 - dependent and inflammation - associated gastric tumorigenesis in gp130 receptor mutant mice. J Clin Invest. (2008), 118:1727-1738.

Faller A, Schünke, M. Der Körper des Menschen. Thieme: Stuttgart, Germany. 2004 (in English), 423-428.

Fierbinteanu - **Braticevici** C, Dina I, Petrisor A, Tribus L, Negreanu L, Carstoiu C.: Noninvasive investigations for non - alcoholic fatty liver disease and liver fibrosis. World J. Gastroenterol. (2010), 16:4784-4791.

Flo TH, Smith KD, Sato S, Rodriguez DJ, Holmes MA, Strong RK, Akira S, Aderem A. Lipocalin 2 mediates an innate immune response to bacterial infection by sequestrating iron. Nature. (2004), 432:917-921.

Flower DR, North AC, Attwood TK. Mouse oncogene protein 24p3 is a member of the lipocalin protein family. Biochem. Biophys. Res. Commun. (1991), 180:69-74.

Flower DR. The lipocalin protein family: structure and function. Biochem. J. (1996), 318:1-14.

Frevert U, Engelmann S, Zougbédé S, Stange J, Ng B, Matuschewski K, Liebes L, Yee H. Intravital observation of Plasmodium berghei sporozoite infection of the liver. PLoS Biol. (2005), 3:e192.

Friedl A, Stoesz SP, Buckley P, Gould MN. Neutrophil gelatinase - associated lipocalin in normal and neoplastic human tissues. Cell type - specific pattern of expression. Histochem. J. (1999), 31:433-441.

Furutani M, Arii S, Mizumoto M, Kato M, Imamura M. Identification of a neutrophil gelatinase - associated lipocalin mRNA in human pancreatic cancers using a modified signal sequence trap method. Cancer Lett. (1998), 122:209-214.

Ganfornina MD, Gutiérrez G, Bastiani M, Sánchez D. A phylogenetic analysis of the lipocalin protein family. Mol. Biol. Evol. (2000), 17:114-126.

Gao J, Serrero G. Adipose differentiation related protein (ADRP) expressed in transfected COS - 7 cells selectively stimulates long chain fatty acid uptake. J. Biol. Chem. (1999), 274:16825-16830.

Godovac - **Zimmermann** J. The structural motif of β - lactoglobulin and retinol - binding protein: a basic framework for binding and transport of small hydrophobic molecules?. Trends Biochem. Sci. (1988), 13:64-66.

Goetz DH, Holmes MA, Borregaard N, Bluhm ME, Raymond KN, Strong RK. The neutrophil lipocalin NGAL is a bacteriostatic agent that interferes with siderophore - mediated iron acquisition. Mol. Cell. (2002), 10:1033-1043.

Goh VJ, Silver DL. The lipid droplet as a potential therapeutic target in NAFLD. Semin. Liver Dis. (2013), 33:312-320.

Grasselli E, Voci A, Pesce C, Canesi L, Fugassa E, Gallo G, Vergani L. PAT protein mRNA expression in primary rat hepatocytes: Effects of exposure to fatty acids. Int. J. Mol. Med. (2010), 25:505-512.

Greenberg AS, Egan JJ, Wek SA, Garty NB, Blanchette - Mackie EJ, Londos C. Perilipin, a major hormonally regulated adipocyte - specific phosphoprotein associated with the periphery of lipid storage droplets. J. Biol. Chem. (1991), 266:11341-11346.

Guo H, Bazuine M, Jin D, Huang MM, Cushman SW, Chen X. Evidence for the regulatory role of lipocalin 2 in high - fat diet - induced adipose tissue remodeling in male mice. Endocrinology. (2013), 154:3525-3538.

Guo H, Jin D, Zhang Y, Wright W, Bazuine M, Brockman DA, Bernlohr DA, Chen X. Lipocalin - 2 deficiency impairs thermogenesis and potentiates diet - induced insulin resistance in mice. Diabetes. (2010), 59:1376-1385.

Guobin H and Karin M. NF - κB and STAT3 – key players in liver inflammation and cancer. Cell Res. (2011), 21:159–168.

Guzmán C, Benet M, Pisonero - Vaquero S, Moya M, García - Mediavilla MV, Martínez - Chantar ML, González - Gallego J, Castell JV, Sánchez - Campos S, Jover R. The human liver fatty acid binding protein [FABP1] gene is activated by FOXA1 and PPARα; and repressed by C/EBPα: Implications in FABP1 down - regulation in nonalcoholic fatty liver disease. Biochim. Biophys. Acta. (2013), 1831:803-818.

Heid HW, Schnölzer M, Keenan TW. Adipocyte differentiation - related protein is secreted into milk as a constituent of milk lipid globule membrane. Biochem J.(1996), 320: 1025-1030.

Horn KD, Wax P, Schneider SM, Martin TG, Nine JS, Moraca MA, Virji MA, Aronica PA, Rao KN. Biomarkers of liver regeneration allow early prediction of hepatic recovery after acute necrosis. Am. J. Clin. Pathol. (1999), 112:351-357.

Hraba - Renevey S, Türler H, Kress M, Salomon C, Weil R. SV40 - induced expression of mouse gene 24p3 involves a post - transcriptional mechanism. Oncogene. (1989), 4: 601–608.

Hvidberg V, Jacobsen C, Strong RK, Cowland JB, Moestrup SK, Borregaard N. The endocytic receptor megalin binds the iron transporting neutrophil - gelatinase - associated lipocalin with high affinity and mediates its cellular uptake. FEBS Lett. (2005), 579:773-777.

Ip E, Farrell GC, Robertson PH, Leclercq GI. Administration of the potent PPARalpha agonist, Wy - 14,643, reverses nutritional fibrosis and steatohepatitis in mice. Hepatology. (2004), 39:1286–1296.

Ito M, Suzuki J, Tsujioka S, Sasaki M, Gomori A, Shirakura T, Hirose H, Ito M, Ishihara A, Iwaasa H, Kanatani A. Longitudinal analysis of murine steatohepatitis model induced by chronic exposure to high - fat diet. Hepatol. Res. (2007), 37: 50–57.

Jaruga B, Hong F, Kim WH, Gao B, IFN - gamma/STAT1 acts as a proinflammatory signal in T cell - mediated hepatitis via induction of multiple chemokines and adhesion molecules: a critical role of IRF - 1. Am J Physiol Gastrointest Liver Physiol. (2004), 287:G1044-G1052.

Jha MK, Jeon S, Jin M, Ock J, Kim JH, Lee WH, Suk K. The pivotal role played by lipocalin - 2 in chronic inflammatory pain. Exp Neurol. (2014), 254:41-53.

Jiang W, Constante M, Santos MM. Anemia upregulates lipocalin 2 in the liver and serum. Blood Cells Mol. Dis. (2008), 41:169-174.

Jin D, Guo H, Bu SY, Zhang Y, Hannaford J, Mashek DG, Chen X. Lipocalin 2 is a selective modulator of peroxisome proliferator - activated receptor - γ activation and function in lipid homeostasis and energy expenditure. FASEB J. (2011), 25:754-764.

Jones MR, Quinton LJ, Simms BT, Lupa MM, Kogan MS, Mizgerd J. Roles of interleukin - 6 in activation of STAT proteins and recruitment of neutrophils during Escherichia coli pneumonia. J Infect Dis. (2006), 193:360-369.

Joshi - Barve S, Barve SS, Amancherla K, Gobejishvili L, Hill D, Cave M, Hote P, McClain CJ, Palmitic acid induces production of proinflammatory cytokine interleukin - 8 from hepatocytes. Hepatology. (2007), 46:823-830.

Kienzl - Wagner K, Moschen AR, Geiger S, Bichler A, Aigner F, Brandacher G, Pratschke J, Tilg H. The role of lipocalin - 2 in liver regeneration. Liver Int. (2014), 35:1195-1202.

Kim JW, Lee SH, Jeong SH, Kim H, Ahn KS, Cho JY, Yoon YS, Han HS. Increased urinary lipocalin - 2 reflects matrix metalloproteinase - 9 activity in chronic hepatitis C with hepatic fibrosis. Tohoku J. Exp. Med. (2010), 222:319-327.

Kirsch R, Clarkson V, Shephard EG, Marais DA, Jaffer MA, Woodburne VE, Kirsch RE, Hall Pde L. Rodent nutritional model of non - alcoholic steatohepatitis: species, strain and sex difference studies. J. Gastroenterol. Hepatol. (2003), 18:1272-1282.

Kjeldsen L, Johnsen AH, Sengeløv H, Borregaard N, Isolation and primary structure of NGAL, a novel protein associated with human neutrophil gelatinase, J. Biol. Chem. (1993), 268:10425–10432.

Kleiner D.E., E.M. Brunt, M. Van Natta, C. Behling, M.J. Contos, O.W. Cummings, L.D. Ferrell, Y.C. Liu, M.S. Torbenson, A. Unalp - Arida, M. Yeh, A.J. McCullough, A.J. Sanyal, Nonalcoholic Steatohepatitis Clinical Research Network. Design and validation of a histological scoring system for nonalcoholic fatty liver disease, Hepatology. (2005), 41:1313–1321.

Kmiec Z. Cooperation of liver cells in health and disease. Adv. Anat. Embryol. Cell Biol. (2001), 161:1–151.

Koopman R., G. Schaart, M.K. Hesselink. Optimisation of oil red O staining permits combination with immunofluorescence and automated quantification of lipids. Histochem. Cell Biol. (2001), 116:63–68.

Krahmer N, Guo Y, Wilfling F, Hilger M, Lingrell S, Heger K, Newman HW, Schmidt - Supprian M, Vance DE, Mann M, Farese RV Jr, Walther TC. Phosphatidylcholine synthesis for lipid droplet expansion is mediated by localized activation of CTP:phosphocholine cytidylyltransferase. Cell Metab. (2011), 14 504-515.

Kubes P, Granger DN. Leukocyte - endothelial cell interactions evoked by mast cells. Cardiovasc Res. (1996), 32:699–708.

Kurtz DT, Feigelson P. Multihormonal induction of hepatic α2u - globulin mRNA as measured by hybridization to complementary DNA. Proc Natl Acad Sci U S A. (1977), 74:4791-4795.

Labbus K, Henning M, Borkham - Kamphorst E, Geisler C, Berger T, Mak TW, Knüchel R, Meyer HE, Weiskirchen R, Henkel C. Proteomic profiling in Lipocalin 2 deficient mice under normal and inflammatory conditions. J. Proteomics (2013), 78:188-196 .

Lai HS, Wu YM, Lai SL, Lin WH: Lipocalin - 2 gene expression during liver regeneration after partial hepatectomy in rats. Int. J. Surg. (2013), 11:314-318.

Lança T, Costa MF, Gonçalves - Sousa N, Rei M, Grosso AR, Penido C, Silva - Santos B. Protective role of the inflammatory CCR2/CCL2 chemokine pathway through recruitment of type 1 cytotoxic γδ T lymphocytes to tumor beds. J Immunol. (2013), 190:6673-6680.

Lang R. Tuning of macrophage responses by Stat3 - inducing cytokines: molecular mechanisms and consequences in infection. Immunobiology. (2005), 210:63–76.

Langer HF, Chavakis T. Leukocyte - endothelial interactions in inflammation. J Cell Mol Med. (2009), 13:1211–1220.

Larter CZ, Yeh MM, James OF. Animal models of NASH: Getting both pathology and metabolic context right Steatohepatitis: A tale of two "hits"? Gastroenterology. (1998), 114:842–845.

Larter CZ, Yeh MM, Williams J, Bell - Anderson KS, Farrell GC. MCD - induced steatohepatitis is associated with hepatic adiponectin resistance and adipogenic transformation of hepatocytes. J. Hepatol. (2008), 49:407-416.

Lee EK, Kim HJ, Lee KJ, Lee HJ, Lee JS, Kim DG, Hong SW, Yoon Y, Kim JS. Inhibition of the proliferation and invasion of hepatocellular carcinoma cells by lipocalin 2 through blockade of JNK and PI3K/Akt signaling. Int. J. Oncol. (2011), 38:325-333.

Lee HJ, Lee EK, Lee KJ, Hong SW, Yoon Y, Kim JS. Ectopic expression of neutrophil gelatinase - associated lipocalin suppresses the invasion and liver metastasis of colon cancer cells. Int. J. Cancer. (2006), 118:2490-2497.

Lee S, Kim JH, Kim JH, Seo JW, Han HS, Lee WH, Mori K, Nakao K, Barasch J, Suk K. Lipocalin - 2 Is a chemokine inducer in the central nervous system: role of chemokine ligand 10 (CXCL10) in lipocalin - 2 - induced cell migration. J Biol Chem. (2011), 286:43855-43870.

Li H, Song Y, Zhang LJ, Gu Y, Li FF, Pan SY, Jiang LN, Liu F, Ye J, Li Q. LSDP5 enhances triglyceride storage in hepatocytes by influencing lipolysis and fatty acid β - oxidation of lipid droplets. PLoS One. (2012), 7:e36712.

Lindberg S, Jensen JS, Mogelvang R, Pedersen SH, Galatius S, Flyvbjerg A, Magnusson NE. Plasma neutrophil gelatinase - associated lipocalinin in the general population: association with inflammation and prognosis. Arterioscler Thromb Vasc Biol. (2014), 34:2135-2142.

Listenberger LL, Brown DA. Fluorescent detection of lipid droplets and associated proteins. Curr. Protoc. Cell Biol. (2007), 24:24.2.

Liu Q, Nilsen - Hamilton M. Identification of a new acute phase protein. J. Biol. Chem. (1995), 270:22565-22570.

Liu Q, Ryon J, Nilsen - Hamilton M. Uterocalin: a mouse acute phase protein expressed in the uterus around birth. Mol. Reprod. Dev. (1997), 46:507-514.

Liu W, Baker SS, Baker RD, Nowak NJ, Zhu L. Upregulation of haemoglobin expression by oxidative stress in hepatocytes and its implication in non - alcoholic steatohepatitis. PLoS One. (2011), 6:e24363.

Liu Z, Petersen R, Devireddy L. Impaired neutrophil function in 24p3 null mice contributes to enhanced susceptibility to bacterial infections. J Immunol. (2013), 190:4692-4706.

Löffler G, Petrides PE. Biochemie und Pathobiochemie. Springer. 1998, 6:1024-1036.

Lögdberg L, Wester L: Immunocalins: a lipocalin subfamily that modulates immune and inflammatory responses. Biochim. Biophys. Acta. (2000), 1482:284-297.

Londos C, Sztalryd C, Tansey JT, Kimmel AR. Role of PAT proteins in lipid metabolism, Biochimie (2005), 87:45-49.

Marchese S, Pes D, Scaloni A, Carbone V, Pelosi P. Lipocalins of boar salivary glands binding odours and pheromones. Eur. J. Biochem. (1998), 252:563-568.

Matarese V, Buelt MK, Chinander LL, Bernlohr DA. Purification of adipocyte lipid - binding protein from human and murine cells. Methods Enzymol. (1990), 189:363-369.

McManaman JL, Bales ES, Orlicky DJ, Jackman M, MacLean PS, Cain S, Crunk AE, Mansur A, Graham CE, Bowman TE, Greenberg AS. Perilipin - 2 - null mice are protected against diet - induced obesity, adipose inflammation, and fatty liver disease. J. Lipid Res. (2013), 54:1346-1359.

Mehrabian M, Sparkes RS, Mohandas T, Fogelman AM, Lusis AJ, Localization of monocyte chemotactic protein - 1 gene (SCYA2) to human chromosome 17q11.2 - q21.1. Genomics. (1991), 9:200–203.

Milner KL, Van der Poorten D, Xu A, Bugianesi A, Kench JG, Lam KS, Chisholm DJ, George J. Adipocyte fatty acid binding protein levels relate to inflammation and fibrosis in nonalcoholic fatty liver disease. Hepatology. (2009), 49:1926-1934.

Mishra J, Dent C, Tarabishi R, Mitsnefes MM, Ma Q, Kelly C, Ruff SM, Zahedi K, Shao M, Bean J, Mori K, Barasch J, Devarajan P. Neutrophil gelatinase - associated lipocalin (NGAL) as a biomarker for acute renal injury after cardiac surgery. Lancet. (2005), 365:1231-1238.

Mishra J, Ma Q, Prada A, Mitsnefes M, Zahedi K, Yang J, Barasch J, Devarajan P. Identification of neutrophil gelatinase - associated lipocalin as a novel early urinary biomarker for ischemic renal injury. J. Am. Soc. Nephrol. (2003), 14:2534-2543.

Mishra J, Mori K, Ma Q, Kelly C, Barasch J, Devarajan P. Neutrophil gelatinase - associated lipocalin: a novel early urinary biomarker for cisplatin nephrotoxicity. Am. J. Nephrol. (2004), 24:307-315.

Monier F, Surla A, Guillot M, Morel F. Gelatinase isoforms in urine from bladder cancer patients. Clin. Chim. Acta. (2000), 299:11- 3.

Motomura W, Inoue M, Ohtake T, Takahashi N, Nagamine M, Tanno S, Kohgo Y, Okumura T. Up - regulation of ADRP in fatty liver in human and liver steatosis in mice fed with high fat diet. Biochem. Biophys. Res. Commun. (2006), 340:1111-1118.

Myers RP. Non - invasive diagnosis of nonalcoholic fatty liver disease. Ann. Hepatol. (2009), 1:S25-S33.

Nagase T, Kikuno R, Ohara O. Prediction of the coding sequences of unidentified human genes. XXI. The complete sequences of 60 new cDNA clones from brain which code for large proteins. DNA Res. (2001), 8:179-187.

Newcomer ME, Ong DE. Plasma retinol binding protein: structure and function of the prototypic lipocalin. Biochim. Biophys. Acta. (2000), 1482:57-64.

Neyzen S, Van de Leur E, Borkham - Kamphorst E, Herrmann J, Hollweg G, Gressner AM, Weiskirchen R. Cryopreservation of hepatic stellate cells. J. Hepatol. (2006), 44: 910–917.

Nielsen BS, Borregaard N, Bundgaard JR, Timshel S, Sehested M, Kjeldsen L. Induction of NGAL synthesis in epithelial cells of human colorectal neoplasia and inflammatory bowel diseases. Gut. (1996), 38:414-420.

Niemann CU, Walia A, Waldman J, Davio M, Roberts JP, Hirose R, Feiner J. Acute kidney injury during liver transplantation as determined by neutrophil gelatinase - associated lipocalin. Liver Transpl. (2009), 15:1852-1860.

Okumura T. Role of lipid droplet proteins in liver steatosis. J Physiol Biochem. (2011), 67:629-636.

Pan H, Ma Y, Wang D, Wang J, Jiang H, Pan S, Zhao B, Wu Y, Xu D, Sun X, Liu L, Xu Z. Effect of IFN - α on KC and LIX expression: role of STAT1 and its effect on neutrophil recruitment to the spleen after lipopolysaccharide stimulation. Mol Immunol. (2013), 56:12-22.

Pervaiz S, Brew K. Homology and structure - function correlations between alpha 1 - acid glycoprotein and serum retinol - binding protein and its relatives. FASEB J. (1987), 1:209-214.

Pervaiz S, Brew K. Homology of β - lactoglobulin, serum retinol - binding protein, and protein HC. Science (1985), 228:335-337.

Pickens MK, Ogata H, Soon RK, Grenert JP, Maher JJ. Dietary fructose exacerbates hepatocellular injury when incorporated into a methionine - choline - deficient diet. Liver Int. (2010), 30:1229-1239.

Pickens MK, Yan JS, Ng RK, Ogata H, Grenert JP, Beysen C, Turner SM, Maher JJ. Dietary sucrose is essential to the development of liver injury in the methionine - choline - deficient model of steatohepatitis. J Lipid Res. (2009), 50:2072-2082.

Pocock G, Richards C. Human Physiology, The basis of Medicine. Oxford University Press. (2006), 3:404.

Przanowski P, Dabrowski M, Ellert - Miklaszewska A, Kloss M, Mieczkowsk J, Kaza B, Ronowicz A, Hu F, Piotrowski A, Kettenmann H, Komorowski J, Kaminska B. The signal transducers Stat1 and Stat3 and their novel target Jmjd3 drive the expression of inflammatory genes in microglia. J Mol Med (Berl). (2014), 92:239-254.

Qureshi K, Abrams GA. Metabolic liver disease of obesity and role of adipose tissue in the pathogenesis of nonalcoholic fatty liver disease. World J Gastroenterol. (2007), 13:3540-3553.

Rathore KI, Berard JL, Redensek A, Chierzi S, Lopez - Vales R, Santos M, Akira S, David S. Lipocalin 2 plays an immunomodulatory role and has detrimental effects after spinal cord injury. J Neurosci. (2011), 31:13412-13419.

Rinella EM, and Green RM, The methionine - choline deficient dietary model of steatohepatitis does not exhibit insulin resistance. J. Hepatol. (2004), 40:47–51.

Rogue A, Anthérieu S, Vluggens A, Umbdenstock T, Claude N, De la Moureyre - Spire C, Weaver RJ, Guillouzo A. PPAR agonists reduce steatosis in oleic acid - overloaded HepaRG cells. Toxicol. Appl. Pharmacol. (2014), 276:73-81.

Roth GA, Nickl S, Lebherz - Eichinger D, Schmidt EM, Ankersmit HJ, Faybik P,Hetz H, Krenn CG. Lipocalin - 2 serum levels are increased in acute hepatic failure. Transplant Proc. (2013), 45:241-244.

Roudkenar MH, Kuwahara Y, Baba T, Roushandeh AM, Ebishima S, Abe S, Ohkubo Y, Fukumoto M. Oxidative stress induced lipocalin 2 gene expression: addressing its expression under the harmful conditions. J. Radiat. Res. (2007), 48:39-44.

Roy AK, Neuhaus OW. Identification of rat urinary proteins by zone and immunoelectrophoresis. Proc Soc Exp Biol Med. (1966), 121:894-899.

Scheiermann P, Bachmann M, Goren I, Zwissler B, Pfeilschifter J, Mühl H. Application of interleukin - 22 mediates protection in experimental acetaminophen - induced acute liver injury. Am. J. Pathol. (2013), 182:1107-1113.

Scheurer B, Rittner C, Schneider PM. Expression of the human complement C8 subunits is independently regulated by interleukin 1 β, interleukin 6, and interferon γ. Immunopharmacology. (1997), 38:167-175.

Schmittgen TD, Livak KJ, Analyzing real - time PCR data by the comparative CT method. Nat. Protoc. (2008), 3:1101–1108.

Seber S, Ucak S, Basat O, Altuntas Y. The effect of dual PPAR alpha/gamma stimulation with combination of rosiglitazone and fenofibrate on metabolic parameters in type 2 diabetic patients. Diabetes. Res. Clin. Pract. (2006), 71:52 - 58.

Seglen PO. Preparation of isolated rat liver cells. Methods Cell Biol. (1976), 13:29–83.

Seki S, Kitada T, Yamada T, Sakaguchi H, Nakatani K, Wakasa K. In situ detection of lipid peroxidation and oxidative DNA damage in non - alcoholic fatty liver diseases. J Hepatol. (2002),37:56–62.

Semba T, Nishimura M, Nishimura S, Ohara O, Ishige T, Ohno S, Nonaka K, Sogawa K, Satoh M, Sawai S, Matsushita K, Imazeki F, Yokosuka O, Nomura F. The FLS [fatty liver Shionogi] mouse reveals local expressions of lipocalin - 2, CXCL1 and CXCL9 in the liver with non - alcoholic steatohepatitis. BMC Gastroenterol. (2013), 13:120.

Shashidharamurthy R, Machiah D, Aitken JD, Putty K, Srinivasan G, Chassaing B, Parkos CA, Selvaraj P, Vijay - Kumar M. Differential role of lipocalin 2 during immune complex - mediated acute and chronic inflammation in mice. Arthritis Rheum. (2013), 65:1064-1073.

Sheng L, Cho KW, Zhou Y, Shen H, Rui L. Lipocalin 13 protein protects against hepatic steatosis by both inhibiting lipogenesis and stimulating fatty acid β - oxidation. J. Biol. Chem. (2011), 286:38128-38135.

Shi H, Luo J, Zhu J, Li J, Sun Y, Lin X, Zhang L, Yao D, Shi H. PPARγ regulates genes involved in triacylglycerol synthesis and secretion in mammary gland epithelial cells of dairy goats. PPAR Res. (2013), 2013:310948

Slamon DJ, Clark GM, Wong SG, Levin WJ, Ullrich A, McGuire WL. Human breast cancer: correlation of relapse and survival with amplification of the HER - 2/neu oncogene. Science (1987), 235:177-182.

Stoesz SP, Friedl A, Haag JD, Lindstrom MJ, Clark GM, Gould MN. Heterogeneous expression of the lipocalin NGAL in primary breast cancers. Int. J. Cancer. (1998), 79:565-572.

Stoesz SP, Gould MN. Overexpression of neu - related lipocalin (NRL) in neu - initiated but not ras or chemically initiated rat mammary carcinomas. Oncogene (1995), 11:2233-2241.

Sultan S, Cameron S, Ahmad S, Malik IA, Schultze FC, Hielscher R, Rave - Fränk M, Hess CF, Ramadori G, Christiansen H. Serum Lipocalin2 is a potential biomarker of liver irradiation damage. Liver Int. (2013) 33:459 - 468.

Sultan S, Pascucci M, Ahmad S, Malik IA, Bianchi A, Ramadori P, Ahmad G, Ramadori G. Lipocalin - 2 is a major acute - phase protein in a rat and mouse model of sterile abscess. Shock (2012) 37:191 - 196.

Sunil VR, Patel KJ, Nilsen - Hamilton M, Heck DE, Laskin JD, Laskin DL. Acute endotoxemia is associated with upregulation of lipocalin 24p3/Lcn2 in lung and liver. Exp. Mol. Pathol. (2007), 83:177 - 187.

Suzuki K, Lareyre JJ, Sánchez D, Gutierrez G, Araki Y, Matusik RJ, Orgebin - Crist MC. Molecular evolution of epididymal lipocalin genes localized on mouse chromosome 2. Gene (2004), 339:49 - 59.

Swirski FK, Robbins CS. Neutrophils usher monocytes into sites of inflammation. Circ Res. (2013), 112:744 - 745.

Tekkesin N, Taga Y, Ibrisim D, Gündogan N. Urinary neutrophil gelatinase - associated lipocalin [uNGAL] levels in patients with nonalcoholic fatty liver disease. Intervent. Med. Appl. Science (2012), 4:132 - 138.

Tietz PS, Larusso NF. Cholangiocyte biology. Current Opinion in Gastroenterology. (2006), 22:279–287.

Triebel S, Bläser J, Reinke H, Tschesche H. A 25 kDa α 2 - microglobulin - related protein is a component of the 125 kDa form of human gelatinase. FEBS Lett. (1992), 314:386 - 388.

Valapala M, Edwards M, Hose S, Grebe R, Bhutto IA, Cano M, Berger T, Mak WT, Wawrousek E, Handa JT, Lutty GA, Samuel Zigler JJr, Sinha D. Increased Lipocalin - 2 in the retinal pigment epithelium of Cryba1 cKO mice is associated with a chronic inflammatory response. Aging Cell. (2014), 13:1091 - 1094.

Viau A, El Karoui K, Laouari D, Burtin M, Nguyen C, Mori K, Pillebout E, Berger T, Mak TW, Knebelmann B, Friedlander B, Barasch J, Terzi F. Lipocalin 2 is essential for chronic kidney disease progression in mice and humans. J. Clin. Invest. (2010), 120:4065–4076.

Wang H, Lafdil F, Kong X, Gao B. Signal transducer and activator of transcription 3 in liver diseases: a novel therapeutic target. Int J Biol Sci. (2011), 7:536-550.

Wang H, Sreenivasan U, Hu H, Saladino A, Polster BM, Lund LM, Gong DW, Stanley WC, Sztalryd C. Perilipin 5, a lipid droplet - associated protein, provides physical and metabolic linkage to mitochondria. J. Lipid Res. (2011), 52:2159-2168.

Wang Y, Lam KS, Kraegen EW, Sweeney G, Zhang J, Tso AW, Chow WS, Wat NM, Xu JY, Hoo RL, Xu A. Lipocalin - 2 is an inflammatory marker closely associated with obesity, insulin resistance, and hyperglycemia in humans. Clin. Chem. (2007), 53:34-41.

Westerbacka J, Kolak M, Kiviluoto T, Arkkila P, Sirén J, Hamsten A, Fisher RM, Yki - Järvinen H. Genes involved in fatty acid partitioning and binding, lipolysis, monocyte/macrophage recruitment, and inflammation are overexpressed in the human fatty liver of insulin - resistant subjects. Diabetes. (2007), 56:2759-2765.

Wolins NE, Brasaemle DL, Bickel PE. A proposed model of fat packaging by exchangeable lipid droplet proteins. FEBS Lett. (2006), 580:5484-5491

Wolins NE, Quaynor BK, Skinner JR, Tzekov A, Croce MA, Gropler MC, Varma V, Yao - Borengasser A, Rasouli N, Kern PA, Finck BN, Bickel PE. OXPAT/PAT - 1 is a PPAR - induced lipid droplet protein that promotes fatty acid utilization. Diabetes. (2006), 55:3418-3428.

Wolins NE, Skinner JR, Schoenfish MJ, Tzekov A, Bensch KG, Bickel PE. Adipocyte protein S3 - 12 coats nascent lipid droplets. J Biol Chem. (2003), 278:37713-37721.

Xu MJ, Feng D, Wu H, Wang H, Chan Y, Kolls J, Borregaard N, Porse B, Berger T, Mak TW, Cowland JB, Kong X, Gao B. The liver is the major source of elevated serum lipocalin - 2 levels after bacterial infection or partial hepatectomy: A critical role for IL - 6/STAT3. Hepatology. (2014), 61:692-702.

Xu SY, Carlson M, Engström A, Garcia R, Peterson CG, Venge P. Purification and characterization of a human neutrophil lipocalin (HNL) from the secondary granules of human neutrophils. Scand. J. Clin. Lab. Invest. (1994), 54:365-376.

Yamaguchi T, Matsushita S, Motojima K, Hirose F, Osumi T. MLDP, a novel PAT family protein localized to lipid droplets and enriched in the heart, is regulated by peroxisome proliferator - activated receptor alpha. J Biol Chem. (2006), 281:14232–14240.

Yan QW, Yang Q, Mody N, Graham TE, Hsu CH, Xu Z, Houstis NE, Kahn BB, Rosen ED. The adipokine lipocalin 2 is regulated by obesity and promotes insulin resistance. Diabetes (2007), 56:2533-2540.

Yang J, Goetz D, Li JY, Wang W, Mori K, Setlik D, Du T. Erdjument - Bromage H, Tempst P, Strong R, Barasch J. An iron delivery pathway mediated by a lipocalin. Mol. Cell. (2002), 10:1045-1056.

Yao ZM, Vance DE. The active synthesis of phosphatidylcholine is required for very low density lipoprotein secretion from rat hepatocytes. J Biol Chem. (1988), 263:2998-3004.

Ye P, Cheah IK, Halliwell B. High fat diets and pathology in the guinea pig. Atherosclerosis or liver damage?. Biochim Biophys Acta (2013), 1832:3553-3564

Ye Z, Wang S, Yang Z, He M, Zhang S, Zhang W, Wen J, Li Q, Huang Y, Wang X, Lu B, Zhang Z, Su Q, Hu R. Serum lipocalin - 2, cathepsin S and chemerin levels and nonalcoholic fatty liver disease. Mol. Biol. Rep. (2014), 41:1317-1323.

Yoshimura A. Signal transduction of inflammatory cytokines and tumor development. Cancer Sci. (2006), 97:439-447.

Zhang J, Wu Y, Zhang Y, LeRoith D, Bernlohr DA, Chen X. The Role of Lipocalin 2 in the Regulation of Inflammation in Adipocytes and Macrophages. Mol Endocrinol. (2008), 22:1416–1426.

Zhang Y, Fan Y, Mei Z. NGAL and NGALR overexpression in human hepatocellular carcinoma toward a molecular prognostic classification. Cancer Epidemiol. (2012) 36:294-299.

Zhang Y, Foncea R, Deis JA, Guo H, Bernlohr DA, Chen X. Lipocalin 2 expression and secretion is highly regulated by metabolic stress, cytokines, and nutrients in adipocytes. PLoS One (2014), 9:e96997.

Zhang Y, Guo H, Deis JA, Mashek MG, Zhao M, Ariyakumar D, Armien AG, Bernlohr DA, Mashek DG, Chen X. Lipocalin 2 regulates brown fat activation via a nonadrenergic activation mechanism. J Biol Chem. (2014), 289:22063-22077.

Zhao CY, Yan L, Wang YD, Wang W, Zhou JY, Zhen Z. Role of resistin in inflammation of hepatocytes in nonalcoholic steatohepatitis. Zhonghua Gan Zang Bing Za Zhi. (2009), 17:683-687.

Zhao P, Elks CM, Stephens JM. The induction of lipocalin - 2 protein expression *in vivo* and *in vitro*, J Biol. Chem. (2014), 289:5960-5969.

10 Appendix

10.1 Supplementary tables

Gene	Acc. No.	Primer (5'→ 3')
ATGL	NM_001163689.1	for: 5'-gaccatctgccttccaga-3' rev: 5'- tgtaggtggcgcaagaca-3'
ATP5-β	NM_016774	for: 5'-gcaaggcagggacagcaga-3' rev: 5'-cccaaggtctcaggaccaaca-3'
CCL2	NM_011333	for: 5'-gtgttggctcagccagatgc-3' rev: 5'- gacacctgctgctggtgatcc-3'
CCR2	NM_009915.2	for: 5'-tcgctgtaggaatgagaa-3' rev: 5'-caaggattcctggaaggtggtcaa-3'
CD45	NM_001111316.1	for: 5'- cttcagagaccacatatcatcca-3' rev: 5'- gtctgcgagtcaggctgtg - 3'
Cox IV	NM_009941	for: 5'-atgtcacgatgctgtctgcc-3' rev: 5'-gtgcccctgttcatctcggc-3'
CPT1	NM_153679	for: 5'-agagaagcctgccagtttgtgaga-3' rev: 5'-tgtacagtgcaaagaggtgacggt-3'
CTP1-β	NM_009948	for: 5'-tctaggcaatgccgttcac-3' rev: 5'-gagcacatgggcaccatac-3'
GAPDH	XM_001473623	for: 5'-actgccacccagaagactg-3' rev: 5'-caccaccctgttgctgtag-3'
HSL	NM_010719.5	for: 5'- agcgctggaggagtgtttt-3' rev: 5'- ccgctctccagttgaacc-3'
HTGL	AY228765.1]	for: 5'- gacaaggcgtgggaacag-3' rev: 5'- tttaatggcttgctagcttcagt-3'
IL-1β	NM_008361	for: 5'- tgtaatgaaagacggcacacc -3' rev: 5'- tcttcttgggtattgcttgg-3'
IL-6	NM_031168	for: 5'-gctaccaaactggatataatcagga-3' rev: 5'-ccaggtagctatggtactccagaa-3'
LCN2	NM_008491.1	for: 5'-ccatctatgagctacaagagaacaat-3' rev: 5'-tctgatccagtagcgacagc-3'
MGL	NM_010719.5	for: 5'- tcggaacaagtcggaggt-3' rev: 5'- tcagcagctgtatgccaaag-3'
Nrf1	NM_010938	for: 5'-tggtccagagagtgcttgtgaag-3' rev: 5'-ggaggctgaggaacgatttcttg-3'
PLIN2	M93275.1	for: 5'-ctccactccactgtccacct-3' rev: 5'-gcttatcctgagcaccctga-3'
PLIN3	NM_025836.3	for: 5'-ccacaggatgctgaaaagg-3' rev: 5'-tgatgtccctgaacatgctg-3'
PLIN5	NM_025874.3	for: 5'-gtcggagaagctggtggac-3' rev: 5'-tcagctgccaggactgcta-3'
PPAR-γ	NM_011146.3	for: 5'-tgctgttatgggtgaaactctg-3' rev: 5'-ctgtgtcaaccatggtaatttctt-3'
STAT1	U06924.1	for: 5'- aaatgtgaaggatcaagtcatgtg-3' rev: 5'- catcttgtaattcttctagggtcttga - 3'
STAT3	NM_213659.2	for: 5'- ggaaataacggtgaaggtgct -3' rev: 5'- catgtcaaacgtgagcgact -3'
Tfam	NC_000076	for: 5' -cactgggaaaccacagcatacag-3' rev: 5'-ggacatctgaggaaaagccttgc-3'
TNF-α	NM_013693	for: 5'- accacgctcttctgtctactga-3' rev: 5'- tccacttggtggtttgctacg-3'

Table 10-i: Oligonucleotides-Primers used for PCR and q-RT-PCR

Antibody	Cat. No.	Clonality*	Supplier	Species*	Dilution*
Primary antibodies					
BAX	2772S	poly, rabbit	Cell signaling	h, m, r, mk	1:1,000
BCL-2	2870S	mono, rabbit	Cell signaling	h, m, r	1:1,000
CD45	553076	mono, rat	BD biosciences	m	1:1,000 (WB), 1:50 (IHC)
cl. CASP-3	9664L	mono, rabbit	Cell signaling	h, m, r, mk	1:1,000
GAPDH	sc-32233	mono, mouse	Santa Cruz	h, m, r	1:10,000
IL-1β	AF401NA	poly, goat	R&D Systems	m	1:1000
LCN2	AF3508	poly, goat	R&D Systems	m, r	1:1,000 (WB), 1:50 (IFC)
MPO	HP9048	poly, rabbit	Hycult Biotech	h, m, r	1:100 (IFH)
PLIN2	NB-110-40877	poly, rabbit	Novus Biologicals	h, m	1:1,000
PLIN3	NB-110-40765	poly, rabbit	Novus Biologicals	h, m	1:1,000
PLIN5	NB-110-60509	poly, rabbit	Novus Biologicals	h, m	1:1,000 (WB), 1:50 (IHC, IFC)
pSTAT1	9167L	mono, rabbit	Cell signaling	h, m	1:1,000
pSTAT3	9131S	poly, rabbit	Cell signaling	h, m, r, c, d	1:1,000
STAT1	sc346	poly, rabbit	Santa Cruz	m, r, h, x	1:1,000
STAT3	sc7179	poly, rabbit	Santa Cruz	m, r, h, z, x	1:1,000
β-ACTIN	A5441	mono, mouse	Sigma-Aldrich	h, m, r	1:10,000
Secondary antibodies					
Alexa Fluor 488 - IgG	A11055	N/A	Life technologies	g	1:200 (IFC)
Alexa Fluor 488 - IgG	A21206	N/A	Life technologies	rb	1:200 (IFH)
Alexa Fluor 555 -IgG	A31572	N/A	Life technologies	rb	1:200 (IFH), 1:500 (IFC)
IgG-Biotinylated	E0353	N/A	DAKO	rb	1:300 (IHC)
IgG-Biotinylated	BA-9400	N/A	Vector Lab.	r	1:300 (IHC)
IgG-HRP	sc-2004	N/A	Santa Cruz	rb	1:5,000
IgG-HRP	sc-2005	N/A	Santa Cruz	m	1:5,000
IgG-HRP	sc-2056	N/A	Santa Cruz	g	1:5,000
IgG-HRP	sc-2032	N/A	Santa Cruz	r	1:5,000
Negative control antibodies					
Normal IgG	sc-2027	rabbit	Santa Cruz	rb	1:100 (IFC, IFHC)
Normal IgG	sc-2028	goat	Santa Cruz	g	1:100 (IFC)
Normal IgG	sc-2026	rat	Santa Cruz	r	1:100 (IHC)

***** Abbreviations used are: mono, monoclonal antibody; poly, polyclonal antibody; N/A, not applicable; h = human, m = mouse, r = rat, rb= rabbit, g = goat, z = zebrafish, x = xenopus, c = cow, d = dog, IHC = immunohistochemistry , IFH = Immunofluorosence-histochemistry, IFC= Immunofluoresence -cytochemistry, WB = Western blot

Table 10-ii: Antibodies used in his study

Plasticware - Glassware	Catalogue no.	Company
Cell Culture 6 well Plate with Lid	353046	Becton Dickinson,Labware Franklin Lakes, USA
Cell culture dish 60 mm x 15 mm	628-160	Greiner Bio-One GmbH, Frickenhausen, Germany
Cell culture dish,10 cm	83.1802	Sarstedt, Nümbrecht, Germany
Cell scraper 240 mm	99002	TPP, Techno Plastic Products, Trasadingen, Switzerland
Centri•Pure P50 Gel Filtration Columns	N/A	Emp Biotech GmbH, Berlin, Germany
Costar® Stripette® serological pipettes, 10 mL	CLS4488	Sigma Aldrich, Steinheim, Germany
Disposable single sealed Cuvettes 50 - 2000 µl	952010051	Eppendorf AG, Hamburg, Germany
Feather disposable scalpel No.11	297511	Feather Safety Razor CO., Osaka, Japan
Folded filters 185 mm	311647	Schleicher & Schuell GmbH, Dassel, Germany
Glass coverslips 24 mm x 24 mm	H875.2	Carl Roth, Karlsruhe, Germany
Glass coverslips 24 mm x 50 mm	1871.2	Carl Roth, Karlsruhe, Germany
Glass Cuvette - QS 10 mm (Precision cells)	108-QS	Hellma Analytics, Mülheim, Germany
GSA centrigugation bottle	N/A	Beckmann, Munich, Germany
Low temeperature Freezer vials- Cryotubes, 2 mL	479-0287	VWR International, Langenfeld, Germany
Microlance Hypodermic Needle 27G x 3/4", 0.4 mm x 19 mm	302200	Becton Dickinson,Labware Franklin Lakes, USA
Microscope glass (76 mm x 26 mm)	03-0004	R. Langenbrinck, Emmendingen, Germany
Microtubes 0.5 mL	72.699	Sarstedt, Nümbrecht, Germany
Microtubes 1.5 mL	72.690.001	Sarstedt Nümbrecht, Germany
Microvette CB 100/200 capillary blood collection tubes	N/A	Sarstedt, Nümbrecht, Germany
MicroAmp® Optical Adhesive Film	4360954	Life technologies, Carlsbad, USA
Original perfusor Syringe 50 mL, Luer Lock, sterile	8728810F	B. Braun, Melsungen, Germany
Parafilm M Laboratory Sealing Film, (100 mm x 75 mm)	7016 06	American National Can, Menasha Wisconsin, USA

Table 10-iii: Material and equipment used in this study

Plasticware - Glassware	Catalogue no.	Company
Petri dish 92 mm x 16 mm with cams	82.1473	Sarstedt, Nümbrecht, Germany
Pipettes Pasteur , glass , Length 150 mm	747715	Brand Wertheim, Germany
Pipettes Pasteur , glass , Length 230 mm	747720	Brand Wertheim, Germany
Pippete tips 10 µl	740011	Biozym Diagnostik, Oldendorf, Germany
Pippete tips 1000 µl	1130401	Heinz Herenz Medizinalbedarf, Hamburg, Germany
Pippete tips 1000 µl with filter	692079	Biozym Diagnostik, Oldendorf, Germany
Pippete tips 200 µl	70.760.02	Starsdedt, Numbrecht, Germany
Pippete tips 200 µl with filter	07.652.7300	Nerbeplus, Winsen, Germany
PS-microplates 96 well, Flat bottom	655101	Greiner Bio-One GmbH, Frickenhausen, Germany
Sterile Syringe Filter 0.20 µm	431219	Corning Inc., NY, USA
Syringe 1mL, Sterile, Concentric Luer Slip	300013	Becton Dickinson, Labware Franklin Lakes, USA
Test Tube 14mL Round BottomPP, with Snap Cap, Sterile, Individually Wrapped	2006	Becton Dickinson, Labware Franklin Lakes, USA
TipOne Filter Pipette Tip, 200µl, sterile, colour: Natural	S1120-8810	Starlab, Merenschwand, Switzerland
Tissue Grind Pestle 21	886001-0021	Kimble & Chase, Gerresheimer, USA
Tissue Grind Tube, size: 21	885752-0021	Kimble & Chase, Gerresheimer, USA
Tissue Tek - Disposable Vinyl Specimen Molds (25 mm x 20 mm x 5 mm)	4557	Sakura Finetek, Tokyo, Japan
Tube 13 mL, 95 mm x 16.8 mm	55.468.001	Sarstedt, Nümbrecht, Germany
Tubes 15 mL	188 280	Greiner Bio-One GmbH, Frickenhausen, Germany
Tubes 50 mL	227 261	Greiner Bio-One GmbH, Frickenhausen, Germany
Vaccum line protector,Vent Filter Unit, Autoclavable	SLFA05010	Millipore, Massachusetts, USA
Whatman Protan BA 83 Nitricellulose Tranfer Membrane	10401396	GE Healthcare, Freiburg, Germany
Whatman Protan BA 85 Nitricellulose Tranfer Membrane	10600002	GE Healthcare, Freiburg, Germany

Table 10-iv: Material and equipment used in this study (cont.)

Chemicals	Catalogue No.	Company
Acetic Acid 99-100%	6052	J.T. Baker, Deventer, The Netherlands
Agarose LE	11685678001	Roche Diagnostics, Mannheim, Germany
Albumin	A-2153	Sigma- Aldrich, Steinheim, Germany
Albumin (cell culture)	A0850,0050	Applichem GmbH, Dramstadt, Germany
Bacto Agar	214010	Becton Dickinson, Labware Franklin Lakes, USA
Bacto Tryptone	211705	Becton Dickinson,Labware Franklin Lakes, USA
Bicine	9162.3	Carl Roth GmbH, Karlsruhe, Germany
Bis-Tris	9140.3	Carl Roth GmbH, Karlsruhe, Germany
Boric acid	1.00165.1000	Merck, Darmstadt, Germany
Bromophenol Blue sodium salt	32768	Sigma- Aldrich, Steinheim, Germany
Chloroform	1.02445.1000	Merck, Darmstadt, Germany
Collagen G from Bovine calf skin, aprox: 4 mg/mLl	L 7213	Biochrom AG, Berlin, Germany
DAKO REAL Hematoxylin	S2020	DAKO Deutschland GmbH, Hamburg, Germany
Deoxycholic Acid (DOC), Na - Salt pure,	18330	Serva Electrophoresis GmbH, Heidelberg, Germany
Deoxynucleoside Triphosphate Set (dNTPs), PCR grade	11969064001	Roche Diagnostics, Mannheim, Germany
Dithiothreitol 1.4 (DTT)	6908.2	Carl Roth, Karlsruhe, Germany
DMSO-Dimethyl sulfoxide	41641	Sigma Aldrich, Steinheim, Germany
Dulbeco's Modified Eagle's Medium (DMEM) 500 mL	D6171	Sigma Aldrich, Steinheim, Germany
Ethannol 70% v/v	64-17-5	Otto Fischer, Saarbrücken, Germany
Ethanol Absolut	27698	Otto Fischer, Saarbrücken, Germany
Ethidium Bromide solution 10 mg/mL	161-0443	Bio-Rad, Munich, Germany
Fetal Bovine Serum 500 mL	F7524	Sigma-Aldrich, Steinheim, Germany
Fluorosence Mounting Medium	S3023	DAKO Deutschland GmbH, Hamburg, Germany

Table 10-v: Material and equipment used in this study (cont.)

Chemicals	Catalogue No.	Company
FORENE Narcotic solution	N01AB06	Abbot, Wiesbaden, Germany
Gentamycin	15710-049	Life technologies, Carlsbad, USA
Glycerol	3783.1	Carl Roth, Karlsruhe, Germany
Glycine Molecular Biology grade	A-1067	Applichem GmbH, Dramstadt, Germany
HepatoZYME SFM (1X) Serum free Medium 500 mL	17705-021	Life technologies, Carlsbad, USA
High fat diet	N/A	Research Diet Services BV, Wijk bij Duurstede, The Netherlands
Hydrochloric acid	100316.1011	Merck, Darmstadt, Germany
Hydrogen Peroxide 30%, H_2O	1.07210.1000	Merck, Darmstadt, Germany
IsoPropanol	6752.4	Carl Roth, Karlsruhe, Germany
Kanamycin sulfate	10106801001	Roche Diagnostics, Mannheim, Germany
L- Glutamine 200mM	G7513	Sigma Aldrich, Steinheim, Germany
Lipofectamin 2000 Reagent 1 mg/mL	11668-019	Life technologies, Carlsbad, USA
Lithium Chloride	1056790250	Merck , Darmstadt, Germany
Magnesium Chloride Hexahydrate	1.05833.1000	Merck , Darmstadt, Germany
Magnesium Sulphate Heptahydrate	1.05886.1000	Merck, Darmstadt, Germany
MES	4256.4	Carl Roth, Karlscruhe, Germany
Methanol	20847.295	VWR Chemicals, Fontenay-sous-Bois, France
Methionine/ Choline deficient diet, pellets	960439	MP Biomedicals, Illkirch, France
MgCl2 Stock solution	14534600	Roche Diagnostics, Mannheim, Germany
MOPS	6979.3	Carl Roth, Karlsruhe, Germany
NEEA (Non Essential Amino Acids) 100X, 100 mL	BE13-114E	Lonza, Verviers, Belgium
Nile Red - Ultra Pure 25 mg	ENZ-52551	Enzo - Life Sciences, Lörrach Germany
Nonidet P40	11754599001	Roche Diagnostics, Mannheim, Germany
NuPAGE® LDS Sample Buffer (4X)	NP0008	Life technologies, Carlsbad, USA
Oil Red O	O-0625	Sigma Aldrich, Steinheim, Germany
Oleic Acid-Albumin	O3008-5ML	Sigma Aldrich, Steinheim, Germany

Table 10-vi: Material and equipment used in this study (cont.)

Chemicals	Catalogue No.	Company
Opti-MEM I; Reduce Serum Medium	31985-070	Life technologies, Carlsbad, USA
Palmitic Acid	P-0500-10G	Sigma Aldrich, Steinheim, Germany
Parafomaldehyde extra pure	K10362105	Merck , Darmstadt, Germany
PCR Buffer 10x without MgCl2	14109300	Roche Diagnostics, Mannheim, Germany
Pen/Strep stock, 10K/10K 100 mL	DE17-602E	Lonza , Verviers, Belgium
Polyethylene Glycole (PEG)	P-2139	Sigma Aldrich, Steinheim, Germany
Ponceau S, sodium salt	P-3504	Sigma Aldrich, Steinheim, Germany
Potassium Phosphate Monobasic	5104	Merck, Darmstadt, Germany
Potassium Acetate	4986.1	Roche Diagnostics, Manheim, Germany
Potassium Chloride	1.04936.0500	Merck, Darmstadt, Germany
Potassium dihydrogen Phosphate	1.04873.1000	Merck, Darmstadt, Germany
Potassium Sulfate	1.05153.0500	Merck, Darmstadt, Germany
Powdered Milk	T-145.3	Carl ROTH GmbH, Karlsruhe, Germany
QIAzol Lysis Reagent	79306	Qiazen Sciences, Maryland, USA
Random Primers 20 µg	c1181	Promega Co. Madison, USA
Rosiglitazone 50 mg	ab120762	Abacam Biochemicals, Cambridge, UK
Roti®-C/I Phenol for DNA/RNA Isolation	A156.1	Carl Roth, Karlscruhe, Germany
Rubidium chloride	R2252	Sigma Aldrich, Steinheim, Germany
SDS	4360.2	Carl Roth Gmbh, Karlsruhe, Germany
Sodium Acetate	6268.1	Merck, Darmstadt, Germany
Sodium Carbonate Anhydrous	106392	Merck, Darmstadt, Germany
Sodium Chloride	106404	Merck, Darmstadt, Germany
Sodium Hydroxide 50%	7067	J.T. Baker,Deventer, Holland
Sodium Pyruvate 100 mL	S8636	Sigma Aldrich, Steinheim, Germany
Standard chow diet	N/A	SSNIFF GmbH, Soest, Germany
SYBR Green ER qPCR SuperMix	11760-500	Life technologies, Carlsbad, USA

Table 10-vii: Material and equipment used in this study (cont.)

Chemicals	Catalogue No.	Company
Sodium Pyruvate 100 mL	S8636	Sigma- Aldrich, Steinheim, Germany
Standard chow diet	N/A	SSNIFF GmbH, Soest, Germany
SYBR Green ER qPCR SuperMix	11760-500	Life technologies, Carlsbad, USA
Tissue Tek - O.C.T. compound	4583	Sakura Finetek, Tokyo, Japan
TITRIPLEX III	108418	Merck, Darmstadt, Germany
Tricine	6977.2	Carl Roth, Karlsruhe, Germany
Trisodium citrate	106448	Merck, Darmstadt, Germany
Triton X 100	3051.2	Carl Roth, Karlsruhe, Germany
Trizma Base	T-1503	Sigma Aldrich, Steinheim, Germany
Tween 20	A 4974.0500	Applichem GmbH, Dramstadt, Germany
Xylene	P2N09208831	Otto Fischer, Saarbrücken, Germany
Yeast extract granulated	1.03753	Merck, Darmstadt, Germany
Enzymes	**Catalogue No.**	**Company**
Complete Protease Inhibitor Coctail Tablets	11849300	Roche Diagnostics, Mannheim, Germany
Fermentas-*EcoRI* restriction endonuclease 10 u/µl	ER0271	Thermo Scientific, Rockford, USA
Fermentas-*HindIII* restriction endonuclease 10 u/µl	ER0501	Thermo Scientific, Rockford, USA
Lysozyme	10837059001	Roche Diagnostics, Mannheim, Germany
***PacI* restriction endonuclease**	R0547S	NEB, Ipswich, MA, USA
Phospahatase Inhibitor Coctail, Aqueous solution	P-5726	Sigma Aldrich, Steinheim, Germany
***PmeI* restriction endonuclease**	R0560S	NEB, Ipswich, MA, USA
PureLink DNase	12185-010	Life technologies, Carlsbad, USA
Rnase A	109169	Roche Diagnostics, Mannheim, Germany
***SalI* restriction endonuclease**	10348783001	Roche Diagnostics, Mannheim, Germany
SuperScript II Reverse Transcriptase	18064-022	Life technologies, Carlsbad, USA
***Taq* DNA Polymerase Recombinant**	10342-020	Life technologies, Carlsbad, USA

Table 10-viii: Material and equipment used in this study (cont.)

Molecular size standards	Catalogue No.	Company
GeneRuler 100bp 100 to 1000bpDNA Ladder	SM0241	Thermo Scientific, Rockford, USA
SeeBlue Plus2 prestained Protein Standard	LC5925	Life technologies, Carlsbad, USA
λ DNA-*HindIII* Digest	N3012L	NEB, Ipswich, USA
Vectors	**Catalogue No.**	**Company**
GeneRuler 100bp 100 to 1000bpDNA Ladder	SM0241	Thermo Scientific, Rockford USA
pCMV-SPORT6-mLCN2 vector	IMAGp998L208764Q	ImaGenes GmbH (Source BioScience LifeSciences, Nottingham, UK
pCMV-SPORT6-mPLIN5 vector	IRAVp968B0772D	ImaGenes GmbH (Source BioScience LifeSciences, Nottingham, UK
Adenoviral shuttle vector pShuttleCMV	N/A	Stratagene, Agilent, La Jolla, USA
pAdEasy-1 vector	N/A	Stratagene, Agilent, La Jolla, USA
AdEasy-CMV-Luc vector	N/A	?
Multi-Component systems	**Catalogue No.**	**Company**
Adeno-X-Maxi purification kit	N/A	Clontech, Carlsbad, USA
DC Protein Assay, Kit	500-0116	Bio Rad, Munich, Germany
Free Fatty Acid Quantification kit	AB65341	Abcam Biochemicals, Cambridge, UK
Nupage 4-12% Bis-Tris Midi Gel 1.0mm 12+2 well	WG1401BX10	Life technologies, Carlsbad, USA
Nupage 4-12% Bis-Tris Midi Gel 1.0mm 20 well	WG1402BX10	Life technologies, Carlsbad, USA
Purelink RNA mini kit	12183018A	Life technologies, Carlsbad, USA
MPO activity Quantification Kit	AB105136	Abcam Biochemicals, Cambridge, UK
SuperSignal West Dura Extended Duration Substrate	34076	Thermo Scientific, Rockford USA
Triglyceride Quantification Kit	AB65336	Abcam Biochemicals, Cambridge, UK
VectaStain ABC Kit	PK-4000	Vector Laboratories, Burlingame, USA.

Table 10-ix: Material and equipment used in this study (cont.)

Cell strains	Catalogue No.	Company
293A	From primary human embryonal kidney	Life Technologies, Carlsbad, USA
Mouse Hepatocytes	From C57BL/6 (WT) and C57BL/6 ($LCN2^{-/-}$)	this laboratory
XL1-Blue Bacteria	Escherichia coli strain	Stratagene, Agilent, La Jolla, USA

Table 10-x: Material and equipment used in this study (cont.)

Apparatus-Equipment	Company
Avanti® J-20 centrifuge	Beckman, Pasadena, CA, USA
Avanti® J-25 centrifuge	Beckman, Pasadena, CA, USA
Axiovert 25 CFL inverted microscope with HBO 50 and fluoresence reflectors	Carl Zeiss Microscopy, Jena, Germany
Blotting chamber, Transphor + 4 cassetes and cooler	GE Healthcare Bio-sciences Co., Piscataway,USA
Cary 50 Scan UV Visible Spectrophotometer	Varian Med. Systems Palo Alto, CA, USA
Centrifuge 5427 R	Eppedorf, Berzdorf, Germany
Dispersing drive Ultra Turrax T 25 basic	IKA, Staufen, Germany
Electrophoresis system, Sub cell, GT	Bio-Rad, Munich, Germany
Eppendorf Microcentrifuge 5415R (5415D)	Eppedorf, Berzdorf, Germany
Eppendorf Reference Pipette adjustable volume, 100-1000ul	Eppedorf, Berzdorf, Germany
Eppendorf Reference Pipette adjustable volume, 10-100 ul	Eppedorf, Berzdorf, Germany
Eppendorf Reference Pipette adjustable volume, 20-200 ul	Eppedorf, Berzdorf, Germany
Eppendorf Reference Pipette adjustable volume, 2-20 ul	Eppedorf, Berzdorf, Germany
Gel documentation system CN UV/WL	MWG-Biotech, Ebersberg, Deutschland
Genevac- Spinfreezer SF50	Biomentra, Göttingen, Germany
Genevac-Vacuum pump Vac CVP MK 1V	Biomentra, Göttingen, Germany
Heraeus HeraFreeze HFC 586 basic	Thermo Fisher Scientific Waltham, MA, USA
Herasafe™ KS (NSF) Class II, Type B3 Biological Safety Cabinet	Heraus, Hanau, Germany
Incubator-shaker/ Certomat orbital shaker incubator BS-1 orbital shaker	B. Brown Biotech International, Melsungen, Germany
KS 260 control shaker	IKA, Staufen, Germany
Laboratory Air Circulation Oven, ,Model UT 20P	Heraus, Hanau, Germany
Lauda Heating Circulator Water Bath E100	Lauda-Brinkmann, Delran, NJ, USA
Leica DM IL LED inverted Microscope	Leica Microsystems, Wetzlar, Germany
Lumi imagerTM Serial No. 1300039	Roche Diagnostics, Manheim, Germany
MELAG Vacuclav 24	Pul Grah GmbH, Düsseldorf, Germany
Microbiological Incubator type B290	Heraus, Hanau, Germany
Nikon ECLIPSE 80i microscope	Nikon, Dusseldorf, Germany
PCR®-Workstation CleneCab®/UV Transilluminators	Herolab, Wiesloch Germany
Pharmacia GeneQuant II RNA/DNA Calculator	Pharmacia Biotech, Amersham, UK
Power Pack P25, power supply	Biometra, Göttingen, Germany
Real-Time PCR System 7300	Life Technologies, Carlsbad, USA
Ultrasonic processor UP100H (100W, 30kHz)	Hielscher, Teltow, Germany,

Table 10-xi: Material and equipment used in this study (cont.)

10.2 Solutions and buffers

Ammonium acetate 10 M, 20 mL: Dissolve 15.42 g Ammonium acetate in final volume of 20 mL sterile dH_2O. Sterilise by filtration with a 0.2 µm syringe filter.

Ampicilin 50 mg/mL, 10 mL: Dissolve 0.5 g ampicillin in final volume of 10 mL sterile dH_2O. Sterilize the antibiotic solution by using a 0.2 µm syringe filter. Aliquot (500 µl - 1 mL) and store at -20 °C until use.

Antigen unmasking solution: Sodium Citrate Buffer 10 mM, 1 L: Add 2.94 g Sodium citrate trisodium salt dehydrate ($C_6H_5Na_3O_7$ * 2 H_2O), to 1 L H_2O. Adjust pH to 6.0.

Blocking solution: 5% v/v fetal calf serum in 1% (v/v) BSA/PBST, 20 mL: Add 1 mL FCS in 199 mL of 1% v/v BSA/PBST wash buffer.

Blocking Solution: 50% (v/v) FCS/0.5% BSA in PBS, 100 mL: Add 50 mL FCS to 50 mL 0.5% BSA in PBS solution.

Bromophenol blue solution 0.5% (w/v), 10 mL: Dissolve 50 mg Bromophenol blue sodium salt in 10 mL H_2O and keep at 4 ^oC.

BSA (Bovine serum albumin) for Protein standards 20 mg/mL, 10mL: Dissolve 200 mg of bovine albumin in 10 mL Ripa CP.

BSA (Bovine serum albumin) for cell culture, 200 µg /µl, 5 mL: Dissolve 1 g bovine albumin, for cell culture, in 5 mL sterile PBS 1X. Filter to sterilise. Keep at -20 ^oC.

BSA 0.5% (w/v) in PBS 1X, 100 mL: Dissolve 0.5 g Albumin in 100 mL of PBS 1X. Sterilise by using a 0.2 µm syringe filter.

BSA 10% (w/v) in PBS 1X, 100 mL: Dissolve 10 g Albumin in 100 mL of PBS 1X. Sterilise by using a 0.2 µm syringe filter.

BSA 2% (w/v) in PBS 1X, 100 mL: Dissolve 2 g Albumin in 100 mL of PBS 1X. Sterilise by using a 0.2 µm syringe filter.

$CaCl_2$ 1 M, 100 mL: Dissolve 14.70 g $CaCl_2$ in final volume of 100 mL dH2O. Sterilization is not required.

$CaCl_2$ 2.5 M, 100 mL (for transfection)**:** Dissolve 36.76 g $CaCl_2$ * 2 H_2O in 100 mL dH_2O and autoclave.

Collagen working solution 0.05 mg/mL, 50 mL, (for coating): Add 1.25 mL of Collagen stock solution 2 mg/mL, in 50 mL 0.1% Acetic acid solution. Mix well and filter – sterilise.

DAPI stock solution, 5 mg/mL (14.3 mM for the dihydrochloride or 10.9 mM for the dilactate) (Life Technologies): Dissolve the contents of one vial (10 mg) in 2 mL dH_2O. The less water-soluble DAPI dihydrochloride may take some time to completely dissolve in water and sonication may be necessary. Keep in small aliquots in -20 ^oC in the dark.

DAPI working solution 100 ng/mL or 300nm, 50 mL: Dilute 1 µl DAPI stock solution in 50 mL PBS. Keep at 4 ^oC in dark.

DTT (Dithiothreitol) 1M, 10 mL: Mix 1.54 g of 1.4DTT and 33.3 µl of NaOAC 3M pH 5.5 in sterile dH_2O. Prepare solution under hood and keep at -20 ^oC.

EDTA (ethylene diamine tetraacetic acid) 0.5 M pH 8.0, 1 L: Dissolve 181.6 TripleX III/EDTA$Na_2$2$H_2$0 in 900 mL dH_2O. Then fix pH to 8.0 with NaOH pellets (around 10 g) while stirring. Add dH_2O to reach volume of 1 L.

EDTA 100 mM pH 8.0, 200 mL (for blood withdrawal): Dissolve 7.264 g TripleX III/EDTA$Na_2$2$H_2$0 in 150 mL dH_2O. Then fix pH to 8.0 with NaOH pellets while stirring. Add dH_2O to reach volume of 200 mL.

Glucose 1M, 100mL: Dissolve 19.8 g Glucose (or 18 g unhydrated glucose) in 100 mL final volume of sterile dH_2O. Sterilise solution by a 0.2 µm syringe filter. Keep solution in 4 ^oC.

Glycerol 50%, 500 mL: Mix 50 mL of Glycerol with 50 mL of dH_2O. Autoclave the solution at 121 ^oC for 15 min.

Hydrogen peroxide (H_2O_2) 3%, 500 mL: Add with great protections 50 mL of 30% Hydrogen peroxide solution to 450 mL dH_2O.

Kalium/Potasium Acetate (CH_3COOK) 5 M, 500 mL: Dissolve 245.38 g CH_3COOK in 500 mL final volume of dH_2O.

Kanamycin 50 mg/mL, 10 mL: Dissolve 0.5 g Kanamycin sulfate powder in final volume of 10 mL dH_2O sterile. Sterilize antibiotic solution by a 0.2 µm syringe filter. Aliquot (500 µl - 1 mL aliquots) and store at -20 °C until use. NOTE: It is best to avoid repeated freeze/thaw cycles of the kanamycin aliquot.

KCl 1 M, 100 mL: Dissolve 7.45 g KCl in 100 mL dH_2O and autoclave.

KOAc 3M, 100 mL: Mix 29.4 g of potassium acetate, 40 mL of dH_2O, add Glacial acetic acid to pH 4.8, and dH_2O to 100 mL. Sterilize by filtering. Store at 4 ^oC.

LB (Lysogeny broth) medium, 1L (with or without Antibiotic)**:** Dissolve 10 g Bacto-tryptone, 5 g yeast extract, and 10 g NaCl in 950 mL dH_2O, adjust the pH of the medium to 7.0 using 1M NaOH and bring volume up to 1 L. Autoclave on liquid cycle for 20 min at 15 psi. Allow solution to cool to 55°C, and add antibiotic if needed (50 µg/mL of Ampicillin or Kanamycin). Store at room temperature or at 4 °C.

LB plates (with or without antibiotic)**:** Prepare LB medium and add 15 g/l Agar after autoclaving. After autoclaving, let it cool to approximately 55 °C, add antibiotic if needed in final concentration of 50 µg/mL, and pour into petri-dishes. Let harden, and then invert plates and store at 4 °C in the dark.

LiCl 5 M, 100 mL: Dissolve 21.2 g LiCl in final volume of 100 mL sterile dH_2O.

Lysozyme solution 10 mg/mL, 5 mL: Mix 50 mg Lysozyme in 5 mL of 10 mM Tris-HCl (pH 8.0) solution. The solution needs to be made fresh.

MES SDS running buffer 20X, 500 mL: Mix 97.6 g (1 M) MES, 60.6 g (1 M) Tris Base, 10 g (69.3 mM) SDS, and 3 g (20.5 mM) EDTA in dH_2O to final volume of 500 mL (pH 7.2, no adjustment necessary).

Methacarn fixative solution: Mix 60% absolut methanol, 30% $CHCl_3$ and 10% glacial acetic acid.

$MgCl_2$ 1 M, 100 mL: Dissolve 20.33 g $MgCl_2 * 6H_2O$ in 100 mL dH_2O and autoclave.

$MgSO_4$ 1 M, 100 mL: Dissolve 24.6 g $MgSO_4 * 7H_2O$ in 100 mL dH_2O and autoclave.

Milk Solution (no fat) 5%, 100 mL: Dissolve 5 g of Milk powder (no fat) in100 mL TBST 1X.

$MnCl_2$ 1 M, 20 mL: Dissolve 3.96 g $MnCl_2$ in final volume of 20 mL sterile dH_2O. Filter-sterilise the solution by using a 0.2 µm syringe filter.

$MnCl_2$ 1 M, 20 mL: Dissolve 3.96 g $MnCl_2 * 4H_2O$ in 20 mL dH_2O and sterilize by filter. Keep in -20 ^oC.

MOPS Buffer (3-(N-morpholino)propanesulfonic acid) **1 M, 100mL:** Dissolve 20.93 g MOPS, in sterile dH_2O. Fix pH to 7.0 with NaOH. Adjust Final volume to 100 mL. Sterilise by a 0.2 µm syringe filter.

MOPS running buffer: MOPS 1M, Tris Base 1M, SDS 2%, EDTA 20mM, (pH 7.4, no adjustment necessary).

Na-Citrat 0.1%/Triton 0.1%, 100 mL: Add 10 mL of 1% NaCitrat and 100 µl in sterile dH_2O to final volume 100 mL.

NaCitrat 1% (for Immunostaining**):** Dissolve 1 g Trisodium citrate in 100 mL dH_2O.

NaCl 1.6 M/PEG 13% (w/v) solution, 100mL: Dissolve 13 g PEG (Polyethylene glycol) and 9.35 g NaCl in final volume of 100mL sterile dH_2O.

NaCl 0.9% (w/v), 100 mL: Dissolve 0.9 g NaCl in 100 mL dH_2O.

NaCl 5 M, 200 mL: Dissolve for extended time 58.44 g NaCl in dH_2O till final volume of 200 mL and autoclave.

NaCl 150 mM, 250 mL: Dissolve 2.19 g NaCl in 250 mL dH_2O.

NaOAC 3 M pH 5.2, 50 mL: Dissolve 20.4 g NaOAC ($C_2H_3NaO_{2)}$ in 40 mL dH_2O. Adjust pH to 5.2 with glacial Acetic acid. Adjust final volume with dH_2O to 50 mL.

NaOH 1 M, 100 mL: Dissolve 4 g of NaOH pellets in 100 mL sterile dH_2O

NaOH 2 M, 100 mL: Dissolve 8 g of NaOH pellets in 100 mL sterile dH_2O.

NaOH 5 M, 100 mL: Dissolve 20 g of NaOH pellets in 100 mL sterile dH_2O.

Nile red stock solution 1 mg/mL in DMSO, 5 mL: Dissolve at a dark room 5 mg Nile Red (ENZO - Life Sciences) in 5 mL DMSO. Aliquot and keep in -20 ^oC for 1 month.

Nile red working solution in 150 mM NaCl: Add at a dark room 1 µl from the Nile red stock solution 1 mg/mL in 10 mL 150 mM NaCl. Make always fresh

NuPAGE 1% (enhanced with 10% Methanol) blotting buffer 1 L: Mix 50 mL NuPAGE blotting buffer 20X and 100 mL Methanol in 850 mL dH_2O.

NuPAGE blotting buffer 20X 1 L: Mix 81.6 g Bicine, 104.64 g Bis Tris, 6 g EDTA and 0.2 mL (1 mM) Chlorobutanol in dH_2O to final volume of 1L (pH 7.2, no adjustment necessary).

Oil Red O stock solution, 100 mL: Dissolve 0.5 g Oil Red O in 100 mL Isopropanol. Initially vortex vigorously and then shake in water bath for 30 min. Then keep in RT in the dark.

Oil Red O working solution, 10 mL: Mix 6 mL of Oil Red O stock solution and 4 mL dH_2O. Then filter through two Whatmman paper filters used at that time. Always prepare fresh.

Oleic acid stock solution 10mM, **20 mL**: Dilute 564µl Oleic acid conjugated to Albumin (Sigma Aldrich, 354 mM) in 19.43 mL HepatoZYME medium or PBS. Keep at -20 ^oC.

Palmitic acid Stock solution, 5mM, 40mL: Dissolve 0.51 g Palmitic acid powder (Sigma Aldrich) in 10 mL vehicle-absolute ethanol (conc.= 200Mm). Heat for 20 min at 70 ^oC or at 37 ^oC overnight. Dillute 1 mL in 39 mL BSA 10% to prepare 5 mM stock solution. Incubate for 30 min at 45^oC to enhance conjugation of Palmitic acid and BSA. Sterilize through a 0.22µm filter. The solution is stable for a month at 4 ^oC or longer at -20 ^oC.

PBS 10X, 1 M, 1 L: Dissolve 80 g NaCl**,** 2 g KCl**,** 14.4 g Na_2PO_4**,** 2.4 g KH_2PO_4 in dH_2O. Adjust pH to 7.4 with HCl/NaOH. Adjust volume to 1L and sterilize by autoclaving.

PBST 1X, 1 L: Add 100 mL PBS 10X in 900 mL dH_2O. Then add 1 mL Tween-20 and mix well.

Permeabilize solution 0.1% Na-Citrat/0.1% Triton, 50 mL: Add 0.5 mL Triton in 49.5 mL 0.1% Na-Citrat solution.

PFA 3% (Parafolmadehyde) **100 mL:** Dissolve 3 g of pure parafolmadehyde respectively in 50 mL warm dH_2O (around 50^oC). Add a couple drops of 5 M NaOH till the color of the solution is clear (not cloudy). Add 10 mL of PBS 10X and adjust pH to 7.4 with phosphoric acid H_3PO_4. Adjust volume with sterile dH_2O to 100 mL. Prepare solution in the hood and keep solution at -20^oC.

PFA 4% (Parafolmadehyde) **100 mL:** Dissolve 4 g of pure parafolmadehyde respectively in 50 mL warm dH_2O (around 50^oC). Add a couple drops of 5 M NaOH till neutral/clear point. Add 10 mL of PBS 10X and adjust pH 7.4 with phosphoric acid H_3PO_4. Adjust volume with sterile dH_2O to 100 mL. Prepare solution in the hood and keep solution at -20 ^oC.

Ponceau S, 1L: Dissolve 0.1% (w/v) Ponceau S powder in 5% (v/v) Acetic acid and adjust final volume with dH_2O to 1 L. Keep in dark.

RbCl 4 M, 20mL: Dissolve 9.67 g RbCl in sterile dH_2O to final volume 20mL.

RIPA Buffer 500 mL: Mix 1% (v/v) NP-40, 0.1% SDS, 50 mM Tris-HCl pH 7.4, 150 mM NaCl, 0.5% (w/v) DOC, 1 mM EDTA in dH_2O of final volume of 500 mL.

RipaC with Phosphatase Inhibitor 1% (v/v): In 5 mL RipaC add 50 µl of Phospahatase inhibitor cocktail, aqueous solution. Make always fresh.

RipaC: In 50 mL RIPA buffer add one Complete protease inhibitor cocktail Tablet and mix well. Keep at -20 ^oC.

RNAse A solution 10 mg/mL, 5mL: Dissolve 50 mg RNAse A in 5 mL sterile dH_2O. Aliquot and keep aliquots at -20 ^oC. Before using, cook the required amount for 10 min.

Rosiglitazone stock solution 10 mM: Dissolve 35.7 mg (Abcam) in 10 mL vehicle-DMSO. For working solution dilute stock in HepatoZYME medium. Notice: DMSO in working solution becomes toxic if above 0.1% in final concentration.

Rubidium Chloride 4 M, 20 mL: Dissolve 9.67 RbCl in 20 mL dH_2O.

SDS 20% (w/v), 100 mL: Dissolve 20 g of SDS in dH_2O in final volume of 100 mL.

Sodium Chloride-Tris-EDTA Buffer (STE buffer) pH 8.0, 1X, 1L: Dissolve 100mM NaCl (20 mL NaCl 5 M) , 1 mM EDTA (2 mL 0.5 M EDTA) and 10 mM Tris-HCl (10 mL Tris-HCl, pH 8,0) in final volume of 1 L sterile dH_2O.

Solution I, 500 mL: Add 50 mM Glucose (25 mL 1 M glucose), 10 mM EDTA (10 mL 0.5 M EDTA, pH 8,0) and 25 mM Tris-HCl (12.5 mL Tris-HCl, pH 8,0) in final volume of 500 mL sterile dH2O. Keep solution 4 ^oC.

Solution II, 100 mL: Add 1% SDS (5 mL of 20% SDS (w/v), 0.2 M NaOH (4 mL 5 M NaOH) in final volume of 100 mL sterile dH_2O. Solution needs to be made always fresh.

Solution III, 500 mL: Mix 300 mL of a 5 M Potassium Acetate (CH_3COOK) solution and 57.5 mL Glacial acetic acid 142.5 mL sterile dH_2O. Keep solution at 4 ^oC.

Standards for protein Quantification 200 µl each, 0 µg/µl: 200 µl RipaC, **0.6 µg/µl:** Mix 6 µl 20 mg/mL BSA in 194 µl RipaC, **0.9 µg/µl:** Mix 9 µl 20 mg/mL BSA in 191 µl RipaC, **1.2 µg/µl:** Mix 12 µl 20 mg/mL BSA in 188 µl RipaC, **1.5 µg/µl:** Mix 15 µl 20 mg/mL BSA in 185 µl RipaC **, 1.8 µg/µl:** Mix 18 µl 20 mg/mL BSA in 182 µl RipaC, **2.1 µg/µl:** Mix 21 µl 20 mg/mL BSA in 179 µl RipaC **, 2.4 µg/µl:** Mix 24 µl 20 mg/mL BSA in 176 µl RipaC. All standards should be kept at -20 ^oC.

STOP Mix 5X, 5 mL: Mix 20mM EDTA (0.2 mL 0.5 M EDTA, pH 8.0), 30% Glycerol (1.7 mL Glycerol), 0.1% w/v Bromophenol blue (1 mL) and 0.5% SDS (w/v) (0.125 mL 20% SDS solution) with dH_2O to final volume 5 mL.

TBE 10X, 1 L: Dissolve 108 g Tris-Base, 55 g Boric acid and 7.44 g EDTA in dH_2O to final volume 1 L.

TBS (Tris-buffered saltine**) 10X:** Dissolve 10 mM (12.1 g) Tris and 150 mM (87.6 g) NaCl in final volume of 1 L dH_2O. Adjust pH to 7.6 with HCl.

TBST (Tris-buffered saltine-Tween20. 0.1%) **1X, 1 L:** Add 100 mL TBS 10X in 900 mL dH_2O**.** Then add 1 mL Tween 20 and mix well.

TE pH 8.0, 100 mL: 10 mM Tris-HCl (1 mL of 1M Tris-HCl pH 8.0) and 1 mM EDTA (0.2 mL of 0.5 M EDTA pH 8.0) in 98.8 mL dH_2O.

TE buffer pH 8.0, 100 mL: Mix 10 mM Tris-Cl (1 mL of 1M Tris-HCl solution, pH 8.0), and 1 mM EDTA (0.2 mL of a 0.5 M EDTA solution pH 8.0) in final volume of 100 mL sterile dH_2O.

TFB I buffer: Mix: 30 mM KOAc (0.6 mL of a 3 M KOAc solution), 50 mM $MnCl_2$ (5 mL of a 1M $MnCl_2$ solution), 100 mM RbCl (2.5 mL of a 4M RbCl solution), 10 mM $CaCl_2$ (1 mL of a 1 M $CaCl_2$ solution) and 15% Glycerol (v/v) in final volume of 100 mL dH_2O. Keep in 4 ^oC degrees.

TFB II buffer: Mix: 10 mM MOPS (1 mL of a 1M MOPS buffer, pH 7.0), 75mM $CaCl_2$ (7.5 mL of a 1 M $CaCl_2$ solution), 10 mM NaCl (1 mL of a 1 M NaCl solution and 15% Glycerol (v/v) (15 mL glycerol) in 100mL final volume of sterile dH_2O. Keep at 4 ^oC.

Tris-HCl pH 7.4, 500 mL: Dissolve 60.55 g Tris-HCl in 350 mL dH_2O, fix desirable pH with HCl and add dH_2O to reach 500 mL of total volume. Autoclave the solution.

YT 2X medium, 1 L: Dissolve 16 g Bacto-tryptone, 10 g yeast extract and 5 g NaCl in dH_2O in a final volume of 1 L. Autoclave.

Wash buffer Citrate/PBST: 1 X PBS/0.1% Tween-20, 1L (for immunohistochemistry): Add 100 mL 10 X PBS to 900 mL dH_2O. Add 1 mL Tween-20 and mix well.

10.3 Table of figures

Figure **4-i**: Phylogenetic tree for human lipocalins 14

Figure **4-ii**: Three dimensional structural architecture of Lipocalin 2 14

Figure **4-iii**: Diagnostic measurement of LCN2 in human specimen 25

Figure **4-iv**: The structure of the hepatic lobule 27

Figure **6-i**: MCD diet leads to sharp alterations of the body weight 48

Figure **6-ii**: Effects of the MCD diet on livers of WT and *Lcn2*$^{-/-}$ mice 49

Figure **6-iii**: Serum analysis 50

Figure **6-iv**: Free fatty acid and triglyceride quantitation 51

Figure **6-v**: Effects of a MCD diet on the protein expression and mRNA level of genes correlated to lipid metabolism 52

Figure **6-vi**: Immunohistochemisty for PLIN5 in the liver tissue 53

Figure **6-vii**: Induction of PLIN5 by LCN2 overexpression in cultured hepatocytes 54

Figure **6-viii**: Effect of LCN2 overexpression in hepatic lipid droplets 55

Figure **6-ix**: Increase in lipid droplets in primary hepatocytes overexpressing PLIN5 56

Figure **6-x**: Immunocytochemical analysis of PLIN5 induction by LCN2 overexpression in primary hepatocytes 57

Figure **6-xi**: Stimulation of primary hepatocytes with oleic acid 58

Figure **6-xii**: Quantitative analysis of lipolytic markers 59

Figure **6-xiii:** Induction of PLN5 expression in hepatocytes by stimulation with fatty acids 59

Figure **6-xiv**: Induction of PLIN5 expression in hepatocytes by stimulation with fatty acids 60

Figure **6-xv**: High fat diet 61

Figure **6-xvi**: Effect of Rosiglitazone on LCN2 and PLIN5 expression 62

Figure **6-xvii**: Expression of mitochondrial marker genes 63

Figure **6-xviii**: Model of LCN2 function in the regulation of PLIN5 expression and control of lipid homeostasis. 66

Figure **7-i**: Inflammation effect after four weeks of MCD diet administration 71

Figure **7-ii**: MCD diet induces the formation of inflammatory infiltrations 72

Figure **7-iii**: MCD diet enhances the recruitment of neutrophils granulocytes 73

Figure **7-iv**: MCD diet affects protein and mRNA expression of genes involved in the inflammation process 74

Figure **7-v**: Proposed scheme of LCN2 role in hepatic inflammation 75

10.4 Table of tables

Table **4-i**: Synonyms of LCN2/NGAL in: human, mouse and rat 16
Table **4-ii**: Sources of LCN2 in human tissues 17
Table **4-iii**: Selected experimental and clinical findings associated with altered hepatic LCN2 expression 20
Table **4-iv**: Selected experimental and clinical findings associated with altered hepatic LCN2 expression 21
Table **4-v**: Selected experimental and clinical findings associated with altered hepatic LCN2 expression 22
Table **4-v**: Selected experimental and clinical findings associated with altered hepatic LCN2 expression
Table **10-i**: Oligonucleotides-Primers used for PCR and q-RT-PCR 92
Table **10-ii**: Antibodies used in his study 93
Table **10-iii**: Material and equipment used in this study 94
Table **10-iv**: Material and equipment used in this study (cont) 95
Table **10-v**: Material and equipment used in this study (cont) 96
Table **10-vi**: Material and equipment used in this study (cont) 97
Table **10-vii**: Material and equipment used in this study (cont) 98
Table **10-viii**: Material and equipment used in this study (cont) 99
Table **10-ix**: Material and equipment used in this study (cont) 100
Table **10-x**: Material and equipment used in this study (cont) 101
Table **10-xi**: Material and equipment used in this study (cont) 102

10.5 Curriculum vitae

Personal Profile

Last Name:	Asimakopoulou
First name:	Anastasia
Date of Birth:	20th October 1986
Nationality:	Greek and Australian
Address:	Rudolfstrasse 8, Aachen 52070, Germany
E-mail address:	natashaasimakopoulou@yahoo.com
Phone number:	+49 1742875000

Academic education

Jan. 2013 - Mar. 2015	PhD thesis 'title of thesis' Institute for Molecular Patho biochemistry, Experimental Gene therapy and Clinical chemistry (Supervisor: Professor Weiskirchen Ralf), RWTH Aachen University, Germany.
Jan. 2012 - Dec. 2013	Master Thesis 'Analysis of non-alcoholic steatohepatitis (NASH) in Lipocalin 2 – deficient mice.', Institute for Molecular Patho biochemistry, Experimental Gene therapy and Clinical chemistry (Supervisor: Professor Weiskirchen Ralf), RWTH Aachen University, Germany.
Jan. 2009 - Jun. 2009	Bachelor Thesis 'Cross amplified microsatellites in the European cherry fly, Rhagoletis cerasi: medium polymorphic – highly informative markers.', Genetics, Cell and Developmental Biology laboratory, (Supervisor: Postdoc Researcher Antonis Avgoustinos), Faculty of Biology, University of Patras, Greece.
Sep. 2005 - Mar. 2010	Bachelors in Faculty of Biochemistry and Biotechnology, School of health sciences, University of Thessaly, Greece.
Aug. 2005	High School-Integrated Lyceum Graduation, Kamares-Egion Achaias.

Publications

2015	**Asimakopoulou A**, Borkham-Kamphorst E, Tacke F, Weiskirchen R. Lipocalin-2 (NGAL/LCN2), a "HELP-ME" Signal in Organ Inflammation. Hepatology (2015), 62: in press.
2014	**Asimakopoulou A,** Weiskirchen R. Lipocalin 2 in the pathogenesis of fatty liver disease and nonalcoholic statohepatitis. Clin Lipidology. (2015), 10:47-67.
2014	**Asimakopoulou A**, Borkham-Kamphorst E, Henning M, Yagmur E, Gassler N, Liedtke C, Berger T, Mak TW, Weiskirchen R. Lipocalin-2 (LCN2) regulates PLIN5 expressionand intracellular lipid droplet formation in the liver. Biochim. Biophys. Acta. (2014), 1841:1513-1524.

2014 Augustinos AA, **Asimakopoulou AK**, Moraiti CA, Mavragani-Tsipidou P, Papadopoulos NT, Bourtzis K. Microsatellite and Wolbachia analysis in Rhagoletis cerasi natural populations: population structuring and multiple infections. Ecol. Evol. (2014), 4: 1943-1962.

2011 Augustinos AA, **Asimakopoulou AK**, Papadopoulos NT, Bourtzis K. Cross-amplified microsatellites in the European cherry fly, Rhagoletis cerasi: medium polymorphic-highly informative markers. Bull. Entomol. Res. (2011), 101: 45-52.

Abstracts

2015 **Asimakopoulou, A**, Borkham-Kamphorst, E, Weiskirchen, R. (2015), Lipocalin 2 (LCN2) in hepatic inflammation. Z. Gastroenterol. 53, A11.

2014 **Asimakopoulou, A**, Borkham-Kamphorst, E, Weiskirchen, R. (2014), Lipocalin-2 (LCN2), a central mediator in inflammatory organ disease. 5. Tag der Medizinischen Forschung Aachen, 5. Dezember 2014, Poster P57.

2013 Weiskirchen, R, Henkel, C, **Asimakopoulou, A**, Borkham-Kamphorst, E. (2013), Lipocalin-2 (LCN2), a central mediator in inflammatory organ disease. 4. Tag der Medizinischen Forschung Aachen, 29. November 2013, Poster P64.

2010 Augoustinos A, **Asimakopoulos A**, Bourtzis K, Papadopoulos N, Mavragani-Tsipidou P. (2010) : Microsatelites markers to the European cherry fly, Rhagoletis cerasi, shows the existence of great genetic variation between the Greek natural populations of this species. 5th Panhellenic Ecology Symposium.

2010 Augoustinos A, **Asimakopoulos A**, Bourtzis K, Papadopoulos N, Mavragani-Tsipidou P. (2010), Microsatelites markers to the European cherry fly, Rhagoletis cerasi, shows the existence of great genetic variation between the Greek natural populations of this species. Ecology Conference 2010, Valencia, Spain.

2009 **Asimakopoulos A**, Bourtzis K, Papadopoulos N, Augoustinos A. (2009), Development of 15 microsatellite markers for the cherry fruit fly, Rhagoletis cerasi (Diptera: Tephritidae) and their use in the analysis of Greek populations of the species. 13th Panhellenic Entomological Symposium.

Internships

Jul. 2009 - Mar. 2009 Internship as Research assistant at Genetics, Cell and Developmental Biology laboratory, Project: 'Microsatellite and Wolbachia analysis in Rhagoletis cerasi natural populations: population structuring and multiple infections.', Faculty of Biology, University of Patras, Greece .Main Tasks: DNA isolation, Radioactivity-labelling, PCR, SDS electrophoresis, Genotyping, Phylogenetic analysis with GENALEX 6.5.

Practical Training

Jul. 2007 - Aug. 2007 At the Heamatology laboratory, General University Hospital of Larissa. Main Tasks: Complete blood test and blood smears, Liver function test, C-reactive protein (CRP) inflammation test.